UNIVERSITY OF FLORENCE

Department of Experimental and Clinical Medicine

PhD COURSE IN

Biomedical Sciences (*Physiological and Nutritional Sciences*)

Cycle XXIX

INFLUENCE OF RELAXIN AND ADIPONECTIN ON MICE GASTROINTESTINAL SMOOTH MUSCLE: MECHANICAL AND ELECTROPHYSIOLOGICAL STUDIES

Candidate: **Eglantina Idrizaj**

Tutor:

Prof. Maria Caterina Baccari

PhD Course Coordinator:

Prof. Persio Dello Sbarba

Years 2013- 2016

Preface

Even if during these three years of PhD course I had the possibility to collaborate with different research groups on various projects, this thesis concerns with the researches aimed to investigate the effects of the hormones relaxin and adiponectin on mice gastrointestinal smooth muscle. These studies indeed combine mechanical and electrophysiological aspects and represent the most recent and innovative results. Moreover, a small part of this study was done in collaboration with the Institute of Diabetic and Cancer (IDC), Helmholtz Zentrum of Munchen (Germany), where I spent a period during my PhD course.

Therefore, I have only reported in brief the results of the other projects (chapter 5), involving additional tissues and techniques, already published on international journals.

Acknowledgements

First and foremost I would like to thank my Professors and collaborators for welcoming me in their research group, making possible the realization of my projects and for creating an amiable work environment. I would like to express my sincere gratitude to my advisor, Prof. Maria Caterina Baccari, for always assisting me with patience and dedication, for her constant professional support, guidance and mentorship and for the helpful suggestions and constructive scientific discussion, also during the writing of this thesis. My deepest thanks to Prof. Fabio Francini for believing in me, teaching me, for his constant advices and his helpful professional inputs. My sincere gratitude goes to Dr. Roberta Squecco for her continuous support and especially for electrophysiological studies, for encouraging me with her boundless optimism and energy and for the useful scientific and non-scientific discussions. I also wish to thank Dr. Rachele Garella, simply a wonderful colleague and friend, making lab life much more enjoyable and much else. I could not have imagined being in a better research team.

I take the opportunity to thank Prof. Corrado Poggesi, Head of the Department of Experimental and Clinical Medicine, for his encouragement and for his enthusiasm on stimulating the researches. My gratitude goes also to Prof. Chiara Tesi for always supporting me and for her constant guidance. I would like to thank Prof. Persio Dello Sbarba for his continuous efforts and helpful advices. Many thanks go to my examiner committee for reading and evaluating my thesis.

With this I also would like to thank Dr. Natalia Pellegata, who gave me the opportunity to join her lab in Munich, were I had the possibility to enrich scientifically and plenty more, for her constant assistance and for making me feel home. Many thanks go to Dr. Hermine Mohr for teaching, supporting and helping me during the time in lab. My appreciation also goes to Elke Pulz for her great help and assistance on performing the experiments concerning on AdipoR1 and AdipoR2 expression and not only. I further want to thank Dr. Tobias Wiedemann for his joyful character and for giving me always helpful and precious advices. Thanks also to Nina, Andrea, Vanessa, and Sebastian for the nice time together at Helmholtz. Special thanks to Anita, Xhimi, Subhamoy and Young-woon that made the life in Munich an unforgettable experience.

I would like to thank Toni for always being there through my highs and lows. My special friends, Tila and Peci, who always find a way to cheer me up.

Last but not least, I would like to express my deepest gratitude to my family: my parents and my sisters for always believing in me and for being my strength.

Thank you one and all!

Abstract

It is well known that the gastrointestinal (GI) smooth muscle is controlled by nervous, myogenic and hormonal mechanisms. This thesis deals with the effects of the two hormones, relaxin (RLX) and adiponectin (ADPN), on GI smooth muscle of female mice. This choice derives from the statement that RLX, which attains high levels during pregnancy, exerts its effects also beyond the reproductive system and that ADPN, which is mainly produced by the white adipose tissue, has been scarcely investigated concerning on its actions on gastric activity. Particularly, by means of a combined mechanical and electrophysiological approach, the muscular effects of RLX on both colon and ileum and of ADPN on gastric fundus have been tested.

Our results demonstrate that both RLX and ADPN are able to influence the mechanical activity and the biophysical properties of GI smooth muscle preparations, causing a decay of the basal tension and, principally, a hyperpolarization of the resting membrane potential. Moreover, the electrophysiological results demonstrate, for the first time, that the two hormones induce similar effects on voltage-dependent Ca^{2+} current and Ca^{2+}-dependent K^+ current (I_{BK}), determining a reduction in size of the amplitude. In contrast, the effects observed on I_{Ks} and I_{Kv} varied in the different preparations. Furthermore, the analysis of the mechanism of action suggests that RLX is likely to exert its effects through the cGMP signalling pathway in colonic preparations, whereas both cGMP and cAMP seem to be involved in the ileal ones.

In conclusions, from a physiological point of view, the myorelaxant effects of RLX on the gut may increase the intestinal transit time, improving water and nutrient absorption. This aspect is particularly important during pregnancy and may also account for the constipation symptom frequently observed in this physiological state. At variance, the relaxant effects induced by ADPN on gastric fundus preparations, may contribute to increase the organ capacity. Since gastric distension represents, a peripheral satiety signal, it could be speculated that the relaxant effects of ADPN might concur to suppress feeding behaviour in rodents. Thus, even if caution is needed when transferring the results obtained in animal models to humans, the present data suggest that ADPN could be regarded as a potential therapeutic tool in the treatment of obesity and eating disorders.

INDEX

Chapter 1

Introduction

It is well known that the gastrointestinal (GI) smooth muscle is controlled by nervous (extrinsic and intrinsic), hormonal and myogenic mechanisms. The extrinsic nervous control is represented by the two sections (sympathetic and parasympathetic) of the Autonomic Nervous System. The latter also includes the Enteric Nervous System (ENS) that is the intrinsic innervation of the GI tract. The ENS controls the majority of the GI functions independently from the extrinsic innervation, even though this latter can modulate its activity.

In addition to noradrenergic and cholinergic nervous fibres, an important role in the control of GI activity is played by non-adrenergic non-cholinergic (NANC) fibres. In fact, the first evidence concerning on the existence of nervous fibres releasing neither acetylcholine nor norepinephrine indeed occurred in the GI tract (*Burnstock et al., 1963*; *Martinson & Muren 1963*). In the following years, the presence of NANC fibres was also found in many other organs and apparatuses such as trachea, lungs, bladder and cardiovascular system (*Coburn & Tomita, 1973; Burnstock 1975; Barnes 1984; Rubino, 1993).*

A number of studies aimed to identify the nature of the neurotransmitters released from NANC fibres, have put in evidence that they may release either excitatory (e.g. substance P) or inhibitory neurotransmitters, such as adenosine triphosphate (ATP), vasoactive intestinal peptide (VIP) and nitric oxide (NO) (*Burnstock, 1972*; *Matsuzaki et al., 1980; Burnstock, 1981; Angel et al., 1983; Biancani et al., 1985; Burnstock, 1986; Lefebvre, 1986; Moncada & Palmer, 1987; Belai et al., 1991; Desai et al., 1991; Lefebvre, 1993*).

Moreover, besides the neurotransmitters, there are many other substances capable to modulate GI activity, such as hormones released by the GI tract itself or by other organs and tissues including the adipose one (see introduction section 2).

The myogenic control also represents another important aspect regarding to GI activity, in particular for the contractile behaviour of smooth muscle cells (SMCs). Notably, SMCs, which are under the control of several systems like neurons, hormones, interstitial cells of Cajal (ICC) and paracrine substances, are the final effectors of force development. As reviewed by Sanders (*2008*), there are intrinsic regulatory pathways in SMCs that can amplify or defeat signalling from higher regulatory systems (ENS and hormones). In fact, signals from the ENS or hormones may fail to produce the contractile behaviours if excitation-contraction (E-C) coupling mechanisms in SMCs are inactivated. The force of contraction is partly due to the firing of excitatory and inhibitory motor neurones, that determines the GI tract motor patterns; however, neural control is superimposed upon intrinsic myogenic mechanisms underlying the excitability and contractility of SMCs (*Sanders, 2008*). The main pathways involved in E-C coupling in GI smooth muscles are illustrated in Fig. 1.

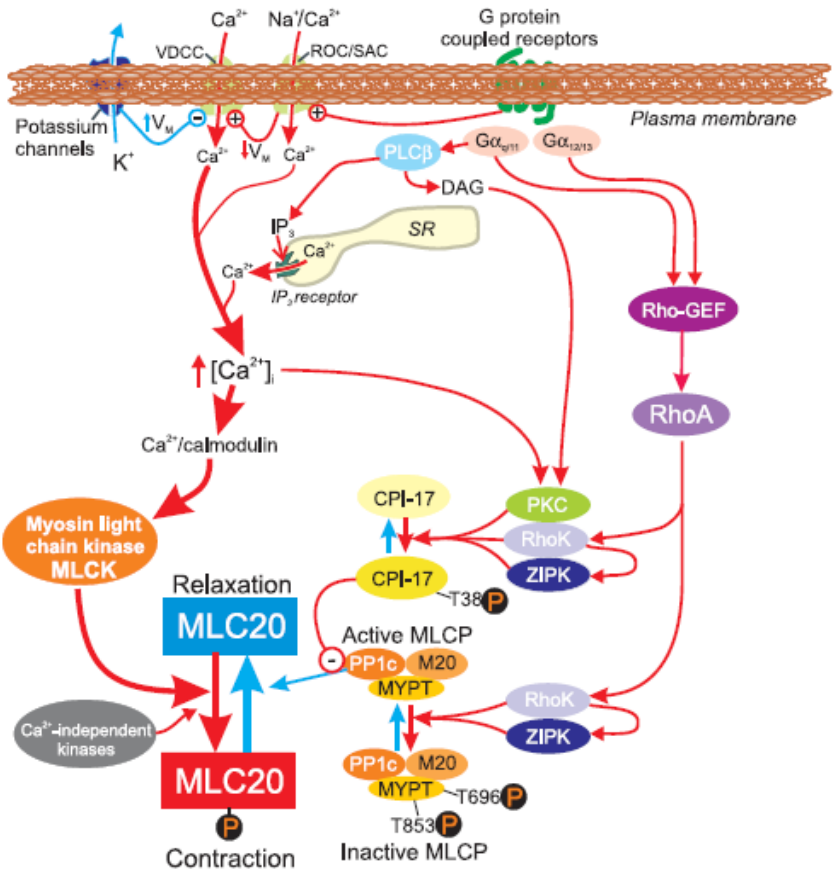

Figure 1. ***Schematic representation of the major pathways involved in excitation-contraction coupling in gastrointestinal smooth muscle***
A rise in cytoplasmic Ca^{2+} ($[Ca^{2+}]_i$) binds to the Ca^{2+} binding protein, calmodulin, and activates myosin light chain kinase (MLCK). MLCK phosphorylates the 20 kDa light chain of myosin (MLC20) and facilitates cross-bridge cycling. There are also Ca^{2+}-independent kinases that can activate MLCK in a Ca^{2+}-independent manner, but under physiological circumstances, excitation-contraction coupling is largely due to the Ca^{2+}-dependent pathway. Phosphorylation of MLC20 is balanced by myosin light-chain phosphatase (MLCP). Dephosphorylation of MLC20 reduces cross-bridge cycling and leads to muscle relaxation. The activity of MLCP is regulated by pathways that regulate the Ca^{2+} sensitivity of the contractile apparatus. One of these pathways is regulated by G protein regulation of GDP-GTP exchange factor (Rho-GEF), RhoA and activation of RhoK (representing ROCK1 and ROCK2 isoforms). Rho kinase and protein kinase C (PKC) can phosphorylate PKC-potentiated inhibitory protein (CPI-17) at T38 which in turn inhibits the catalytic subunit of MLCP (PP1c). Rho kinase can also phosphorylate the regulatory subunit of MLCP (MYPT) at T696 and T853. Phosphorylation of MYPT decreases the activity of MLCP and its ability to target dephosphorylation of MLC20. Other kinases including zipper-interacting kinase (ZIPK) can also phosphorylate CPI-17 and MYPT. Red arrows depict pathways leading to enhanced contraction; blue arrows indicate pathways leading to reduced contraction (From: *Sanders, 2008*).

As in skeletal muscle cells *(Friedrich et al., 1999)*, the raise of $[Ca^{2+}]_i$ is the primary driving force for contraction (*Morgan et al., 1981*). Calcium can enter into the cell

through the channels opened by membrane depolarization, stretch or chemical signals. The most part of Ca^{2+} that initiates contraction comes from the external solution through voltage dependent Ca^{2+} channels (VDCC). Moreover, Ca^{2+} enters from the extracellular fluid also through non-voltage dependent non-selective cation channels (NSCC) that include stretch-activated channels (SAC) and receptor-operated channels (ROC). The VDCC are negatively regulated by a variety of K^+ channels and positively by ROC and SAC that, conversely, depolarize the SMCs. Furthermore, Ca^{2+} entry can be supplemented under various conditions by the release of Ca^{2+} from intracellular stores (*Sanders, 2008*) as in skeletal muscle cells (*Fink & Veigel, 1996*). Calcium release can determine either the stimulation of the contractile apparatus or the activation of Ca^{2+}-dependent K^+ channels (BK) which determines membrane hyperpolarization that induces two oppose effects: it reduces the activation of VDCC, in turn decreasing the Ca^{2+} entry from VDCC, and increases the driving force for Ca^{2+}, determining an increase of Ca^{2+} entry from NSCC. Moreover, variations in $[Ca^{2+}]_i$ also regulate the activity of Na^+/Ca^{2+} exchanger and Ca^{2+} pump present in the sarcolemma and sarcoplasmic reticulum membrane.

There are many regional differences in ion channels expression in SMCs but VDCC, BK and the delayed rectifier (since they do not undergo a fast inactivation) K^+, which includes the fast-activated (Kv), the slow-activated (Ks) and the transient-activated (I_{to}) ones, are expressed in almost every region of the GI tract (*Benham et al., 1985; Carl & Sanders, 1989*; *Schmalz et al., 1998; Matsuyama et al., 1999; Sanders & Koh 2006; Dirk & Richard, 2008; Sanders, 2008*). Moreover, GI SMCs express many other K^+ channels such as ATP-sensitive K^+ channels (K_{ATP}) (*Koh et al., 1998*), small conductance Ca^{2+}-activated K^+ channels (SK) (*Koh et al., 1997; Vogalis & Goyal,*

1997) and intermediate-conductance Ca^{2+}-activated K^+ channels (IK) (*Vogalis et al., 1997*), which I simply schematized below.

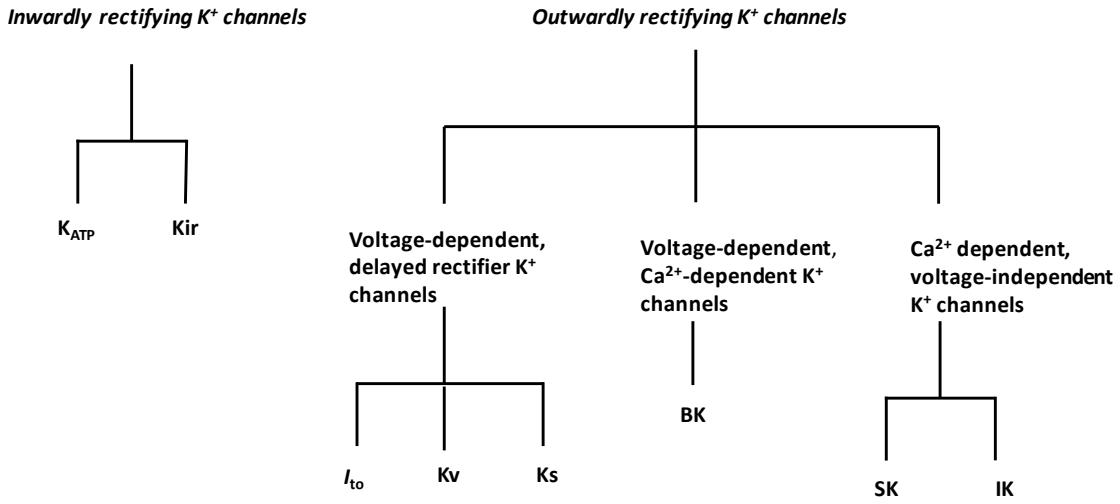

In addition to the above-reported potassium channels, the presence of other species has been also reported in GI SMCs. Among them, the two-pore K^+ (*Koh et al., 2001; Cho et al., 2005; Sanders & Koh 2006*), ether-a-go-go related gene (*Akbarali et al., 1999; Farrelly et al., 2003*), M-current (*Sims et al., 1985*), MinK channels (*Ohya et al., 2002*) and also additional types of VDCC, such as T-Type channels that may contribute in delivering Ca^{2+} to the contractile apparatus (*Xiong et al., 1995*).

The relative permeability of the plasma membrane to physiological ionic species regulates, at resting, the membrane potential. The regulation of the resting membrane potential (RMP) is an important aspect related to the control of excitability in SMCs. Among the different ion species involved in RMP regulation (*Morgado et al., 2012*), SMCs demonstrate a dominant permeability to K^+ ions but other cations inflowing

through NSCC can decrease and thus depolarise the membrane potential considerably from the equilibrium potential of K^+ ions (*Sanders, 2008*).

Finally, also the Na^+/K^+ ATPase pump contributes to several mV on the resting potential. The RMPs of SMCs in different districts of the GI tract may largely vary (from about -75 to -40 mV), due to the differential expression of ion channels and differences in their relative open probabilities (*Sanders, 2008*). Excitatory agonists can influence RMP leading to depolarization of membrane potential by activating inward currents, whereas the activation of outward or suppression of ionic inward currents, contribute to hyperpolarize or stabilize the membrane potential.

Another important role in regulating GI smooth muscle contractions is played by the interstitial Cajal-cells (ICC) that generate the pacemaker activity, in the form of electrical slow waves, and propagate actively through the network of ICC (*Sanders et al., 2006*). SMCs are electrically coupled by gap junctions to each other and to ICC, forming a multicellular syncytium. Changes in ionic conductance, in any cell type, affect the total input resistance and the excitability of the syncytium. For example, K^+ channels opening in ICC can reduce the excitability of the coupled SMCs, thus reducing the probability of reaching the action potential threshold (*Burns et al., 1996*). The slow waves change the membrane potential from a state of low opening probability of VDCC (e.g., resting potential more negative than −55 mV) to an elevated probability of channel opening (peak depolarization from approximately −30 to −25 mV). Thus, there is a sharp relationship between activation of Ca^{2+} channels and membrane potential during slow waves and even small changes in potential at the peak of slow waves can greatly affect the access of Ca^{2+} and contraction (*Sanders et al., 2006*). However, electrical activity in the gut varies among regions (*Szurszewski et al., 1987*). Differences

between SMCs and ICCs or differences in ion channels expression can explain the diversity of electrical behaviour in GI smooth muscles (*Sanders et al., 2006*).

In summary, the control of motor patterns starts with the basic properties of SMCs and leads to contraction or relaxation of the smooth muscle according to various stimuli. Particularly, different inputs from the ENS, hormonal influences, and paracrine factors regulate motor activity during physiological responses. SMCs integrate the inputs from all levels of control and generate appropriate responses. Thus, stimuli such as hormones produced by peripheral tissues as well as by the central nervous system (CNS), which possess stimulatory or inhibitory actions, can change the electrophysiological proprieties of SMCs and have an important role in modulating E-C coupling mechanisms and thus GI activity.

Accordingly, among the different substances that may influence GI smooth muscle activity, I focused this thesis on the effects of two particular hormones, relaxin (RLX) and adiponectin (ADPN).

1.1 Relaxin

The peptide hormone relaxin (6000Da) was identified, for the first time, in 1926 by Hisaw (*Hisaw, 1926*) and is the equivalent of the peptide successively known as Human relaxin-2 peptide (see below). Human relaxin-2 (H2 relaxin), that is the major circulating form into the blood (*Bathgate et al., 2006b*), is simply referred with the more generic term relaxin (*Grossman & Frishman, 2010*) and throughout this thesis work, it will be simply designated as RLX. For a long time the activity of RLX has been reported only in the reproductive system: in fact, the first scientific evidence is referred in a study about the modification of pelvic girdle occurring during the childbirth and the hormone gets the name from its capacity to induce relaxation (*Fevold et al., 1930*). RLX is mainly produced by the corpus luteum, uterus and placenta, attaining high circulating levels during the luteal phase of the menstrual cycle (*Ivell et al., 1989*) and even more during pregnancy (*Weiss et al., 1976; Bell et al., 1987*). Moreover, it has been established that RLX is also produced in the endometrium and mammary gland (*Sherwood et al., 2004; Bathgate et al., 2006a*). In the male, the primary source is the prostate (*Ivell et al., 1989; Sokol et al., 1989; Hansell et al., 1991*), from which the hormone is secreted in the seminal plasma (*Winslow et al., 1992*). Furthermore, RLX is also expressed in the non-reproductive organs. Indeed, its expression has been revealed in human heart (*Dschietzig et al., 2001*) as well as in many other tissues (brain, lung, kidney, liver, thymus, spleen and heart) of mice (*Bathgate et al., 2002; Du et al., 2003; Samuel et al., 2006*).

RLX is considered a pleiotropic hormone (*Bani, 1997*). Actually, the hormone has been reported to exert numerous activities in different districts, such as epidermis (*Unemori & Amento, 1990*), lung (*Unemori et al., 1996*), kidney (*Garber et al., 2001*), liver

(*Williams et al., 2001*) heart (*Samuel et al., 2004; Sherwood, 2004*), central nervous system (*McGowan et al., 2005*) and GI tract (*Baccari & Calamai, 2004*). RLX, in addition to its physiological functions, has been reported to have a potential therapeutic role in some pathological conditions such as inflammatory processes (*Masini et al., 1994*), musculoskeletal diseases (*Dehghan et al., 2014*), renal and cardiovascular diseases (*Bani, 1997; Samuel et al., 2006; Samuel & Hewitson, 2006*), including cardiac fibrosis (*Samuel et al.,* 2004; *Squecco et al., 2015a).*

1.1.1 Relaxin family peptides and receptors

RLX has been isolated and purified in several animal species, including humans, and its amino acidic sequence was identified (*Sherwood & O'Byrne, 1974*; *Schwabe et al., 1976; James et al., 1977; Sherwood 1979; Hudson et al., 1983; Hudson et al., 1984).* The hormone belongs to the *relaxin-insulin peptide* family, and is believed to be evolved from insulin early in the evolution of vertebrates (*Bathgate et al., 2006b*). In humans, this peptide family includes relaxin-1 (H1 relaxin), relaxin-2 (H2 relaxin or RLX) and relaxin-3 (H3 relaxin) (*Hudson et al., 1983; Hudson et al., 1984; Bathgate et al., 2002; Bathgate et al., 2006c*), as well as insulin like peptides (INSL) 3, 5 and 6 (*Adham et al., 1993*; *Chassin et al., 1995*; *Lok et al., 2000*).

In the relaxin family peptide, relaxin-3 is the most recently identified. It is believed to be the ancestral peptide of the family (*Wilkinson et al., 2005*) and seems to be involved in stress, memory, and appetite regulation (*McGowan et al., 2005*; *Tanaka et al., 2005; Ma et al., 2007; Banerjee et al., 2010; Ganella et al., 2013; Ryan et al., 2013; Smith et al., 2014*). INSL3, discovered in the Leydig cells of the testis (*Adham et al., 1993*), appears to have a role in the maintenance of ovarian function and in gubernaculum development involved in the first stage of testis descent (*Spanel-Borowski et al., 2001; Kawamura et al., 2004; Glister et al., 2013*). Concerning on peptide INSL5, it appears

to be widely distributed with high expression in the GI tract (*Conklin et al., 1999*), particularly in L cells isolated from colon (ascending, transverse, and descending) and proximal rectum of mouse (*Grosse et al., 2014*).

All relaxin family peptides are synthesized as a pro-hormone, termed pre-pro-relaxin, constituted by a signal peptide (the B-chain), a connecting peptide (the C-peptide) and an A-chain. Pre-pro-relaxin is processed to the mature hormone by sequential proteolytic digestion of the signal peptide and of the connecting peptide between the two chains (*Kemp & Niall, 1984*). RLX is composed by two disulfide-linked chains, A and B: the A-chain consists of 24 amino acid residues (25 in the mouse), with 2 to α-helix structures localized in A3-9 and A13-20 position (thus, allowing only the interaction with its specific receptors), while the B-chain (where the hormone-receptor binding site is located) consists of 29 amino acid residues with a single structure to α-helix in B7-22 position (Fig.2). The chains are covalently linked by two inter-chain disulfide bonds and an intra-disulfide link (in the A-chain), which stabilize the tertiary structure (*Schwabe et al., 1978; Bathgate et al., 2006b*).

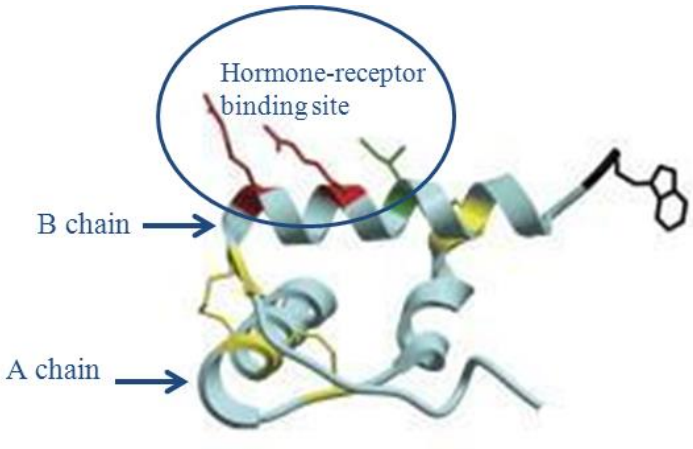

Figure 2. ***Relaxin structure***
Characteristic two-peptide chain hormone held together by disulphide bonds, shown in yellow, which provides the tertiary form of the molecule. There is a relaxin-receptor binding site, shown in red and green (Modified from: *van der Westhuizen et al., 2008*).

Although the hormone is structurally similar to insulin, it acts on different receptors and signalling pathways (*Teichman et al., 2009*). Relaxin family peptide receptors (RXFP) include RXFP1 (LGR7*), RXFP2 (LGR8*), RXFP3 (GPCR135*) and RXFP4 (GPCR142*) which are G-protein-coupled receptors (*names used previously for the RXFP receptors prior to reclassification by NC-IUPHAR) *(Bathgate et al., 2006b*).

However, although relaxin peptides resemble each other closely in structure, each of them binds specific G protein–coupled receptor (GPCR) and possesses a large variety of physiologic functions (*Halls et al., 2015*). The cognate ligands for each receptor have been identified: RLX for RXFP1; INSL3 for RXFP2; RLX 3 for RXFP3 and INSL5 for RXFP4. There are no specific receptors identified yet for INSL4 and INSL6 *(Bathgate et al., 2006b*).

RXFP1 is the cognate receptor for H2 relaxin (RLX) in humans, found in a wide range of reproductive organs including ovary, uterus, mammary gland, placenta, prostate, and testis but also in the heart, liver, kidney, lung and blood cells (*Bathgate et al., 2013*). It is also expressed in a number of areas of brain such as cortex, organum vascuosum of the lamina terminalis (OVLT), and subfornical organ (SFO) (*Bathgate et al., 2005; Samuel & Hewitson, 2006; Samuel et al., 2006; Bathgate et al., 2013)*. RXFP2 is present in uterus, testis, brain, kidney, thyroid and bones, RXFP3 in testis and brain, RXFP4 is mainly distributed in placenta, testis, prostate, brain, kidney, colon, salivary glands, heart, skeletal muscle and liver (*Boels & Schaller, 2003; Bathgate et al., 2005*).

The different types of RLX receptors and their principal localization are summarized in Table 1.

Table 1. Receptors for relaxin family peptides

Official IUPHAR nomenclature	***Ligand***	***Receptor Distribution***
RXFP1	H2 relaxin	ovary, uterus, mammary gland, placenta, prostate, testis, heart, liver, kidney, lung, blood cells, and brain
RXFP2	INSL3	uterus, testis, brain, kidney, thyroid and bones
RXFP3	H3 relaxin	testis and brain
RXFP4	INSL5	placenta, testis, prostate, brain, kidney, colon, salivary glands, heart, skeletal muscle, and liver

It has been shown that the activation of RXFP1 or RXFP2 by porcine relaxin causes a dose-dependent increase of cAMP (*Hsu et al., 2002*), whereas RXFP3 and RXFP4 both inhibit adenylate cyclase (AC) and, in addition, RXFP3 activates Erk1/2 signalling (*Halls et al., 2007*). Indeed, different signalling pathways have been reported to be engaged by RLX (*Sarwar et al., 2015*), including sphingosine-1-phosphate *(Frati et al., 2015)* or cGMP: increased cGMP levels have been found in different cell types as the result of activation by RLX of the endogenous nitric oxide (NO) pathway (*Bani et al., 1995; Bani et al., 1998; Sarwar et al., 2016*).

1.1.2 Relaxin and the gastrointestinal tract

The observation that during pregnancy there is a decrease of GI motility, that rapidly returns to normal during the follicular phase in the period after childbirth (*Datta et al., 1974; Lawson et al., 1985*), suggested a strong correlation between intestinal motor alterations and hormonal variations (*Wald et al., 1982; Everson, 1992*). Some studies directed to further investigate this hypothesis have suggested progesterone as the hormone responsible for the inhibition of GI motility (*Kumar, 1962; Ryan & Bhoiwani,*

1986). However, following studies have demonstrated that progesterone alone determines opposite effects and that it was able to delay gastric emptying only in the presence of estradiol (*Coeskum et al., 1995*). For a long time the attention of the researchers was focused on ovarian hormones, without considering the hypothesis that RLX too could be involved in the regulation of intestinal motility, even if the relaxant effects of RLX on the smooth muscle of numerous anatomical districts were already known (*Bani et al., 1999; Downing & Hollingsworth, 1993*). Early reports have indicated that a purified ovarian RLX preparation reduces the strength and frequency of contractions in the isolated rat ileum (*Del Angel Meza et al., 1991*) and that RLX had disruptive effects on the migrating myoelectric complex of the rat small intestine *in vivo* (*Dekeratry et al., 1993*). In a study conducted on 28 non-pregnant women with intestinal motility disorders, high levels of RLX were found in 68% of cases (*Mathias et al., 1993*). Despite this evidence, only in the recent years it was observed that, in addition to ovarian steroids, also RLX was able to influence GI motility (*Bani et al., 2002; Baccari et al., 2004a; Baccari et al., 2004b; Baccari et al., 2007; Vannucchi et al., 2011*). The effects of RLX on GI motility have been reported to mainly occur through NO, which relaxes the GI smooth muscle (*Rand, 1992*) and alterations of its production/release are involved in numerous motor dysfunctions (*Vallance et al., 2003*). In this view, RLX, in addition to its physiological role, may be also useful in the treatment of pathological conditions related to NO production. For example, it has been reported that RLX is able to counteract, in the dystrophic (mdx) mouse (*Baccari et al., 2007; Vannucchi et al., 2011*), the altered GI motility attributed to a reduction of NO production (*Azzena & Mancinelli, 1999; Baccari et al., 2000*; *Mulè et al., 2001; Garella et al., 2010*).

Notably, NO released from NANC fibres or produced by SMCs is considered the main

inhibitory substance causing GI relaxation (*Grider et al., 1992; Rand, 1992*).

NO is a free radical signal-transducing agent, that easily diffuses within the cell or across the cell membrane and is involved in both autocrine and paracrine actions. It is synthesized endogenously by nitric oxide synthase (NOS) isoenzymes that, in the presence of oxygen, nicotinamide adenine dinucleotide phosphate (NADPH) and co-factors such as flavin mononucleotide (FMN), flavin adenine dinucleotide (FAD), haem and tetrahydrobiopterin (BH4), catalyse the oxidation of the terminal guanidine nitrogen of the amino acid L-arginine to form L-citrulline and NO (Fig. 3) (C*alabrese et al., 2007*).

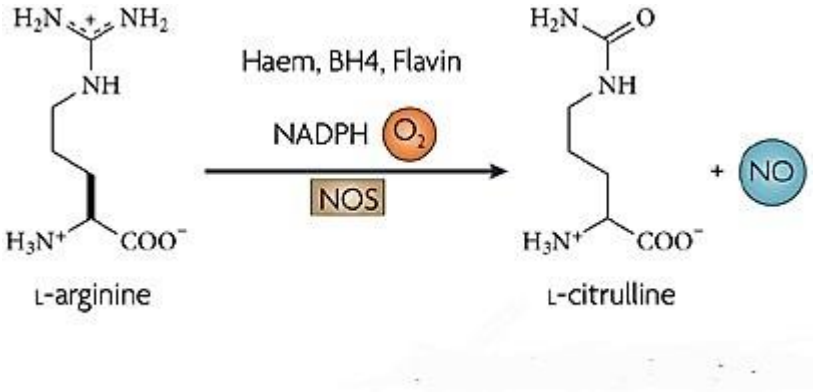

Figure 3. ***The metabolic pathway that leads to NO formation***
In the presence of oxygen, flavin adenine dinucleotide (FAD), NADPH and co-factors such as flavin mononucleotide (FMN), haem and tetrahydrobiopterin (BH4), NOS catalyses the oxidation of the terminal guanidinyl nitrogen of the amino acid L-arginine to form L-citrulline and NO (From: *Calabrese et al., 2007*).

The classical major NOS isoforms are the constitutive NOS, i.e. the neuronal nNOS (type I) and the endothelial eNOS (type III) isoforms as well as an inducible NOS (iNOS, type II), present in a variety of cell types, including vascular endothelial cells, smooth muscle cells, platelets, neuronal cells, macrophages, and neutrophils (*Moncada*

& Higgs 1991; Mayer & Hemmens 1997). The constitutive isoforms, nNOS and eNOS, are enzymes activated by calcium through calcium-calmodulin binding. Both isoforms stimulate the production of NO under the action of various factors such as stretch or some physiological molecules. The inducible isoform, iNOS, is expressed in Kupffer cells, macrophages, neutrophils, fibroblasts, vascular SMCs and endothelial cells in response to a variety of stimuli, including proinflammatory mediators and hormones. The iNOS activity does not depend on calcium, although containing a binding site for calcium-calmodulin complex: the high affinity of the site for its ligand, allows the activation of the enzyme already at very low Ca^{2+} concentrations. The two types of NOS isoforms also differ for the regulation of their expression: constitutive NOS isoforms are expressed in cells at basal levels, while the inducible isoform is not normally expressed, but there are specific transcriptional stimuli, such as interferon γ, interleukin 1β or other cytokines that induce its expression (*Moncada et al., 1991; Mayer & Hemmens 1997*). Finally, NO activates the guanylate cyclase (GC) enzyme, present in the cytoplasm and in the inner part of the cell membrane, which synthesizes the second messenger cyclic guanosine monophosphate (cGMP) able to mediate many of the physiological effects of NO. The ability of cGMP to counteract the effects evoked by the increase of the intracellular Ca^{2+} concentration, such as platelet aggregation or smooth muscle contraction, has been also reported (*Wang et al., 1998; Rybalkin et al., 2003*).

In the GI tract, RLX has been observed to regulate the expression of the different NOS isoforms related to the segment considered (*Baccari & Bani 2008*), as summarized in Table 2, in which the effects of the hormone on the mechanical activity of both healthy and mdx mice are also reported.

Table 2. ***Site-related effects of relaxin on isolated preparations from mouse gastrointestinal (GI) tract by the selective regulation of the different nitric oxide synthase (NOS) isoforms expression.***

GI segment	Site of action	Mechanical effects	NOS isoform regulation	References
Gastric Fundus	Nervous	Decreased motility	↑nNOS-eNOS(protein)	(*Baccari et al., 2004b*)
		Normalization of hypermotility in mdx mice	↑nNOS (protein)	(*Vannucchi et al., 2011*)
Ileum	Muscular	Decreased motility	↑iNOS-eNOS (protein)	(*Bani et al., 2002*)
		Normalization of hypermotility in mdx mice	↑iNOS (protein)	(*Baccari et al., 2007*)
Proximal Colon	Nervous and muscular	Decreased basal tension and increased spontaneous contractions.	↑nNOSβ-eNOS ↓nNOSα-eNOS (protein)	(*Baccari et al., 2012*)

At variance with the gastric fundus where RLX has been shown to act at the nervous level, in the mouse ileum, the hormone was able to reduce the spontaneous contractile activity through a direct action on the smooth muscle mainly by increasing NO biosynthesis (*Bani et al., 2002*). In agreement, immunohistochemistry and Western Blot analysis have put in evidence that, 18h following systemic RLX administration, iNOS and eNOS expression in ileal SMCs was enhanced. Despite this evidence, it was hypothesized that the NO/cGMP could not be the only pathway through which RLX exerted its effects, but probably the cAMP signalling pathway could be also implicated, as observed in the smooth muscle of the mouse uterus (*Bani et al., 1999).*

Moreover, in contrast to the other GI segments in which RLX always depressed the motility, in the isolated mouse proximal colon (the gut region mainly involved in motor

symptoms of pregnancy and menstrual cycle), the hormone determined two opposite effects: a decrease of muscle tone associated with an increase in amplitude of spontaneous contractions (*Baccari et al.,2012*). In agreement, immunohistochemistry revealed that exposure of colonic preparations to RLX increased the two nNOS splice variants (nNOSβ and nNOSγ) expression in the myenteric neurons and downregulated muscular nNOSα and eNOS expression.

Indeed, besides the classical three major NOS isoforms (eNOS, nNOS and iNOS), several NOS splice variants have been identified. Particularly, one of the nNOS variants is membrane-associated (nNOSα) (*Salapatek et al., 1998; Vannucchi et al., 2002*) and two are soluble cytosolic (nNOSβ and nNOSγ) (*Huber et al., 1998*; *Saur et al., 2000; Vannucchi et al., 2002),* whereas the eNOS variants are one full-length and two shorter variants (*Lorenz et al., 2007*). In the GI tract, enteric neurons express a nNOS (isoform likely corresponding to the nNOSβ variant), a full-length eNOS and an iNOS variants, whereas at the SMCs level all the above NOS isoforms are expressed even if the nNOS likely corresponds to the nNOSα variant (*Vannucchi et al., 2002*).

Thus, in the mouse colon, RLX appeared to exert opposite mechanical effects through the up-regulation of neuronal nNOSβ and eNOS and the downregulation of muscular nNOSα and eNOS expression. The depression of NOS activity in these cells could explain the increased mechanical contractility caused by RLX, likely occurring through an enhancement of intracellular Ca^{2+} concentration (*Baccari et al., 2012*).

1.2 Adiponectin

In recent years, the increasing occurrence of obesity has focused scientific research on the study of adipose tissue leading to the discovery that the white adipose tissue is able to secrete important molecules with endocrine, paracrine and autocrine meaning, known together as adipokines. Adipose tissue is today considered a proper endocrine organ (*Scherer, 2006; Harwood, 2012*). Actually, the molecules produced by the white adipose tissue significantly interfere with many kinds of metabolic activities (lipid and glucose metabolism) and are also involved in the regulation of the cardiovascular functions (blood pressure, homeostasis, angiogenesis), immune system and feeding behaviour (*Wajchenberg, 2000; Kershaw et al.,2004*). The same adipokines seem also to be involved in the initiation of the molecular mechanisms that lead to the appearance of the metabolic syndrome that often accompanies obesity and its associated complications (*Smith et al., 2001; Scherer, 2006; Nedergaard et al., 2007*). Moreover, some of the substances secreted by the white adipose tissue, such as the protein hormone leptin, are able to act on the CNS and to modify animal feeding behaviour (*Wilding, 2002; Coope et al., 2008*). In this regard, it has been shown that the mutation of the murine or human gene, preventing the complete synthesis of leptin or the synthesis of its functional receptor, induces a severe obesity mainly characterized by an uncontrollable intake of food (*Wilding, 2002*).

Among the adipokines, adiponectin (ADPN), also known as complement-related protein (ACRP30), gelatin-binding protein-28 (GBP28), ADIPOQ, and apM1 gene product, was discovered in 1995 and is one of the most abundant substances secreted by adipocytes in the blood plasma (*Scherer et al., 1995*). ADPN is induced during adipocyte differentiation and its secretion is stimulated by insulin (*Hotta et al., 2001; Fu et al.,*

2005). Structurally, it belongs to the superfamily of collagen and occurs in three major oligomeric forms with different molecular weight. ADPN is a 244-amino acid polypeptide protein, encoded on chromosome 3q27 (human adiponectin gene, apM1) and exists in both its proteolytic and full-length (30 kDa) forms in plasma *(Maeda et al., 1996*). The full length ADPN (244-amino acid) consists of four domains (Fig. 4): an amino-terminal signal peptide made up of 17 amino acids, a species-specific variable domain of 28 amino acids, a 65-amino acid collagen-like domain, and a 137-amino acid carboxy-terminal globular domain (*Maeda et al., 1997).* Even though ADPN is expressed as a single subunit, full-length ADPN circulates in four isoforms in plasma (*Scherer et al., 1995*). The specific activity of ADPN depends on the complex quaternary structure it forms. Its four isoforms consist of: homotrimers (90KDa), a hexamer (complex of two trimers), a 180 KDa low molecular weight form, and a 360–400 KDa high-molecular weight form (*Hu et al., 1996).*

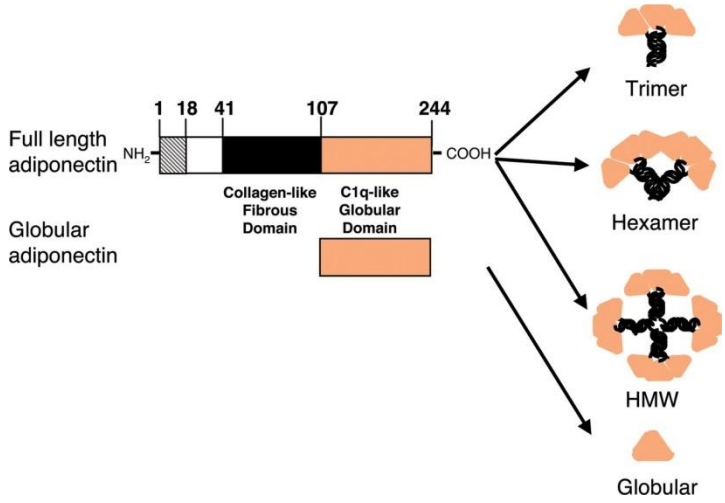

Figure4. ***Domains and structure of adiponectin.***
Full-length adiponectin is composed of 244 amino acids, including a collagen-like fibrous domain at the N-terminus and a C1q-like globular domain at the C-terminus. In plasma, full-length adiponectin combines via collagen domain and forms multimer complexes, such as trimers and hexamers, and a high-molecular-mass (HMW) form. A smaller form of adiponectin that consists of globular domain also exists in plasma in very small amounts (From: *Okamoto et al., 2006*).

Experimental evidence suggests that different forms of ADPN fractions exhibit different biological activities. For example, complexes with lower molecular weight ADPN show stronger anti-inflammatory actions, whereas the high molecular weight form, whose active form constitutes nearly 70% of circulating ADPN in healthy people, may be related to insulin sensitivity (*Nakano et al., 1996; Arita et al., 2002*).

Although ADPN is most abundantly expressed in white adipose tissues (*Scherer et al., 1995*), it has been also found in brown adipose tissue, smooth and skeletal muscle, cardiomyocytes, liver, brain, osteoblasts, placenta and pituitary of several animal species (*Fujimoto et al., 2005; Kaser et al., 2005; Blüher et al., 2006; Psilopanagioti et al., 2009; Boyraz et al., 2013; Ghantous et al., 2015*). ADPN mRNA was recently detected also in the antral mucosa of mice (*Kentish et al., 2015).*

The circulating level of the hormone, in humans, ranges from 5 to 30 μg/ml (*Maeda et al., 1996*) which represents up to 0.05% of total plasma proteins and is typically found at levels 35% lower in men than in women (*Hu et al., 1996; Arita et al., 1999*).

Although ADPN derives from the adipose tissue, it has been observed that plasma ADPN concentrations was lower in obese (3.7±3.2 μg/ml) compared to non-obese subjects (8.9±5.4 μg/ml) (*Arita et al., 1999*). Studies in humans also reported that, in both genders, plasma ADPN concentrations are negatively correlated with body mass index (*Arita et al., 1999*) and visceral fat area (*Ryo et al, 2004*). Other studies described similar results in rodent models (*Hu et al., 1996; Hotta et al., 2001*). This negative correlation appears stronger in visceral than in subcutaneous adiposity (*Cnop et al., 2003; Yatagai et al., 2003*). Therefore, it seems that there is a close correlation between reduced ADPN plasma levels (less than 6 μg/ml) and obesity (*Hotta et al., 2000; Weyer et al., 2001; Arita et al., 2012*).

1.2.1 Receptors and biological activities of adiponectin

ADPN receptors, AdipoR1 and AdipoR2, were identified by expression cloning for the first time in 2003 (*Yamauchi et al., 2003*). They share approximately 67% sequence identity and possess homologous molecular structures but exhibit different binding affinities for the different ADPN forms. AdipoR1 exhibits high affinity for globular ADPN, while AdipoR2 more strongly binds full-length ADPN (*Kadowaki & Yamauchi, 2005).* Another ADPN receptor is the tumor-suppressor protein Tcadherin (CDH-13 gene) that shows affinity for hexameric and high-molecular weight ADPN isoforms but not for the trimeric or globular forms (*Hug et al., 2004).* AdipoR1 (42.4 kDa, 375 amino acids) and AdipoR2 (35.4 kDa, 311 amino acids) both contain an internal (cytoplasmic) N-terminal collagenous domain and an external (extracellular) globular C-terminus with an orientation opposite to all reported G protein-coupled receptors (GPCRs) (Fig. 5) (*Delort et al., 2012).*

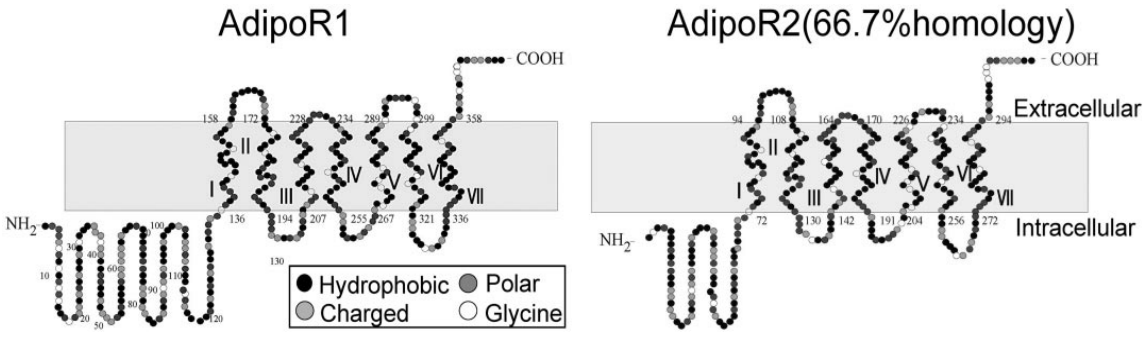

Figure 5. ***Structure of adiponectin receptors*** (From*: Kadowaki & Yamauchi, 2005*).

ADPN receptors are expressed in various peripheral tissues such as liver, skeletal muscle, adipose tissue (*Yamauchi et al., 2003*), macrophages (*Chinetti et al., 2004*) and

pancreatic beta cells (*Kharroubi et al., 2004*). In addition, the expression of the hormone receptors has been reported also in the GI tract: González and co-workers (*2009*) show that AdipoR2 was expressed in the stomach and colon of rats. Moreover, a recent study reported that both AdipoR1 and AdipoR2 are expressed in nodose ganglia, vagal afferent neurons and antral mucosa of mice (*Kentish et al., 2015*). At the central level the AdipoR1 is ubiquitous while AdipoR2 is more expressed on cortex, hippocampus and hypothalamus (*Qi et al., 2004; Kos et al., 2007; Coope et al., 2008; Kadowaki et al., 2008*).

The biological effects of ADPN depend not only on its concentration in the circulation, but also on the activity and expression of tissue-specific receptors (*Oh et al., 2007*). Notably, Palin and co-workers (*2012*) have demonstrated that ADPN is an important regulator of female reproduction, as it interacts with the receptors AdipoR1, AdipoR2 and T-cadherin, which are expressed centrally as well as on peripheral reproductive tissues. Moreover, studies conducted by Yamauchi and collaborators (*2007; 2013*) have shown that AdipoR1 predominantly increases the phosphorylation of AMP-activated protein kinase (AMPK), suppressing lipogenesis and gluconeogenesis. At variance, the interaction of the hormone with AdipoR2 activates peroxisome proliferator-activated receptor alpha (PPARα) ligand, leading to an increase of fatty acid oxidation and energy consumption. Furthermore, AdipoR1 and AdipoR2 demonstrated ceramidase activity determining a decrease in serum ceramide levels and an increase of sphingosine-1-phosphate (S1P) in pancreatic beta cells and cardiomyocytes with protective effects from apoptosis (*Holland et al., 2011*). Denzel *et al.* (*2010*) demonstrated that binding of ADPN with T-cadherin receptors in responsive tissues, such as heart and blood vessels, determines cardio-protective effects. A schematic representation of the above ADPN intracellular signalling is summarized in Figure 6.

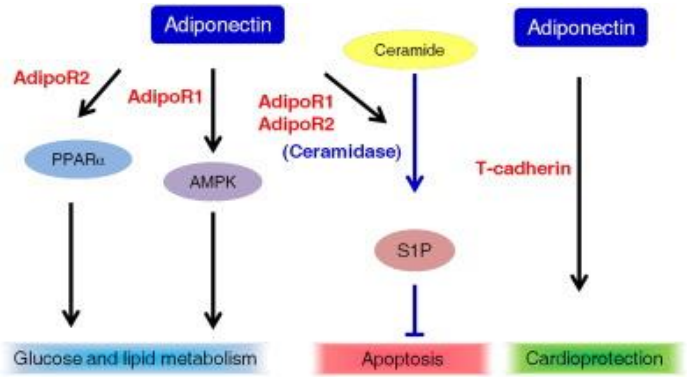

Figure 6. ***Adiponectin intracellular signalling.***
Binding of adiponectin to adipoR1 activates the AMP-activated protein kinase (AMPK) while binding to adipoR2 activates PPARα. The activation of these pathways results in reduced gluconeogenesis and increased fatty acid oxidation. Moreover, adiponectin via AdipoR1 and AdipoR2 decreases ceramide, increases sphingosine-1-phosphate (S1P), to account for the anti-apoptotic effects. T-cadherin is critical for adiponectin's cardioprotective effects on mice (From: *Fu et al., 2016*).

ADPN seems to play an important role also in inflammatory responses. In this view, it has been reported to increase interleukin 6 (IL-6) in macrophages via activation of nuclear factor kappa *β* (NFk*β*) through a still unidentified ADPN receptor, AdipoRX (different from AdipoR1 or AdipoR2), leading to an increase of insulin receptor substrate 2 (IRS-2) in hepatocytes (*Hui et al., 2012).* Furthermore, its anti-inflammatory effects were shown also on vascular system and were attributed to its ability to inhibit NFk*β* signalling through a cAMP-dependent pathway (*Ouchi et al., 2000*).

Interestingly, several studies indicate that hypothalamic AMPK is probably involved in the control of food intake, since it is stimulated by orexigenic ghrelin and conversely inhibited by anorexigenic leptin and insulin (*Andersson et al., 2004; Minokoshi et al., 2004*). In the hypothalamus, AMPK activity is negatively correlated with malonyl-coenzyme A content whose hypothalamic accumulation inhibits food intake (*Hu et al., 2003; Wolf 2006*). Concerning on the metabolic pathways of ADPN, it has been demonstrated that the hormone was also able to initiates AMPK-mediated eNOS

activation leading to an increase of NO production in vascular system (fig. 7) (*Chen et al., 2003; Han et al., 2007*).

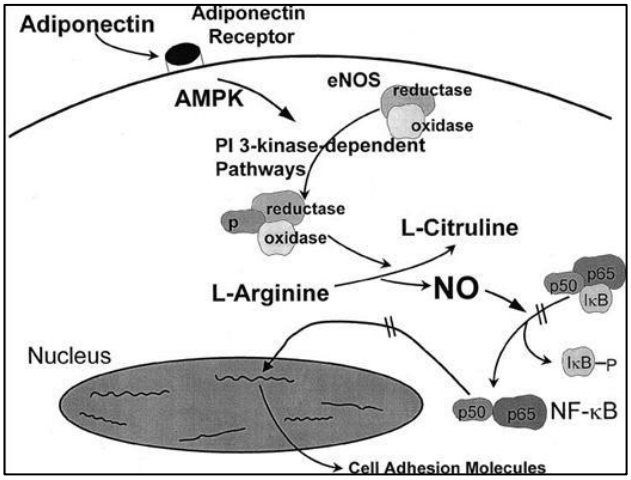

Figure 7. ***Adiponectin increases NO production in endothelial cells of vascular system.*** Adiponectin has novel vascular actions to directly stimulate production of nitric oxide (NO) using phosphatidylinositol (PI) 3-kinase-dependent pathways involving phosphorylation of endothelial nitric oxide synthase (eNOS) by adenosine-monophosphate-activated protein kinase (AMPK) (*Chen et al., 2003*) and reduces expression of adhesion molecules and decreases cytokine production from macrophage by inhibiting nuclear transcription factor kappa B (NF-κB) signalling through cyclic adenosine-monophosphate-dependent pathways (From: *Han et al., 2007*).

Indeed, ADPN was shown to exert through NO many physiological actions on the vascular system such as prevention of atherosclerosis, inhibition of vascular SMCs proliferation and regulation of vascular contraction and blood pressure (*Ewart et al., 2008*).

Thus, ADPN, acting through different pathways, seems to exert antiatherogenic, antiapoptotic, antidiabetic, antiinflammatory effects both in animals and humans (*Yamauchi et al., 2003; Kadowaki et al., 2006*). Recently, a role of ADPN in preventing cardiac dysfunctions has been also described (*Francisco et al., 2016*).

ADPN, besides its peripheral metabolic effects, appears to be a regulator of food intake, sending signals to the hypothalamus, the key region of the CNS involved in the regulation of feeding behaviour (*Murphy & Bloom, 2004*). In this view, many

adipokines such as leptin, that regulate centrally food intake, are also capable of acting at the level of the GI smooth muscle (*Yarandi et al., 2011; Okumura & Nozu, 2016*). On the other hand, peripheral factors, such as motor variations of the GI tract may influence the hypothalamic centres deputies to the adjustment of food intake thanks to the afferent nerves and through the interposition of extra-hypothalamic structures (*Duca & Covasa, 2012*).

In fact, as reviewed by Konturek *et al.* (*2004*), signals arising from a variety of sensors in the gut that respond to various stimuli, such as mechanical (including distension), chemical (including nutrients) and neuro-hormonal (gut hormones, neurotransmitters and neuromodulators), reach the CNS through the afferent vagal and sympathetic nerves (*Holzer et al., 1992; Langley et al., 1994*).

Several hormones from the GI tract, as well as signals from adipose tissue, have been reported to modulate appetite in humans (*Tschöp et al., 2001; Batterham et al., 2003; Stanley et al., 2005*), as shown in Fig. 8.

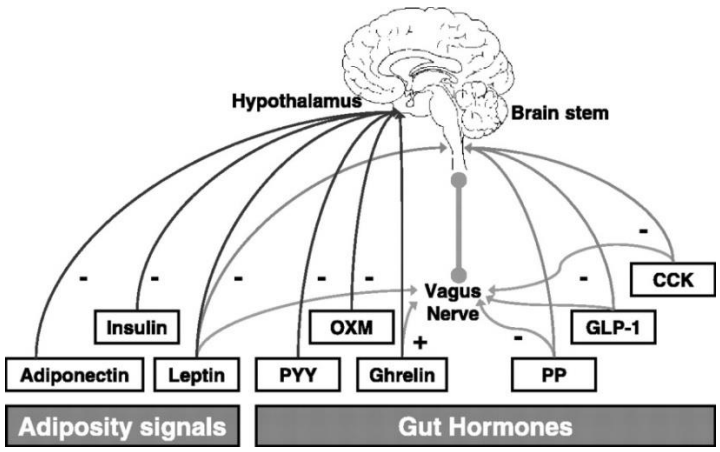

Figure 8. ***Adiposity signals and gut hormones influence on CNS.***
Peripheral signals from the gut include, peptide YY (PYY), oxyntomodulin (OXM), ghrelin, pancreatic polypeptide (PP), glucagon-like peptide 1 (GLP-1), and cholecystokinin (CCK), and adiposity signals from adipose tissue or pancreas include adiponectin, leptin or insulin, influence central circuits in the hypothalamus and brain stem sanding negative (-) or positive (+) signals and thus influencing feeding behaviour and energy expenditure (From: *Stanley et al., 2005*).

Among the adipokines, also ADPN may have a role on regulating feeding behaviour by sending anorexigenic signals to hypothalamus (*Coope et al., 2008)*. Notably, it has been shown that peripherally overexpression of ADPN reduced food intake in rats (*Shklyaev et al., 2003*). Moreover, intracerebroventricular ADPN treatment determines weight loss through the increase of energy expenditure in mice (*Qi et al., 2004*).

Notwithstanding the above results, Kubota and co-workers (*2007*) reported that ADPN appears to increase food intake and to cause weight gain by activation of its receptors in the hypothalamus.

Thus, although ADPN has been shown to affect satiety, acting both centrally and peripherally, there is absence of consensus regarding to its ability to decrease food intake (*Kentish et al., 2015*). Therefore, ADPN action deserves to be better explored to extend our knowledge about its physiological effect and its role in feeding behaviour. In fact, despite the observation that ADPN may influence feeding behaviour and the suggestion of its involvement in a stomach–vagal–brain pathway (*Kentish et al., 2015*), at present, there are no data in the literature concerning on its physiological effects on GI motility.

1.3 Aim of the present research

We have already mentioned that SMCs from diverse segments of GI tract may show different electrical behaviour due to typical changes in ion channel expression. SMCs integrate the inputs from different levels of control and many substances can modify and modulate their contractile behaviour.

This thesis work is centred on the effects of two particular hormones, RLX and ADPN, on SMCs of different GI tracts of female mice, in order to clarify the modulatory action of these endogenous substances. Particularly, the effects of RLX have been studied on both colonic and ileal preparations, whereas those of ADPN in gastric fundus as follows:

Effects of RLX on colonic smooth muscle

As mentioned in the introduction section, previous mechanical studies showed that RLX always depressed gastric and small intestine motility in female mice, mainly through the activation of the L-arginine/NO pathway (*Bani et al., 2002; Baccari et al., 2004a; Baccari et al., 2004b*). More recently, unexpected effects of the hormone on mice proximal colonic preparations have been observed: a decay of the basal tension coupled to an increase of spontaneous contractions (*Baccari et al., 2012*). Since this latter was an unusual phenomenon, we decided to better investigate the effects of RLX on colonic smooth muscle by a combined mechanical and electrophysiological approach.

Thus, this study aims *to better understand the mechanism of action of RLX on the proximal colonic smooth muscle and to find a possible correlation between its mechanical and electrophysiological effects*. For this purpose, we investigated: i) the expression of the RLX receptor, RXFP1, by immunohistochemical experiments

performed in collaboration with the Histology and Embryology Research Unit of the Anatomy and Histology Section of our Department; ii) the ability of RLX to affect the biophysical properties of the colonic SMCs, particularly the RMP and the voltage-dependent and independent Ca^{2+} and K^+ currents; iii) the contribution of the NO/cGMP/PKG pathway in the observed mechanical and electrophysiological RLX effects.

Effects of RLX on ileal smooth muscle

Although most of the effects of RLX on the GI tract have been ascribed to the ability of the hormone to increase NOS expression (*Baccari & Bani 2008*), previous experiments, carried out on ileal preparations from female mice (*Bani et al., 2002*), have hypothesized the involvement of additional signalling pathways, such as cAMP, as occurs in other SMCs (*Bani et al., 1999).*

Accordingly, this research attempts *to investigate whether, in addition to cGMP, cAMP may contribute to the direct muscular effects of the hormone on ileal preparations*. Therefore, the effects of RLX on distal ileum of female mice, in the absence or presence of the two signalling pathway inhibitors, were tested on: i) the mechanical activity; ii) the biophysical properties of ileal SMCs, particularly on the RMP and on voltage-dependent and independent Ca^{2+} and K^+ currents.

Effects of ADPN on gastric smooth muscle

As stated above, hormones such as some adipokines, act at the level of the CNS to regulate food intake and can affect GI motility. Since at present no data are available in the literature about the physiological effects of ADPN on gastric motility, this further part of the research aims *to investigate if ADPN influences the gastric smooth muscle activity.* Therefore, we evaluated on the gastric fundus of female mice: i) the expression of ADPN receptors (in collaboration with IDC, Helmholtz Zentrum of Munchen,

Germany); ii) the mechanical effects of ADPN ; iii) the influence of the hormone on the SMC membrane passive properties and on voltage-dependent and independent Ca^{2+} and K^+ currents.

Chapter 2

Materials and methods

Ethics statement

The experimental protocols that included animals were performed according the European Community guidelines for animal care (DL 116/92, application of the European Communities Council Directive of 24 November 1986; 86/609/EEC) and approved by the Committee for Animal Care and Experimental Use of the University of Florence. The ethical policy of the University of Florence conforms to the *Guide for the Care and Use of Laboratory Animals* of the US National Institutes of Health (NIH publication no. 85-23, revised 1996; University of Florence assurance no. A5278-01). The protocols were communicated to local authorities and to Italian Ministry of the Health, according to the Italian law (Art.7/D.lgs 116/92).

Animals Treatments

Adult albino female mice, CD1 strain (Envigo, Udine, Italy), weighing 25 ± 1.5 g were used. The animals had free access to food and water and were housed on a 12 h–12 h light–dark cycle at 22°C room temperature (RT). The experiments were designed to minimize pain and the number of animals used. Mice were killed by prompt cervical dislocation. For the studies conducted to identify the role of RLX on ileum and colon, only mice in proestrous or estrous (i.e., the estrogen- dominated phases of the ovarian cycle), entered the experiments. This choice was made because estrogen is known to

favour RLX responsiveness of several target organs and tissues (*Mercado-Simmen et al., 1980*). After 1 week of acclimatization, the mice underwent assessment of the phase of the estrous cycle by light microscopic examination of vaginal smears stained with Papanicolaou, according to the method of Austin and Rowlands (*1969*).

Mechanical experiments

After the cervical dislocation of the mouse, the abdomen was opened and the portion of the GI tract (stomach, ileum or colon) was rapidly removed and cleaned with Krebs-Henseleit solution, with the following composition (in mM): 118 NaCl, 4.7 KCl, 1.2 $MgSO_4$, 1.2 KH_2PO_4, 25 $NaHCO_3$, 2.5 $CaCl_2$, and 10 glucose (pH 7.4). Full-thickness gastric strips (2 × 10 mm) were cut from the fundus region in the direction of the longitudinal muscle layer. Full-thickness segments from the distal ileum and longitudinal preparations from the proximal colon were also dissected. One end of each preparation was tied to a platinum rod while the other was connected to a force displacement transducer (Grass model FT03) by a silk thread for continuous recording of isometric tension. The transducer was coupled to polygraph systems (Grass model 7K). Muscle preparations were mounted in 5-ml double-jacketed organ baths containing Krebs-Henseleit solution, gassed with 95% O_2-5% CO_2 mixture. Prewarmed water (37°C) was circulated through the outer jacket of the tissue bath via a constant-temperature circulator pump. The temperature of the Krebs-Henseleit solution in the organ bath was maintained constant within ±0.5°C. Preparations were allowed to equilibrate for 1 h under an initial load of 0.8 g, 1.5 g or 0.5 g for gastric fundus, ileum and colon, respectively. During this period, repeated and prolonged washes of the preparations with Krebs-Henseleit solution were done to avoid accumulation of metabolites in the organ baths.

Electrophysiological experiments

For electrophysiological recordings, as in mechanical experiments, the abdomen of the animal was opened and the portion of GI tract was rapidly removed and cleaned with Krebs-Henseleit solution. Then a full-thickness strip was cut and pinned to a Sylgard (Dow Corning, Midland, MI, USA)-coated dissecting Petri dish filled with Krebs-Henseleit solution. First, we pinned the mucosal side up to dissect carefully the mucosa and submucosa away under a dissecting microscope. The residual tissue was re-pinned serosal side up and the connective tissue was removed in order to expose the smooth muscle layer. The obtained tissue was finally pinned, serosal side up, in the recording chamber with a Sylgard floor. During the experiments, the tissue was continuously superfused (Pump 33, Harvard Apparatus) at a rate of 1.8 ml min^{-1} with a Krebs-Henseleit solution. Intracellular recording was made by a conventional high resistance glass microelectrode (*Squecco et al., 2011*) inserted in a cell of the longitudinal smooth muscle layer. Microelectrodes were obtained by using a micropipette vertical puller (Narishige PC-10) from borosilicate glass (GC 100-7.5; Clark) and were filled with the following solution (mM): 150 CsBr, 5 $MgCl_2$, 10 Ethylene-bis(oxyethylenenitrilo)tetraacetic acid (EGTA), 10 (4-(2-hydroxyethyl)-1-piperazineethanesulfonic acid) (HEPES). Once filled, the pipette resistance measured 60-70 MΩ. The pH was set to 7.4 with NaOH and to 7.2 with tetraethylammonium hydroxide (TEA-OH) for bath and pipette solution, respectively. For RMP recording in current-clamp experiments we used the Krebs-Henseleit as control bath solution. For delayed rectifier K^+ current records we used a modified Krebs-Henseleit solution with different specific channels blockers added: $BaCl_2$ to block the inward rectifier K^+ current, I_{Kir}, nifedipine to block L-type Ca^{2+} current, Tetrodotoxin (TTX) to block Na^+ current, 4-aminopyridine (4-AP) to block transient outward K^+ current (I_{to}). The type of

voltage-dependent delayed rectifier current involved in the total outward K^+ records was evaluated by pharmacological dissection (*Baglioni et al., 2012*). Accordingly, three types of delayed rectifier currents, $I_{BK,}$ I_{Ks} and I_{Kv} were identified by the following specific blockers: iberiotoxin (IbTx), chromanol (Chr) and α-dendrotoxin (α-DTX), respectively.

To record only Ca^{2+} currents we used a Na^+- and K^+-free high-TEA solution with the following composition (mM): 10 $CaCl_2$, 145 TEABr and 10 HEPES. Nifedipine was used to selectively block $I_{Ca,L}$.

In some experiments, Glybenclamide (Glbn) and gadolinium chloride ($GdCl_3$) were employed to block the voltage-independent ATP-sensitive K^+ channels (K_{ATP}) and the non-selective cation channels (NSCC), respectively. ODQ was used to block guanylate cyclase and KT5823 to inhibit the cGMP-dependent protein kinase (PKG) (*Wang et al., 2009*). Moreover, 9-cyclopentyladenine mesylate (9-CP-Ade**)** was used as an adenylate cyclase inhibitor.

Any current amplitude was normalized to cell linear capacitance C_m (in pA/pF) to consent the evaluation of test current recorded from cells of different size; in fact, C_m is usually considered an index of cell-surface area presuming that membrane-specific capacitance has a constant value of 1 µF/cm^2.

Pulse protocols of stimulation

By using the current clamp mode of our amplifier, with a stimulus waveform: I = 0 pA, we recorded the RMP of the SMCs before and after drug stimulation.

By the voltage clamp mode of our amplifier, the membrane passive properties ($R_{m,}$ G_m and C_m) were consistently estimated by applying two step voltage pulses 75 ms long to -80 and -60 mV starting from a holding potential (HP) of -70 mV.

Always in this mode, ionic currents were evoked by the following pulse protocols: Ca^{2+} current (I_{Ca}) activation was evoked in the SMCs held at -80 mV, and 1-s long step pulses were applied in 10-mV increments from -70 to 50 mV; an interval of 20 s between episodes was given to allow recovery. I_{Ca} inactivation was investigated by a two-pulse protocol with a 1-s pre-pulse to different voltages followed by 1-s test pulse to 10 mV (*Squecco et al., 2011*). When we applied the two-pulse protocol, we used again a 20-s interval between stimulating episodes to consent to recovery. Outward K^+ current activation was elicited by 1-s long voltage step pulses ranging from -80 to 50 mV applied in 10-mV increments from HP= -60 mV. Capacitive, linear leak and voltage-independent ionic currents were cancelled on-line using the P/4 procedure. Among these latter currents we include those flowing through intermediate and slow Ca^{2+}-dependent K^+ channels (IK and SK) as well as non-selective cation channels, NSCC.

To evaluate the steady-state ionic current activation of voltage dependent channels we used the following equation

$$Ia(V) = Gmax\,(V - Vrev)/\{1 + exp[(Va - V)/ka]\} \quad (1)$$

and the following was used for the steady-state current inactivation:

$$Ih(V) = I/\{1 + exp[-(Vh - V)/kh]\}, \quad (2)$$

where Gmax represents the maximal conductance for Ia; Vrev is the apparent reversal potential; Va and Vh are the voltages causing the half-maximal activation and inactivation, respectively; ka and kh are steepness factors of activation and inactivation, respectively.

Immunohistochemistry

To identify RXFP1-expressing cells in the colonic tissue, full-thickness samples of the proximal colon were taken and immediately fixed in 4% paraformaldehyde. Transverse

sections, 7 µm thick, were cut and then incubated with rabbit polyclonal anti-RXFP1 (1:5000, 4°C, overnight; Immundiagnostik). Immune reaction was revealed by biotinylated anti-rabbit secondary antibody (1:600 for 1h at room temperature; Dako, Glostrup, Denmark) and avidin-peroxidase complex (Dako) by using 3-3′diaminobenzidine as chromogen and hematoxylin for nuclear counterstaining. Negative controls were carried out by omitting the primary antiserum.

Western Blot analysis

To evaluate RLX receptor (RXFP1 protein) expression in colonic tissue, full-thickness samples of the proximal colon were quickly minced and homogenized with a tissue homogenizer (Ing. Terzano,) in a cold lysis buffer (10 mM Tris/HCl, pH 7.4, 10 mM NaCl, 1.5 mM, MgCl2, 2 mM Na2 EDTA, 1% Triton X-100), added with 10X Sigmafast Protease Inhibitor cocktail tablets (Sigma-Aldrich, Milan, Italy). Upon centrifugation at 13.000 g for 20 min at 4°C the supernatants were collected and the total protein content was measured spectrophotometrically using micro-BCA™ Protein Assay Kit (Pierce, IL, USA). Sixty µg of total proteins were electrophoresed by SDS–PAGE and blotted onto nitrocellulose membranes (Amersham, Cologno Monzese, Italy). The membranes were blocked with PBS containing 0.1% Tween (Sigma-Aldrich) and 5% bovine serum albumin (Sigma-Aldrich) for 1h at room temperature and then incubated with rabbit polyclonal anti-RXFP1 (1:3000, over night at 4°C; Immundiagnostik, Bensheim Germany). Specific band was detected using rabbit peroxidase-labeled secondary antibody (1:15.000, 1h, room temperature; Vector, Burlingame, CA) and ECL chemiluminescent substrate (BioRad, Milan, Italy).

Polymerase chain reaction (PCR)

PCR for RLX receptors

To evaluate the presence of mRNA for the high-affinity RLX receptor RXFP1 in colonic tissue, full-thickness samples of the proximal colon were quickly minced and homogenized with a tissue homogenizer (Ing. Terzano, Milan, Italy) in TRIzol Reagent (Invitrogen, Groningen, NL) and total RNA was extracted according to the manufacturer instructions. One μg of total RNA was reverse transcribed and amplified with SuperScript One-Step *Reverse Transcription-PCR* (RT-PCR) System (Invitrogen): after cDNA synthesis for 30 min at 55°C, the samples were pre-denatured for 2 min at 94°C and then subjected to 38 cycles of PCR performed at 94°C for 15 s, alternating with 53°C for 30 s and 72°C for 1 min; the final extension step was performed at 72°C for 5 min. The following mouse gene-specific primers were used: RXFP1 (NM_ 212452.1), forward 5'- ACG AGC TGT CCC ATC AGT TT -3'and reverse 5'- ATG TGC TGA CAG AGG GGT TT -3'. PCR products were electrophoresed on a 2% agarose gel stained with ethidium bromide.

PCR for ADPN receptors

Mouse tissues were snap-frozen in liquid nitrogen and stored at −80 °C until use. Then, from frozen tissue sections, RNA was extracted using RNeasy Mini Kit (Qiagen, Hilden, Germany) following the manufacturer's instructions. Semiquantitative RT-PCR was performed for AdipoR1 and AdipoR2 receptors and the following primers were used:

AdipoR1 forward 5'- CAG AGA AGC TGA CAC AGT GGA G -3' and reverse 5'- GTC CCT CCC AGA CCT TAT ACA C -3';

AdipoR2 forward 5'- GGA CTC CAG AGC CAG ATA TAC G -3' and reverse 5'- ACT CTT CCA TTC GTT CCA TAG C -3'

The following mixtures were prepared in thin walled 0.2 ml tubes and analysed by Biometra PCR cycler (Table 3):

Table 3. ***PCR components***

Reagents	**Volume**
forward primer (10 pmol/µl)	1 µl
reverse primer (10 pmol/µl)	1 µl
GOTaq colorless Master Mix sample (Promega^{R})	12.5 µl
H2O	9.5 µl
cDNA template	1 µl

PCRs were run with the following program (table 4):

Table 4. ***PCR Setup***

Step	**Temperature [°C]**	**Time**	**Note**
1	94	3 min	-
2	94	20 sec	-
3	64	30 sec ***	***-0.5C per cycle
4	72	35 sec	Repeat steps 2-4 for 12 cycles
5	94	20 sec	-
6	58	30 sec	-
7	72	35 sec	Repeat steps 5-7 for 25 cycles
8	72	2 min	-
9	4		Hold

Agarose gel electrophoresis

The PCR amplicons were analysed by agarose gel electrophoresis. For this purpose, the samples were mixed with 6x loading dye loaded onto a 1% agarose gel containing

0.001% ethidium bromide. Samples were separated in 1x TBE alongside a DNA standard [100bp Marker (NEB)] at 120 V (for about 40 min).

A negative control without cDNA template, as well as a positive control containing cDNA of inguinal fat pad were analysed in parallel. DNA bands were made visible under UV light

Data analysis and statistical tests

For functional experiments, amplitude of contractile activity is expressed as absolute values (grams) and measured when the maximal effect was reached. The values of the treated preparations were expressed as percentage changes of the basal (control) values or as grams. Basal tension was evaluated as changes in the recording baseline.

Statistical analysis was performed by Student's *t*-test (Prism 3.0; GraphPad Software, San Diego, CA) to compare two experimental groups or one-way ANOVA followed by Newman-Keuls posttest when more than two groups were compared. For electrophysiological experiments, mathematical and statistical analysis of data was performed by pClamp9 (Axon Instruments).

The number of muscle preparations/cells was designated by *n.* Results are expressed as mean ± SEM and $P \leq 0.05$ was considered significant (confidence limits used are the 95%) unless otherwise specified.

Drugs

The following drugs were used:

α-dendrotoxin (α-DTX, 10 nM); 1H-[1,2,4]oxadiazolo[4,3-*a*]-quinoxalin-1-one (ODQ, 1 µM); 9-cyclopentyladenine mesylate (9-CP-Ade, 100 µM**)**; 4-aminopyridine (4-AP, 2mM); barium chloride ($BaCl_2$, 0.4 mM); chromanol (Chr, 50 µM); gadolinium chloride

($GdCl_3$, 50 μM); glybenclamide (Glbn, 10 μM); iberiotoxin (IbTx, 100 nM); KT5823 (20 nM); mouse recombinant adiponectin (ADPN, 20nM); nifedipine (10 μM); porcine relaxin (RLX, 50 nM); tetrodotoxin (TTX, 1 μM)

In our experiments, we used porcine relaxin (RLX), since it has been reported that porcine relaxin activates both RXFP1 and RXFP2 with similar potency and efficacy as Human relaxin 2 (RLX) (*Hsu et al., 2002; Sudo et al., 2003*).

We employed mouse recombinant adiponectin (ADPN), as it has been shown that mouse ADPN shares about 83% amino acid identity with that of human (*Wong et al., 2004*).

All drugs were obtained from *Sigma Chemical* (St. Louis, MO), except for highly purified porcine RLX (2,500–3,000 U/mg) that was generously provided by *Dr. O. D. Sherwood* (University of Illinois, Urbana, IL). Solutions were prepared on the day of the experiment, except for TTX, for which a stock solution was kept stored at −20°C. Drug concentrations are given as final bath concentrations and are in the range of those previously shown to be effective in *in vitro* preparations (*Bani et al., 2002; Baccari et al., 2007; Baccari et al., 2012; Kentish et al., 2015*).

Chapter 3

Results

3.1 Relaxin effects on colonic smooth muscle

Mechanical experiments

RLX exerts two opposite effects on the mechanical activity

Longitudinal colonic preparations (n= 22 preparations, 11 mice) as previously observed by Baccari and co-workers (*2012*) in the circular ones, exhibited spontaneous contractile activity consisting of rhythmic changes in isometric tension (mean amplitude 0.5±0.04 g). Addition of RLX (50 nM) to the bath medium, induced (*n* = 12 preparations; 6 animals) two opposite effects: a decay of the basal tension (mean amplitude 0.42±0.05 g), that persisted for the whole period of exposure (up to 1 h, longer time not observed), coupled to a long-lasting increase in amplitude of the spontaneous contractions (mean amplitude 1.7±0.2 g; $P<0.05$) (Fig. 9). In the presence of the guanylate cyclase inhibitor ODQ (1 μM), RLX was no more able to influence either the basal tension or the amplitude of the spontaneous contractions (Fig. 9) suggesting the involvement of cGMP signalling pathway (*n* = 10 preparations; 5 animals). .

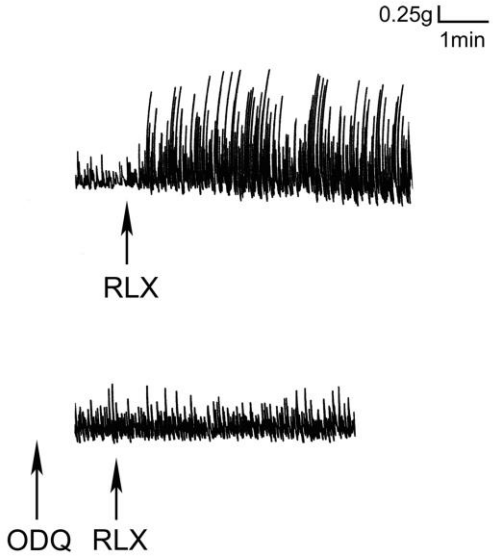

Figure 9. ***Involvement of cGMP signalling pathway in the effects of RLX on the spontaneous mechanical activity of the mouse colon.***
Upper trace: typical tracing showing the effects of RLX (50 nM) on the spontaneous mechanical activity of the mouse colonic longitudinal preparation. RLX causes a progressive decay of the basal tension coupled to an increase of the spontaneous contractions. Lower trace: RLX (50 nM) in the presence of ODQ (1 μM) has no longer effects on either basal tension or spontaneous contractions.

Electrophysiological experiments

Spontaneous electrical activity of the SMCs

In order to better clarify the effects of RLX on colonic smooth muscle mechanical activity, we first focused on the membrane properties of SMCs by making experiments in current-clamp conditions. The RMP measured in a SMC from the longitudinal layer of colonic strips did not show a steady value owing to the occurrence of spontaneous rapid rhythmic waves of membrane potential (Figs. 10 and 12, panels a, control, Ctr). These waves were asynchronous, without a regular shape or a dominant rhythmicity. Therefore, the RMP was considered that at the maximal hyperpolarization value of the

waves and was -40±3 mV (range from -15 to -60 mV). The amplitude of these asynchronous waves evaluated from the maximal hyperpolarized value to the maximal depolarized value was 15±3 mV. Data from Ctr n= 96 cells (45 strips; 26 mice).

The effects of RLX on RMP are abolished by ODQ

As shown in figure 10 on panels Ab and Bb, the addition of RLX induced immediately a slight hyperpolarisation, occurring right after 40-60 sec, followed by cycles of slow hyperpolarization/depolarization oscillations, superimposed on a hyperpolarisation trend. In fact, the maximal hyperpolarization reached after 4-6 min was -48 ± 7 mV and -58 ± 8 mV after 15-20 min (n = 24 cells; 10 strips; 5 mice) (Fig. 10 AB).

ODQ itself did not significantly affect the RMP, determining only a not significant hyperpolarization (1-3 mV). Furthermore, RLX, added at least 15 min after ODQ, was no more able to affect the RMP (Fig. 10 C). In agreement, RMP values were: -44±2 mV in control (Ctr), -46±7 mV in the presence of ODQ and -46±8 mV after adding RLX; the amplitudes of the asynchronous waves were 15±2, 16±2 and 16±3 mV, respectively. All data were not statistically different in respect to the relative Ctr (*n* = 22 cells, 10 strips, 6 mice).

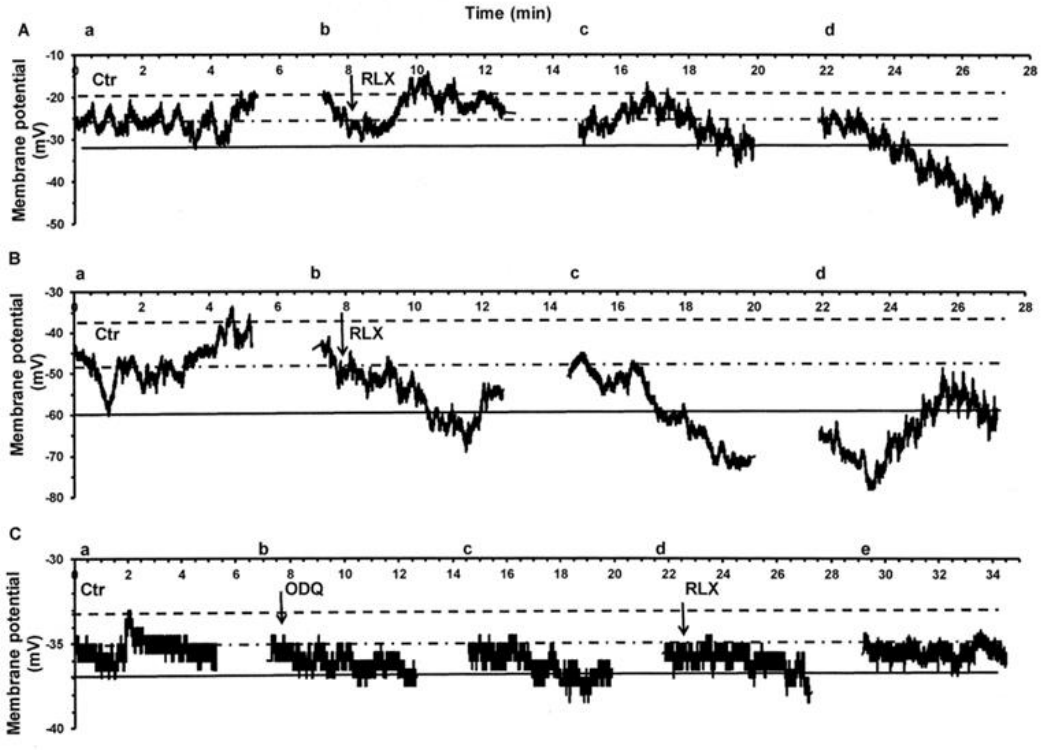

Figure 10. ***Effects of RLX on membrane potential recorded from colonic SMC.***
Typical tracings of membrane potential from a single colonic SMC. A-C) Asynchronous and irregular waves of RMP recorded in basal condition (panels a; control, Ctr). A,B) 50 nM RLX (arrow) induces a slow hyperpolarisation that occurred early, right after 40-60 sec (see panels b) and lasted 2-4 min, from its application. Such a hyperpolarization is followed by a series of slow depolarization/hyperpolarisation oscillations (peak to peak time of about 5-7 min) superimposed on a hyperpolarization trend as shown in panels Ab,c,d and Bb,c,d (the maximal depolarization and hyperpolarization value were shifted towards more negative values). C) 1µM ODQ (arrow) induces only a slight hyperpolarization of resting membrane potential (b and c) with respect to Ctr (a), whereas adding RLX does not further affect membrane potential (d and e). In all the panels, horizontal straight lines are referred to Ctr tracings. Particularly, the continuous lines indicate the maximal hyperpolarization values (considered as the resting membrane potential), point-dash lines represent the mean values of the spontaneous waves and the dashed lines the maximal peak values of depolarization.

RLX decreases the voltage-dependent Ca^{2+} current

To better understand the origin of the increase in amplitude of the spontaneous contractions elicited by RLX we decided to evaluated its effects on the inward voltage-dependent Ca^{2+} currents through L-type channels (I_{Ca}), by performing experiments in voltage-clamp condition and by using the high-TEA solution.

In this set of experiments, no T-type Ca^{2+} current were recorded. In Fig. 11A we shown a typical example of the time course of current traces, $I_{Ca,}$ recorded from a SMC in control condition (Aa) and after adding RLX (Ab). Since, this current was high voltage activated, having a voltage threshold at about -30 mV, with a slow activation and inactivation phases and was blocked by nifedipine, it was assumed to be an L-type Ca^{2+} current.

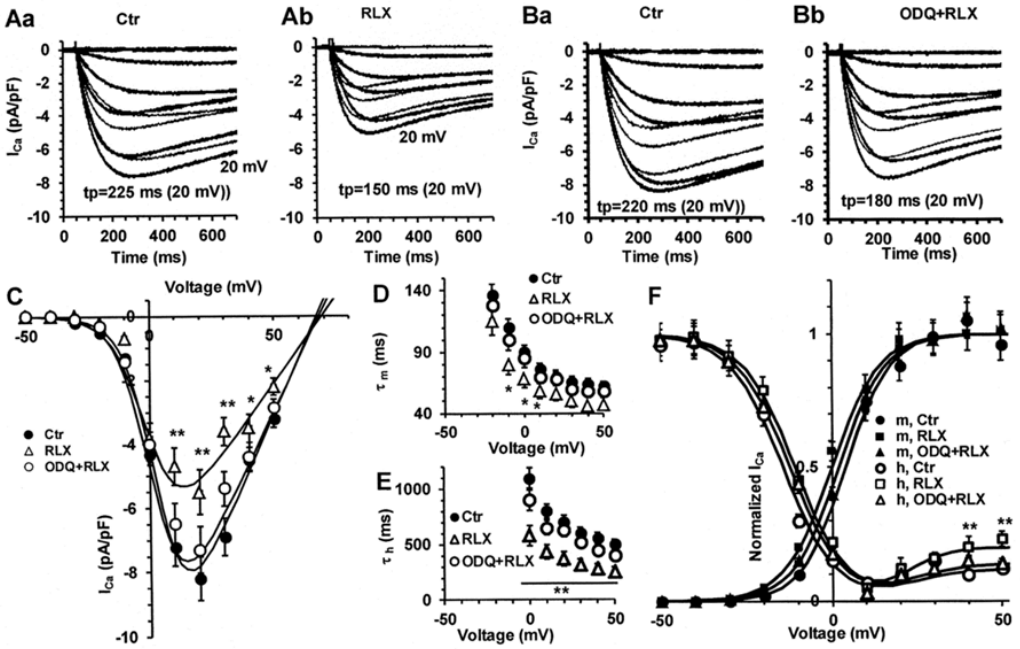

Figure 11. ***RLX treatment affects inward L-type Ca^{2+} currents.***
A) Typical L-type Ca^{2+} currents (I_{Ca}) recorded in high TEA-Ca^{2+} solution in control (Aa) and after 50 nM RLX treatment (Ab); (Ba) I_{Ca} records from a different control cell of another colonic strip and after 1µM ODQ plus 50 nM RLX treatment (Bb). RLX is added 15 minutes after ODQ. A,B) only the first 700 ms of the pulse are depicted. C) *I-V* plots of L-type Ca^{2+} currents (I_{Ca}) for Ctr, RLX and ODQ+RLX treated tissue from experiments as in panels A and B, respectively. Single Boltzmann fits are superimposed to experimental data. D,E) voltage dependence of the time constant of I_{Ca} activation (D) and inactivation (E). F) Related steady-state activation (m, filled symbols) and inactivation curves (h, open symbols) in control (Ctr, circles), RLX (squares) and ODQ+RLX (triangles). RLX (50 nM) in the presence of ODQ (1µM) has no longer significant effects. Best fit to the data is obtained by the sum of two Boltzmann terms. Boltzmann parameters, statistical analysis are listed in Table 5. Current values were normalized to cell capacitance. All data are mean values ± SEM. Data from RLX: n = 27 cells (12 strips; 6 mice), from ODQ+RLX: n = 22 cells (10 strips; 5 mice) and from Ctr n= 49 cells (20 strips; 11 mice) that is the sum of the two sets of experiments. * $P < 0.05$, ** $P < 0.01$ RLX *vs* related Ctr; ODQ+RLX all values are not significantly different in respect to Ctr ($P > 0.05$).

It can be clearly seen (Fig. 11 Aa, Ab) that RLX reduced the maximal peak current size at 20 mV step and the time to peak value (225 msec on control condition vs 150 msec after RLX treatment).

Fig. 11B shows a typical current recorded from another cell in control condition (Ba) and pre-treated with ODQ 15 min before RLX addition (Bb). In the presence of ODQ, RLX no longer changed the voltage that induced the maximal current amplitude (20 mV- pulse): it was no more able to reduce to a lesser degree either the peak current amplitude or the time to peak value in respect to (Ab) (180 msec *vs* 220 msec). Then, to better evaluate the general behaviour of the phenomenon, we calculated the *I-V* relationship related to all the experiments done, reporting the normalized mean I_{Ca} maximal amplitude for any voltage step applied (Fig. 11C). The analysis of the *I-V* plot confirmed that RLX decreases the current amplitude and that ODQ pre-treatment abolished the effect of RLX.

RLX treatment significantly altered the voltage dependence of the current activation time constant, $\tau_{m,}$ (Fig. 11D) as well as that of inactivation, τ_h (Fig. 11E) and again, ODQ pre-treatment abolished the effects of RLX.

The effect of RLX on the voltage-dependent L- type Ca^{2+} current was analysed by the steady-state activation and inactivation curves (Fig. 11F). Inactivation curve was U-shaped and the best fit to the data was obtained by the sum of two Boltzmann terms. All the Boltzmann parameters and statistical analysis are listed in Table 5.

Table 5. ***Boltzmann parameters of $I_{Ca,L}$ activation and inactivation in longitudinal SMC in control (Ctr), in the presence of RLX alone (RLX) or with ODQ pre-treatment (ODQ+RLX)***

Parameters	**Ctr**	**RLX**	**ODQ+RLX**
$I_{Ca,L,max}/C_m$ (pA/pF)	7.9 ± 0.5	5.3 ± 0.3**	7.7 ± 0.7§§
G_m/C_m (pS/pF)	178.7 ± 11	110.3 ± 18***	169.7 ± 14§§
V_p (mV)	15.2 ± 2	10.9 ± 2*	15.1 ± 2§
V_a (mV)	4.1 ± 1	0.2 ± 0.3***	2.1 ± 1§§
k_a (mV)	6.5 ± 0.4	7.3 ± 0.5*	6.3 ± 0.4§
V_{rev} (mV)	67.2 ± 4	68.5 ± 4	67.1 ± 4
V_h (mV)	-14.4 ± 3	-10.9 ± 3	-13.2 ± 3
k_h (mV)	7.6 ± 0.4	7.5 ± 0.5	7.4 ± 0.5
V_h(+) (mV)	22.2 ± 2	21.8 ± 2	23.0 ± 2
k_h(+) (mV)	8.3 ± 2	4.2 ± 2*	7.9 ± 3

RLX decreases the normalized maximum peak size of the specific $I_{Ca,L}$, $I_{Ca,L,max}/C_m$, and the related G_m/C_m; moreover it shifts the voltage values eliciting the maximal current in the *I-V* plots (V_p) and affect the $I_{Ca,L}$ kinetics changing the V_a and k_a Boltzmann parameters of activation. In the U shaped inactivation curve, the Boltzmann parameters for the curve at more negative potential was indicated as V_h and k_h and those for more positive as V_h(+) and k_h (+). The only altered Boltzmann parameters are k_h(+).Cells of ODQ+RLX group were slightly affected but were not statistically different from Ctr. Data from: RLX n = 27 cells (12 strips, 6 mice); ODQ+RLX n = 22 cells (10 strips, 5 mice) and Ctr n= 49 cells (20 strips, 11 mice) that is the sum of the two sets of experiments. * P < 0.05, ** P < 0.01 and *** P < 0.005 RLX respect to the related Ctr; § P < 0.05 and §§ P < 0.01 values from ODQ+RLX respect to RLX.

The effects of RLX involve voltage-independent NSCCs

Also the voltage-independent ionic channels, such as NSCC, may have a significant role in regulating the RMP and thus the contraction (*Dwyer et al., 2011*). Therefore, also this group of channels was taken into account to justify the increased contractility caused by RLX. We observed that in control solution the NSCC blocker $GdCl_3$, determined "per se" a slight (about 3 mV) but significant hyperpolarization of the RMP

(n = 14 cells; 7 strips; 5 mice) (Fig. 12, panels b and c). RLX, in the presence of $GdCl_3$ was no more able to induce any of its effects on RMP (Fig. 12, panels d,e) suggesting the involvement of NSCC in its mechanism of action. In fact, RMP values were: -26±2mV in the Ctr, -31±2mV in the presence of $GdCl_3$ ($P<0.05$ vs Ctr) and -26±4 mV after RLX ($P>0.05$ vs Ctr and $GdCl_3$); the amplitude of the asynchronous waves was not significantly different among them (15±2, 16±2 and 16±2 mV).

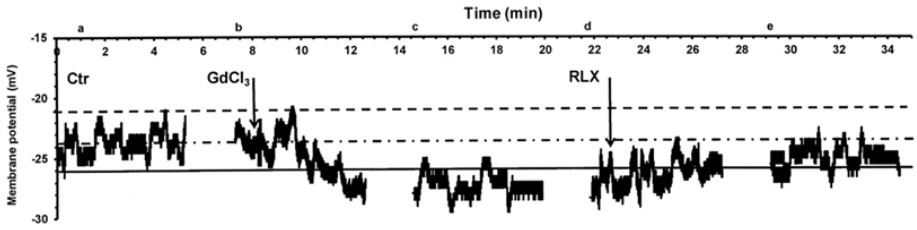

Figure 12. ***Effect of RLX on membrane potential in SMC pre-treated with Gadolinium chloride ($GdCl_3$).***
Typical records from a single impaled cell of smooth muscle tissue strips. Column a represent the Ctr trace. NSCC blocker $GdCl_3$ (50 µM, panels b and c) induces a slow hyperpolarization; adding RLX (50 nM) in the presence of $GdCl_3$ (panels d and e), other than reducing such hyperpolarization, no longer induces any of its effects. Horizontal straight lines are as in Fig. 10.

RLX affects the voltage-dependent outward K^+ currents

In order to comprehend how RLX could affect RMP and excitability, we successively investigated its effect on the main voltage-dependent delayed rectifier K^+ currents ($I_{K,DR}$) known to be expressed on SMC of the colon (*Koh et al., 2012*). Typical outward K^+ current traces were evoked by proper voltage pulse stimulation protocol (see methods section) and elicited in the modified bath control solution containing nifedipine to avoid the occurrence of inward Ca^{2+} currents. The different types of voltage-dependent K^+ channels, involved in the total K^+ current recorded, were

separated by pharmacological tools according to previous literature (*Koh et al., 2012*). We distinguished the large conductance Ca^{2+} activated K^+ current that was IbTx-sensitive, namely BK current (I_{BK}), the slowly activating Chr-sensitive I_{Ks}, and the fast activating α-DTX-sensitive I_{Kv} (Figs. 13 and 14).

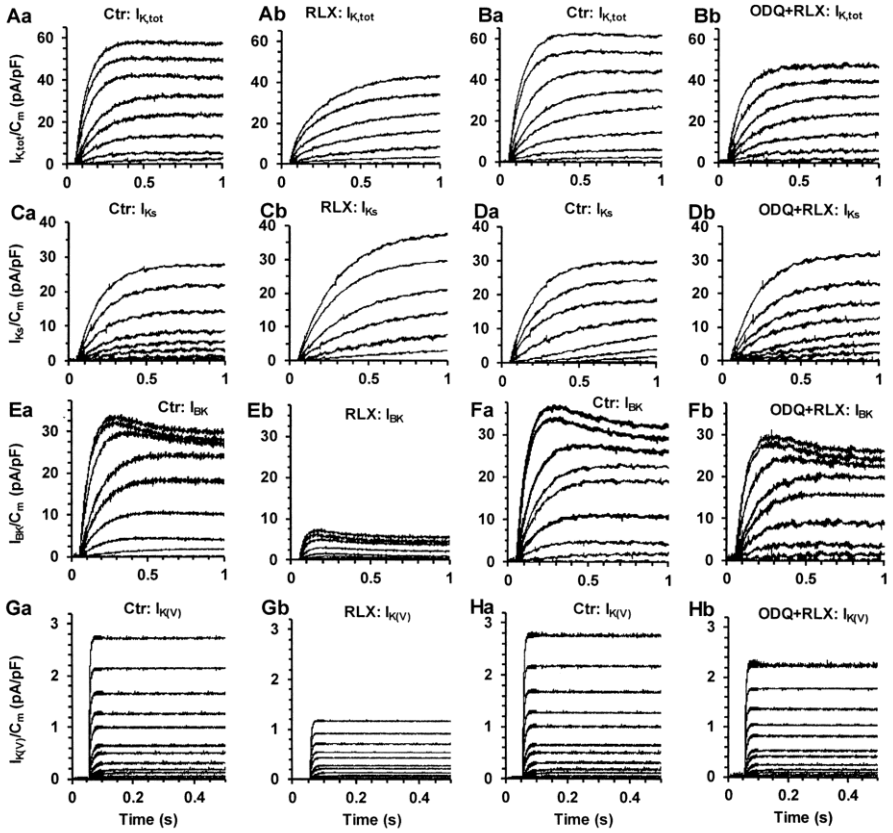

Figure 13. ***Effect of RLX on outward delayed rectifier K^+ currents.***
Outward K^+ currents, elicited by voltage steps from -80 to 50 mV (HP= -60 mV) in control solution containing nifedipine (10 μM). A) Representative total outward K^+ currents ($I_{K,tot}$) recorded in a Ctr cell (a) and in the presence of 50 nM RLX (b). B) Same current traces recorded from another Ctr cell (a) from a different colonic strip and with RLX added in the presence of 1μM ODQ (b). By pharmacological dissection $I_{K,tot}$ could be systematically distinguished into three kinds of K^+ currents: I_{Ks} (C,D), I_{BK} (E,F) and I_{Kv} (G,H); examples from a cell in control solution are reported in Ca, Ea and Ga, whereas Cb, Eb and Gb, report the different components under RLX treatment. Same current traces recorded from a different Ctr cell from another colonic strip (Da, Fa and Ha) and with RLX added in the presence of ODQ (Db, Fb and Hb). Current values are normalized to cell capacitance.

The voltage threshold of activation for the different type of currents was -41±5, -31±4 and -19±4 mV for I_{Kv}, I_{BK} and I_{Ks}, respectively (Fig. 14).

Note that I_{Kv} that has the lowest threshold of activation was also the smallest in amplitude. We could clearly observe that RLX treatment caused a decrease of the total outward K^+ current (Figs. 13Ab and 14A) and that such a decrease was mostly due to the greater reduction of I_{BK} and I_{Kv} amplitudes (Figs. 13Eb, Gb and 14Ca, Da). The reduced activation of the low threshold I_{Kv} and I_{BK} may contribute to a minor membrane hyperpolarization. Notably, the activation time constant of I_{Ks} was increased whereas that of I_{BK} was reduced (Fig. 14Bb and Cb, respectively).

Therefore, we conclude that RLX treatment mainly affect the K^+ currents with a more negative voltage threshold and a higher opening probability next to resting membrane potential. In contrast, the high threshold I_{Ks} is slightly increased by RLX (Figs. 13Cb and 14Ba), thus leading to hyperpolarization when the membrane reaches depolarized values next to the voltage threshold for its activation.

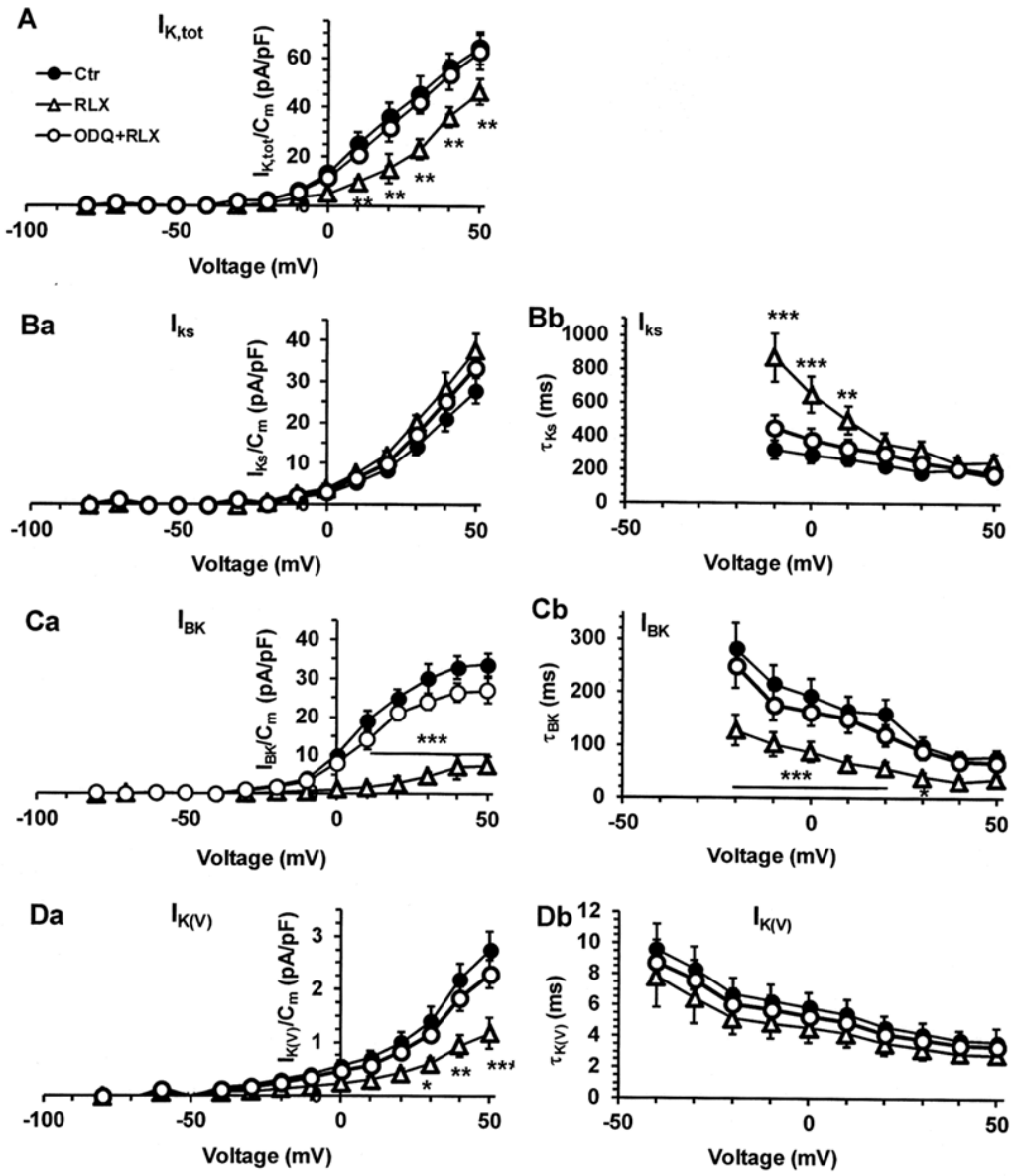

Figure 14. ***RLX inhibits I_{BK} and I_{Kv} and such effect is reverted by ODQ.***
A) I-V plot related to the total delayed rectifier K^+ current ($I_{K,tot}$). Ba-Da) *I-V* curves related to the pharmacologically dissected components I_{Ks} (B), I_{BK} (C) and I_{Kv} (D). Bb-Db) *I-V* activation curves related to all the experiments done. Current values were normalized to cell capacitance. * $P < 0.05$, ** $P < 0.01$ and *** $P < 0.005$ RLX vs related Ctr; ODQ+RLX all values are not significantly different from Ctr. RLX: $n = 20$ cells (10 strips; 5 mice), ODQ+RLX: $n = 16$ cells (8 strips; 5 mice); Ctr $n = 36$ cells (18 strips; 10 mice) that is the sum of the two sets of experiments.

Once again we tested the effect of RLX on K^+ currents after ODQ pre-treatment (Fig. 13, panels Bb, Db, Fb, Hb). As for Ca^{2+} current, also the K^+ current traces (Fig. 13 right panels), the *I-V* plot values and the voltage-dependence of the time constants (Fig. 14B-

D) were not statistically different to those detected in control conditions, suggesting that the blockade of guanylate cyclase prevents RLX effects also on these ion channels.

The effects of RLX involve voltage-independent ATP-sensitive K^+ channels

Since Kv and BK channels were strongly inhibited by RLX, the capability of cell membranes to hyperpolarize through the activation of these channels was reduced. In this regard, another good candidate that affect cell hyperpolarization could be the voltage-independent ATP-sensitive K^+ channel, K_{ATP}, that is well related to the muscle contractile activity (*Currò, 2014*) and is functionally expressed in gut muscle. To evaluate the involvement of these channels, we added to the control solution the typical blocker of K_{ATP} sensitive channels, glybenclamide (Glbn), and we tested the effect of RLX on RMP by current clamp experiments (Fig. 15). The use of this specific blocker, as expected, induced a slow transient depolarization of RMP (7 ± 2 mV) with rapid synchronized rhythmic waves superimposed (n = 16 cells; 9 strips; 5 mice).

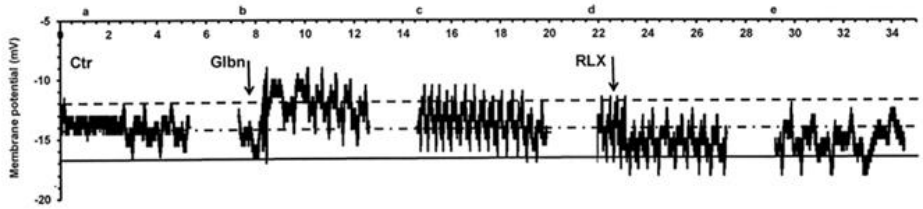

Figure 15. ***Effect of RLX on membrane potential in SMC pretreated with glybenclamide (Glbn).***
Typical records from a single impaled cell of smooth muscle tissue strip. Column a represents the Ctr trace. K_{ATP} channels blocker, Glbn, induces a transient depolarization of resting membrane potential with rapid synchronised rhythmic waves superimposed (b and c). RLX (50 nM) in the presence of 10 µM Glbn, reduces the rapid synchronised rhythmic waves and induces a slight hyperpolarization (d and e) with respect to control SMC (a, Ctr), but it is no more able to generate either the slow oscillations or the rapid rhythmic waves. Horizontal straight lines are as in Fig. 10.

RLX, in the presence of Glbn, was no more able to induce the slow oscillations or the rapid rhythmic waves of the membrane potential, suggesting an important involvement of K_{ATP} channels in these effects. SMCs pretreated with Glbn were depolarized (-18±2 vs Ctr -25±4 mV; $p<0.05$) and the amplitude of the asynchronous waves was slightly increased (17±3 vs Ctr 10±2 mV; $p<0.05$). RLX added at least 15 min after Glbn, did not affect the RMP, being RMP at -27±4 mV and the amplitude of the asynchronous waves of 11±2 mV.

The effects of RLX involve PKG

In order to evaluate whether PKG was involved in RLX effects, a specific inhibitor of PKG, KT5823, was added to the control solution (*Wang et al., 2009*) and we tested the effect of RLX on RMP by current clamp experiments (Fig.16).

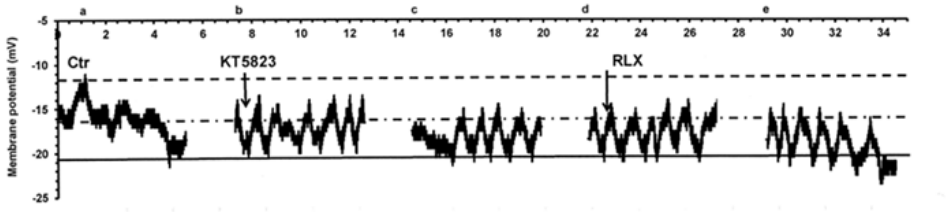

Figure 16. ***Effect of RLX on membrane potential in SMC pretreated with KT5823.***
Typical records from a single impaled cell of smooth muscle tissue strip. Column a represents the Ctr trace. KT5823 (20 mM), a specific inhibitor of PKG, slightly affects the cell spontaneous activity. RLX (50 nM) added 15 after KT5823 does not induce any evident further changes. Horizontal straight lines are as in Fig. 10.

SMCs pre-treated with KT5823 were slightly hyperpolarized, -27±4 mV (Ctr -25±3 mV) and the amplitude of the asynchronous waves was slightly increased, 14±2 mV (Ctr 12±2 mV), but there were no statistically significant differences compared to controls. RLX added about 15 min after KT5823, did not further affect the RMP, being

RMP at -26±4 mV and the amplitude of the asynchronous waves of 13±2 mV (*n* = 20 cells; 9 strips; 5 mice).

RXFP1 is expressed in colonic SMCs

In collaboration with the section of Anatomy and Histology (Department of Experimental and Clinical Medicine, University of Florence) RT-PCR and Western Blot were performed. In our colonic tissue (from 5 mice) we revealed RXFP1 mRNA and protein, respectively (Fig. 17 A,B). Immunohistochemical investigation showed that RXFP1 was expressed in colonic SMCs, especially by muscular wall and by the neurons of the myenteric plexus (Fig. 17C).

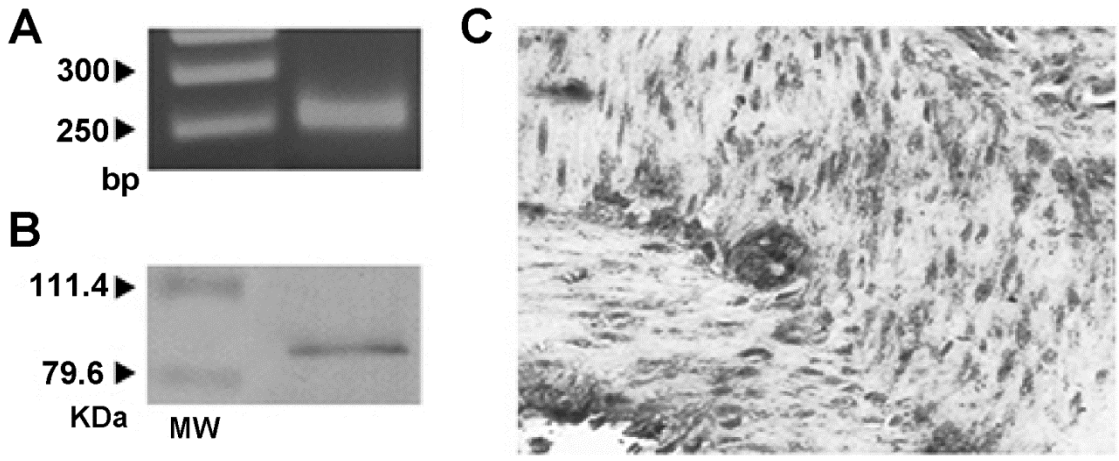

Figure 17. ***Expression of RLX receptor, RXFP1, by mouse proximal colon.***
RT-PCR (A), Western Blot (B) and Immunohistochemistry (C) revealed that mouse colon expressed RXFP1 receptor. In particular, RXFP1 is expressed by SMCs of muscular wall and by neurons of the myenteric plexus (C).

We have already published the above results (*Squecco et al., 2015*)

3.2 Relaxin effects on ileal smooth muscle

Mechanical experiments

RLX reduces the mechanical activity

In agreement with previous observations (*Bani et al., 2002*), ileal preparations (n = 20) showed, at basal tension, spontaneous and rhythmic phasic contractions (mean amplitude 0.59 ± 0.04 g) (Fig. 18), that were unaffected by the neural blocker TTX (1 µM), indicating their myogenic nature. Addition of RLX (50 nM) to the bath medium (n = 18) caused a TTX-insensitive clear-cut decay of muscle tension (62.3 ± 2.2%) and a reduction in amplitude (36.1 ± 1.8%) of the spontaneous contractions (Fig. 18). The action of the hormone on basal tension and on spontaneous activity was just evident 10 and 20 min, respectively, after its addition to the bath medium. The influence of RLX on ileal motility was long lasting, because they could still be present 1 h after addition of the peptide to the organ baths (longer time not observed).

The effects of 50 nM RLX (*n* = 12) on both spontaneous contractions and muscle tension were reduced by the guanylate cyclase (GC) inhibitor ODQ (1 µM) ($p<0.05$) and by the adenylate cyclase (AC) inhibitor 9-CP-Ade (100 µM) (Fig. 18) ($p<0.05$). RLX (50 nM) added to the bath medium in the presence of ODQ (1 µM) plus 9-CP-Ade (100 µM) had no longer effects (n=6) on both muscle tension and spontaneous contractions (Fig. 18).

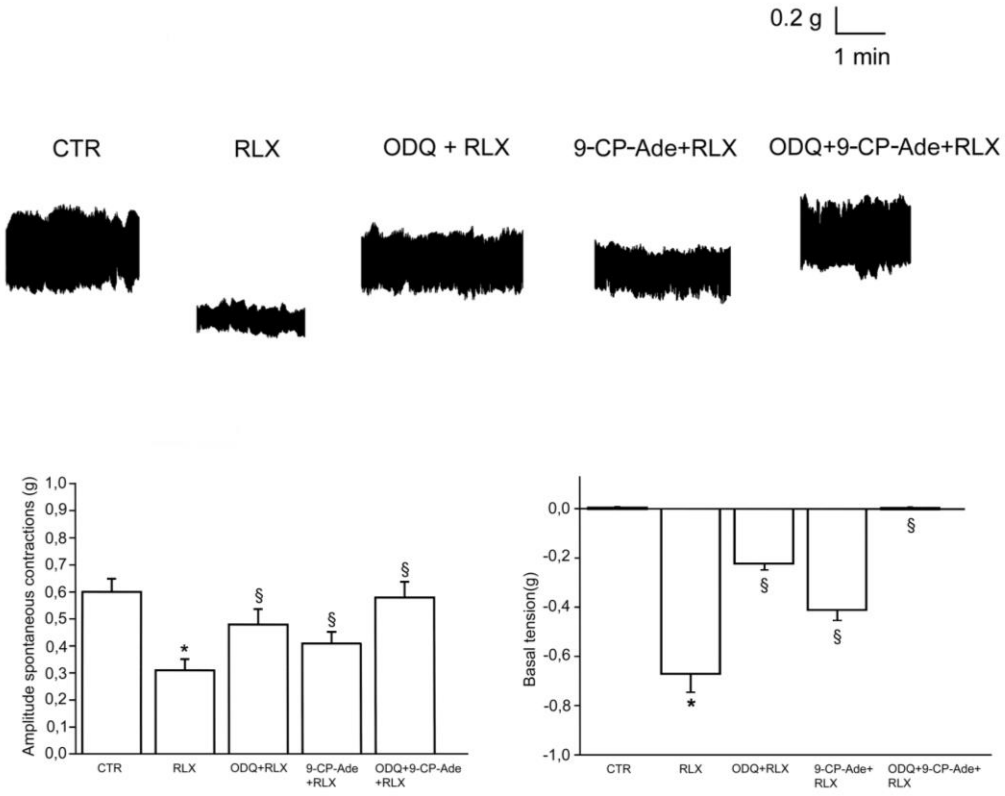

Figure 18. ***Influence of guanylate- and adenylate-cyclase inhibitors (ODQ and 9-CP-Ade, respectively) on relaxin (RLX) effects on the mechanical activity of the mouse ileal preparations.***

Upper panel. A: typical tracing showing the spontaneous activity of the ileal longitudinal segments. B: RLX (50 nM), 30 min from its application to the bath medium, causes a decrease in amplitude of the spontaneous contractions and a decay of the basal tension compared to A. Both these effects are reduced when RLX is added to the bath medium in the presence of 1 µM ODQ (C) or 100 µM 9-CP-Ade (D) and abolished by ODQ plus 9-CP-Ade (E). Traces C-E are obtained from different preparations.

Lower panel: Bar charts showing the influence of ODQ and 9-CP-Ade on RLX effects on the mean amplitude of spontaneous contractions (left hand histogram) and basal tension (right hand histogram) with respect to the control. All values are means ± SEM of 6 preparations. **P* < 0.05 *vs.* ctr; § *P* < 0.05 *vs.* RLX (one-way ANOVA and Newman-Keuls post-test).

Electrophysiological experiments

RLX influences the SMC passive membrane properties

The effect of RLX was investigated on the SMC resting membrane properties in voltage clamp mode. RLX applied alone did not alter significantly the mean membrane capacitance, neither in the presence of ODQ (ODQ+RLX), nor with 9-CP-Ade (9-CP-Ade+RLX) or in the concomitant presence of both inhibitors (ODQ+9-CP-Ade+RLX). In contrast, RLX reduced significantly G_m and G_m/C_m. This decrease was counteracted when RLX was applied in the presence of both inhibitors (Fig. 19).

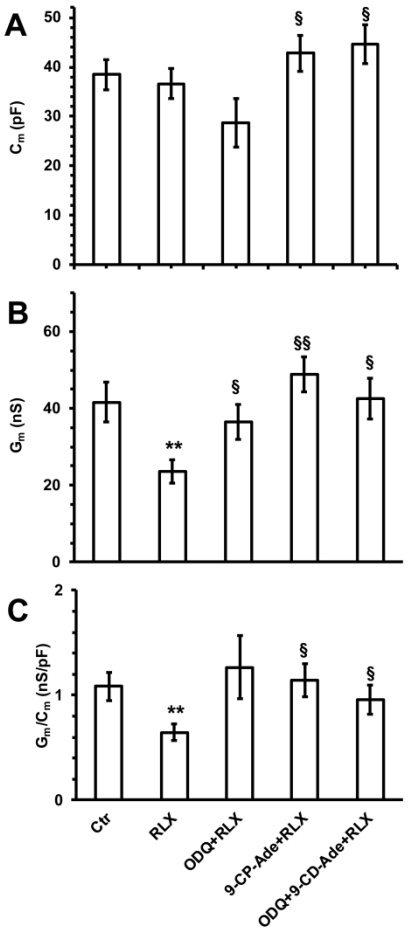

Figure 19. ***Effect of RLX on SMC membrane passive properties.***
Only data obtained in the presence of RLX are significantly affected compared to control. ** $P < 0.01$ *vs.* control (Ctr); § and §§ $P < 0.05$ and $P < 0.01$ solution with inhibitors *vs.* RLX alone. In each experimental condition, data are from n = 15-18 cells (of 6-7 ileal preparations).

Since the above results indicate that RLX may regulate the SMC mechanical activity by a dual mechanism, the AC-cAMP-PKA and the NO-GC-cGMP-PKG pathway, we evaluated the ability of ODQ and 9-CP-Ade to antagonize RLX effects on the RMP and on the main voltage-dependent ionic channels, such as the L-type Ca^{2+}- and the delayed rectifier K^+- channels (Ks, BK and K_V).

RLX influences the SMC resting membrane potential

We then focused on the membrane electrical activity of SMC by performing experiments in current-clamp conditions using the control bath and control microelectrode filling solution (see method section). Spontaneous asynchronous and irregular waves of RMP were detected by intracellular recording in basal condition. These irregular waves of the membrane potential showed cyclically recurring periods of electrical activity with low frequency of 0.5 ± 0.1 wave/min alternating with periods of increased frequency, lasting 8-10 min, to 1.1 ± 0.2 wave/min. The RMP measured at the negative peak was -53.6 ±5 mV, in accord to previous literature (*Ryoo et al., 2014*) and the size of the irregular wave was 37.5±4 mV (n= 26). Therefore, the positive peak reached a value of -20.3±2.2 mV that is near the voltage threshold for L-type Ca^{2+} and the delayed rectifier K^+ current activation (see below).

When RLX was added to the bath solution, we observed a hyperpolarization, typical feature of NO stimulation (*Matsuyama et al., 1999*), already appreciable 1-3 min after its application. The asynchronous and irregular waves were always recorded during the hyperpolarization due to RLX that maintained similar amplitude but had a greater frequency (2 ±0.1 that could increase in train of 8-10 min to 4 ± 0.2 waves min^{-1}) (Fig. 20A). The RMP reached -98,8±5 mV in the presence of RLX (Fig. 20A) and its maximal peak reached -63,8±5 mV, a value that was definitely under threshold for the activation of L-type Ca^{2+}- and the delayed rectifier K^+-currents studied (see below).

This prevalent tendency of RMP to hyperpolarization and the parallel reduction of the

membrane conductance observed above, strongly justify the decrease of the basal tension and the reduced amplitude of the spontaneous contraction induced by RLX observed in the mechanical experiments.

In order to investigate the signalling pathway involved in this RLX effect, we used the inhibitors ODQ and 9-CP-Ade also in this set of experiments. RLX added at least 15 min after ODQ or 9-CP-Ade did not appreciably affect the wave amplitudes (Fig. 20B, C) but hyperpolarized the cell to a lesser extent (25.7 ± 3 and 27.4 ± 4 mV, respectively), suggesting that both cGMP and cAMP signalling pathways were involved in this effect of RLX. Particularly, the hyperpolarization caused by RLX in the presence of ODQ was less than that observed in the presence of 9-CP-Ade (Fig. 20B,C). In fact, the positive peak of the membrane potential reached -30.7 ± 3 and -43.7 ± 4 mV, respectively. In agreement with the observations from the mechanical experiments, RLX added in the presence of both inhibitors had no longer effects (Fig. 20D).

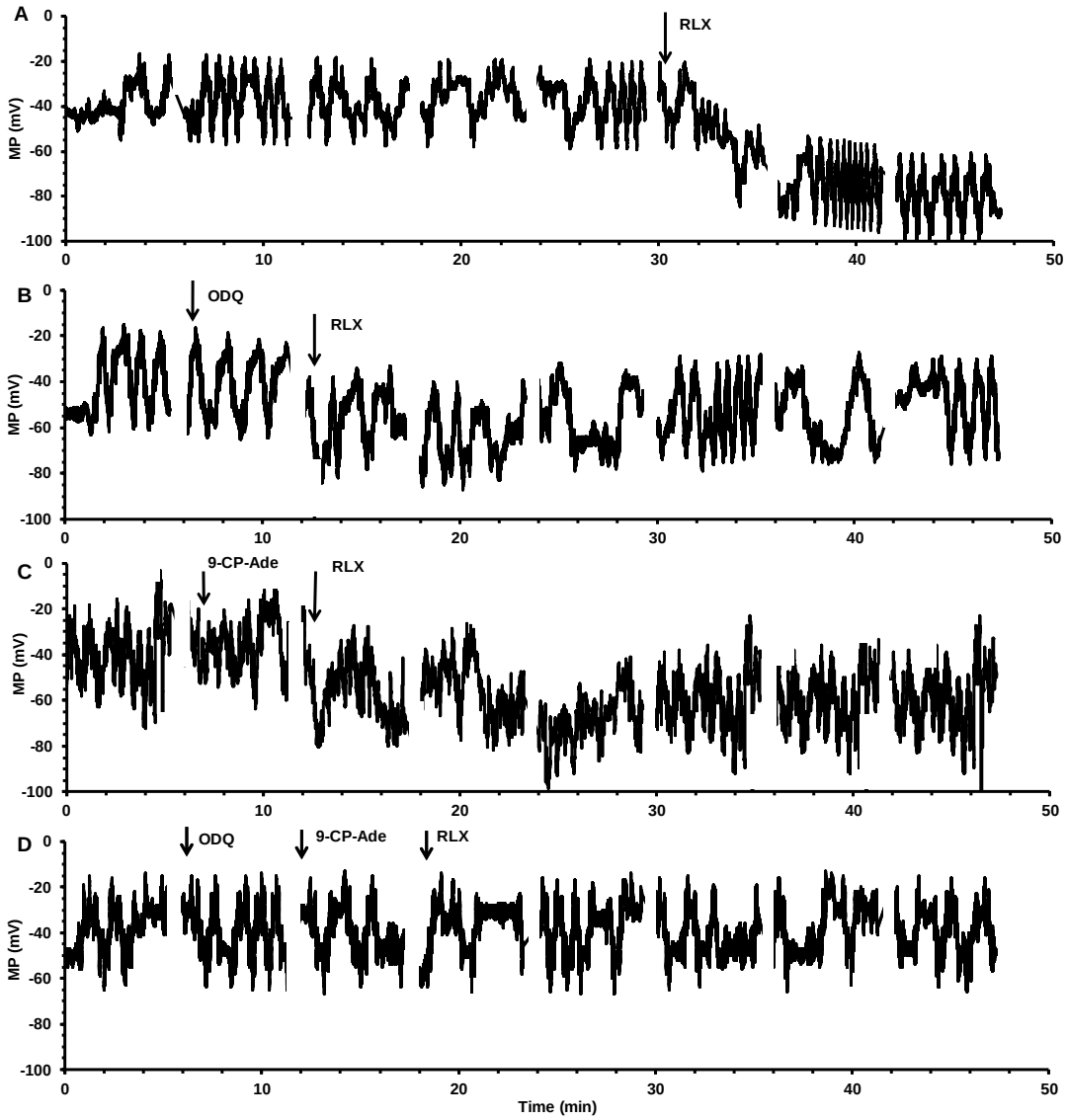

Figure 20. ***Effects of guanylate and adenylate cyclase inhibitors (ODQ and 9-CP-Ade, respectively) on RLX action on membrane potential recorded from a SMC of mouse ileum.***
Typical tracings of membrane potential from four different single ileum SMCs. A-D) Asynchronous and irregular waves of resting membrane potential recorded in basal condition (control, Ctr). A. RLX addition (arrow) induced a persistent hyperpolarization occurring right after about 2 min from its application. The hyperpolarization caused by RLX was reduced in the presence of ODQ (B) or 9-CP-Ade (C) and was abolished when both blockers were concomitantly added (D).

RLX reduces the voltage-dependent Ca^{2+} current

The effects of the hormone were then evaluated on the inward voltage-dependent ionic currents by switching to the voltage-clamp mode of our device. It is to note that, in our experiments, we did not consistently record TTX-sensitive Na^{+} current or T-type Ca^{2+} currents. Accordingly, to better put in evidence the appearance of voltage-dependent Ca^{2+} currents (I_{Ca}), we used appropriate filling pipette solution and bath recording high TEA-Ca^{2+} solution (see method section).

The time course of typical I_{Ca} traces recorded from a cell in control (Aa) and after RLX treatment (Ab) is shown in Fig. 21. Since this kind of current was high voltage activated, having a voltage threshold at about -30 mV, had a slow activation, a slow inactivation and was blocked by nifedipine, we assumed that it was an L-type Ca^{2+} current *(*$I_{Ca,L}$). It can be clearly seen (Fig. 21 Aa, Ab) that RLX reduced the maximal peak current size as well as the time to peak (190 *vs.* 250 ms in ctr). In any case, the maximum current amplitude was evoked by the 20 mV step.

Then, to evaluate the general behaviour of the phenomenon, we calculated the *I-V* relationship related to all the experiments done, reporting the normalized mean I_{Ca} maximal amplitude for any voltage step applied (Fig. 21C). The analysis of the *I-V* plot confirmed that RLX caused the decrease of current amplitude. The ODQ or 9-CP-Ade pre-treatment did not completely abolish the effect of RLX, but slightly reduced the time to peak (240 vs. 250 ms in control and 235 vs. 250 ms in control, respectively) (Fig. 21 B,C).

The voltage dependence of the current activation time constant, $\tau_{m,,}$ (Fig. 21D) as well as that of inactivation, τ_{h} (Fig. 21 E), was significantly speeded by RLX treatment. Particularly, the ODQ pre-treatment did not entirely eliminate the effects of RLX on $\tau_{m,}$, whereas 9-CP-Ade resulted more effective in counteracting RLX effects (Fig. 21D).

Instead, the action of RLX on $\tau_{h,}$ was similarly prevented by the pre-treatment with each of the inhibitors (Fig. 21 E).

The effect of RLX and of the effector inhibitors on the L-type Ca^{2+} current voltage dependence was analysed by the steady-state activation and inactivation curves (Fig. 21 F): RLX shifted the activation curve towards more negative potentials and positively shifted the inactivation curve, making it more U-shaped for positive potentials.

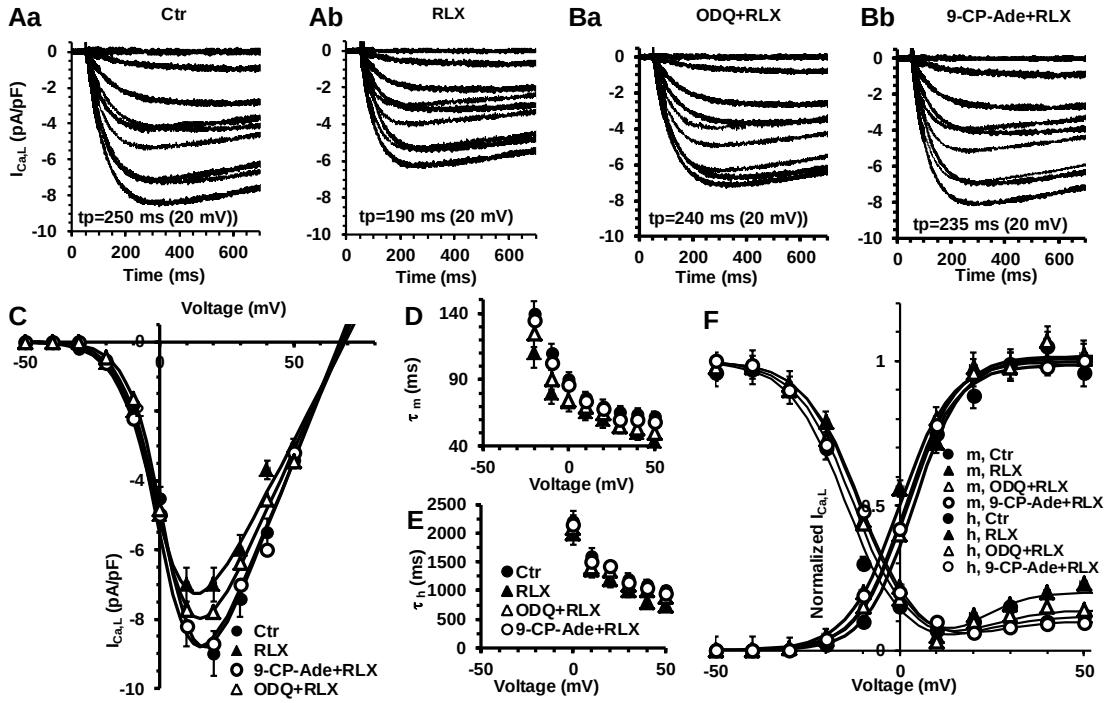

Figure 21. ***RLX treatment affects L-type Ca^{2+} currents.***
A) Typical L-type Ca^{2+} currents ($I_{Ca,L,}$) recorded in the high TEA-Ca^{2+} solution from a control cell (Aa) and after RLX treatment (Ab). Ba) $I_{Ca,L}$ records from a different control cell where RLX is added 15 minutes after ODQ treatment. Bb) $I_{Ca,L}$ records from another different control cell where RLX is added 15 minutes after 9-CP-Ade treatment. A, B) only the first 700 ms of the pulse are depicted. C) *I-V* plots of L-type Ca^{2+} currents ($I_{Ca,L}$) for Ctr (filled circles), RLX (filled up triangles), ODQ+RLX (open up triangles) and 9-CP-Ade +RLX (open circles) from experiments as in panels A and B. The single Boltzmann fits are superimposed to experimental data as continuous lines. D) Voltage dependence of the time constant of $I_{Ca,L}$ activation (τ_m).
E) Voltage dependence of the time constant of $I_{Ca,L}$ inactivation (τ_h). F) Steady-state $I_{Ca,L}$ activation (m) and inactivation curves (h) in Ctr, RLX, ODQ+ RLX and 9-CP-Ade +RLX; the best fit to the inactivation data is obtained by the sum of two Boltzmann terms. Data are mean values ± SEM. Boltzmann parameters, statistical analysis and number of analysed cells are listed in Table 6. Current values are normalized to cell capacitance.

The best fit parameters (mean values ± SEM), statistical analysis and number of analysed cells are listed in Table 6. Notably, the voltage threshold for $I_{Ca,L}$ activation was not significantly affected among the different treatments and the control and was 28.7±3 mV.

Table 6. ***Boltzmann parameters of $I_{Ca,L}$ activation and inactivation in a SMC from longitudinal muscle layer in control (Ctr), in the presence of RLX alone (RLX) or with ODQ (ODQ+RLX) or 9-CP-Ade (9-CP-Ade+RLX)***

Parameters	Ctr	RLX	ODQ+RLX	9-CP-Ade +RLX
$I_{Ca,L,max}/C_m$ (pA/pF)	8.9 ± 0.6	7.3 ± 0.4**	8.1 ± 0.8§	9.0 ± 0.8§§
G_m/C_m (pS/pF)	199.7 ± 12	120.3 ± 18***	174.8 ± 15§§	203.3 ± 16§§§
V_p (mV)	17.2 ± 2	15.1 ± 2*	15.9 ± 2	17.4 ± 2§
V_a (mV)	4.0 ± 1	0.2 ± 0.3***	2.0 ± 1§§	3.9 ± 1§§
k_a (mV)	6.5 ± 0.4	6.4 ± 0.5	6.7 ± 0.4	6.6 ± 0.4
V_{rev} (mV)	67.0 ± 4	68.8 ± 4	68.1 ± 5	68.3 ± 4
V_h (mV)	-14.4 ± 2	-10.8 ± 1*	-12.3 ± 1	-14.2 ± 2§
k_h (mV)	7.6 ± 0.5	7.5 ± 0.5	7.5 ± 0.6	7.6 ± 0.7
$V_h(+)$ (mV)	22.0 ± 2	20.3 ± 2	23.1 ± 2	22.2 ± 2
$k_h(+)$ (mV)	8.3 ± 1	5.3 ± 0.6**	7.6 ± 1§	8.1 ± 1§

In the U shaped inactivation curves (h) the best fit to the data is obtained by the sum of two Boltzmann terms named V_h and k_h that for negative and $V_{h(+)}$ and $k_h(+)$ for positive potential. * $P < 0.05$, ** $P < 0.01$ and *** $P < 0.005$ RLX compared to the related control; § $P < 0.05$, §§ $P < 0.01$ and $P < 0.001$ values from ODQ+RLX and 9-CP-Ade +RLX compared to RLX. Data from RLX: n = 20 cells (10 ileum preparations), from ODQ+RLX: n = 18 cells (5 ileum preparations), from 9-CP-Ade +RLX: n = 15 cells (5 ileum preparations) and from Ctr n= 53

RLX influences the voltage-dependent outward K^+ currents

We successively investigated the effect of RLX on the main voltage-dependent delayed rectifier K^+ currents in order to comprehend how RLX could affect RMP and excitability. Typical outward K^+ current traces, were evoked by proper voltage pulse stimulation protocol (see methods section) and elicited in the modified bath control solution containing nifedipine (10 μM) to avoid the occurrence of inward Ca^{2+} currents. Fig. 22 A shows typical total outward K^+ currents ($I_{K,tot}$) recorded in a Ctr cell (a) and in the presence of RLX (b). It can be clearly seen that RLX strongly reduced the outward current. When RLX was added in the presence of the GC or AC inhibitors we observed only a slight reduction, being the current amplitude in the presence of ODQ (ODQ+RLX, panel Ba) and 9-CP-Ade (9-CP-Ade +RLX, panel Bb) similar to that observed in control records (Fig. 22 A, B).

As for the previous study in the colonic preparation, we made a pharmacological dissection of $I_{K,tot}$ to distinguish the principal voltage-dependent K^+ currents expressed in the gastrointestinal SMC and we were able to discriminate three different kinds of K^+ currents: I_{Ks} (C-D), I_{BK} (E-F) and I_{Kv} (G-H); examples of current traces normalized to cell capacitance from a cell in control solution are reported in Ca, Ea and Ga, whereas Cb, Eb and Gb, report the different components under RLX treatment. It can be easily observed that RLX reduced all the types of K^+ currents, especially I_{BK}.

When RLX was added in the presence of ODQ (Ba, Da, Fa and Ha) we still could note a current amplitude reduction, indicating that the blockade of cGMP signalling pathway was not the only one involved in RLX action. In contrast, when RLX was added in the presence of 9-CP-Ade (Bb, Db, Fb and Hb) all the outward K^+ currents showed an amplitude similar to control, suggesting that RLX effect was also strongly influenced by the blockade of AC pathway.

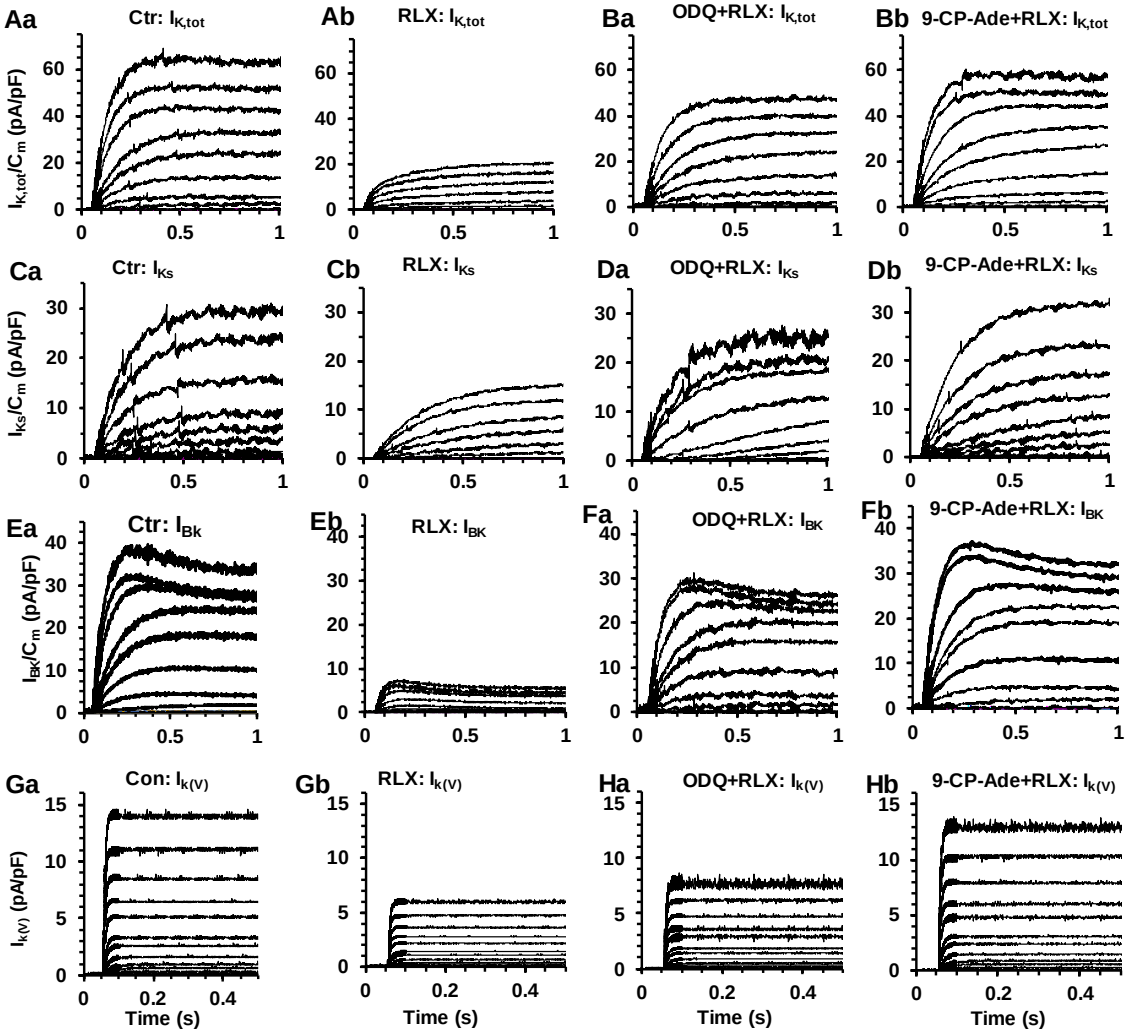

Figure 22. ***Effect of RLX on voltage-dependent delayed rectifier K^+ currents.***
Time course of outward K^+ currents, elicited by voltage steps from -80 to 50 mV (HP= -60 mV) in control solution containing Nifedipine (10 μM). A) Representative total outward K^+ currents ($I_{K,tot}$) recorded in a Ctr cell (a) and in the presence of RLX (b). B) Same current traces recorded from a different cell with RLX added in the presence of ODQ (Ba) or 9-CP-Ade (Bb). By pharmacological dissection $I_{K,tot}$ could be systematically separated into three kinds of K^+ currents: I_{Ks} (C-D), I_{BK} (E-F) and I_{Kv} (G-H); examples from the cell in control solution are displayed in Ca, Ea and Ga, whereas Cb, Eb and Gb report the different components under RLX treatment. Current traces recorded from different cells with RLX added in the presence of ODQ are in Ba, Da, Fa and Ha or of 9-CP-Ade in Bb, Db, Fb and Hb. Current values are normalized to cell capacitance.

The analysis of the *I-V* plot related to the $I_{K,tot}$ and to the individual components, confirmed the above observation: RLX inhibited I_{Ks}, I_{BK} and I_{Kv} and its effect was partially reverted by ODQ and almost completely reverted by 9-CP-Ade (Fig 23). We also studied the voltage dependence of each K^+ current time constant (Fig 23 Bb-Db):

especially for negative voltages, RLX was able to affect almost I_{Kv}, making its kinetics faster. Notably the voltage threshold for I_{Ks}, I_{BK} and I_{Kv} were -15.8±2, -25.2±3 and -42.1±4 mV, respectively and were not affected by the treatments used (Fig. 23). Consequently, in resting condition only I_{BK} and I_{Kv} could be somewhat activated by the spontaneous depolarizing wave.

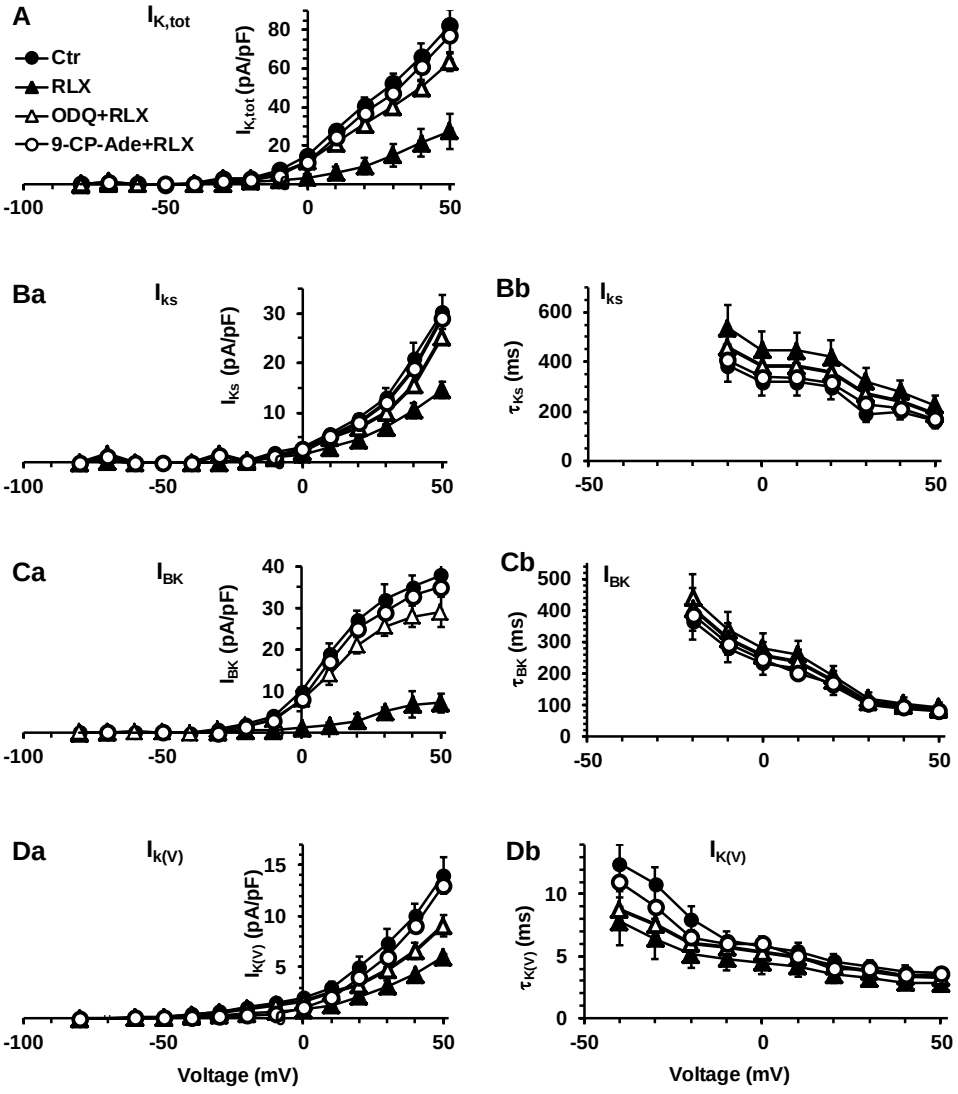

Figure 23. ***RLX inhibits IKs, I_{BK} and I_{Kv} and such effect is partially or almost reverted by ODQ and 9-CP-Ade, respectively.***
A) *I-V* plot related to the total delayed rectifier K^+ current ($I_{K,tot}$). Ba-Da) *I-V* curves related to the pharmacologically dissected components I_{Ks} (B), I_{BK} (C) and I_{Kv} (D). Bb-Db) τ-V curves related to all the experiments done. Current values are normalized to cell capacitance. Ctr n = 21, RLX: n = 20 cells (10 ileum preparations), ODQ+RLX: n = 11 cells (6 ileum preparations); Ctr n = 21.), 9-CP-Ade +RLX: n = 11 cells (6 ileum preparations).

3.3 Adiponectin effects on gastric smooth muscle

Mechanical experiments

ADPN causes a decay of the basal tension

Addition of ADPN (20 nM) to the bath medium induced on longitudinal strips of gastric fundus (*n* = 6), a progressive and long-lasting decay (P<0.05) of the basal tension (mean amplitude 0.15±0.02 g), that persisted for the whole period of exposure (30 min, longer time not observed). In the presence of TTX (1µM), ADPN was still effective, indicating a direct muscular action of the hormone (Fig. 24).

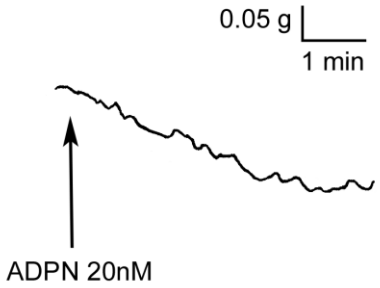

Figure 24. ***Effects of adiponectin on the basal tension of the longitudinal muscle strip from the mouse gastric fundus.***
Typical tracing showing the progressive decay of the basal tension caused by adiponectin (20nM).

Electrophysiological experiments

ADPN affects the passive proprieties of SMCs

In order to investigate the effects of ADPN on the biophysical properties of the gastric fundus SMCs we performed some electrophysiological recordings using the microelectrodes technique.

In order to estimate possible modification of the cell size, we evaluated in voltage clamp mode the cell capacitance (Cm) in control and after ADPN added to the bath medium. ADPN induced a significant increase of the Cm (32± 5pF) in respect with the control (17±2pF) (Fig.25A). The analysis of the membrane conductance, Gm, (Fig.25B) and specific membrane conductance normalized to cell capacitance, Gm/Cm, (Fig.25C) in the presence of ADPN revealed a significant decrease with respect to the control (Gm: 0.033±0.02 pS in CTR vs 0.017±0.02pS in the presence of ADPN; Gm/Cm: 0.0021±0.0003pS/pF in CTR vs 0.0006±0.0002pS/pF in the presence of ADPN). This decrease on membrane conduction may account for the decay of the basal tension observed in the mechanical experiments and could justify the hyperpolarization of the sarcolemma membrane in the SMCs at resting (see below).

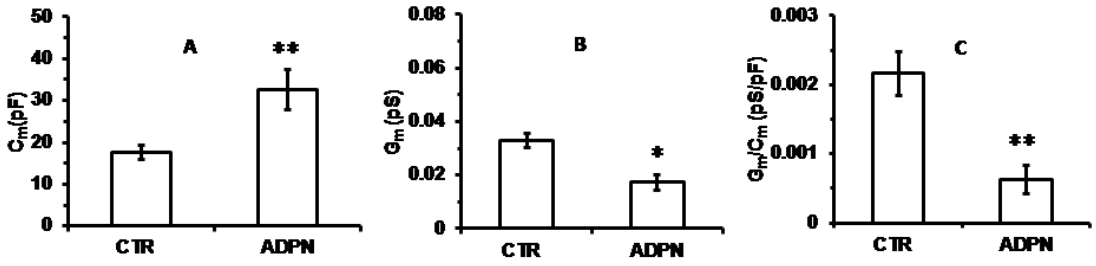

Figure 25. ***Passive properties of fundus gastric cells in control conditions (CTR) and in the presence of adiponectin.***
A–C, data evaluated in control condition (CTR) and after adding adiponectin to the bath solution (after 5 min). *A*, cell capacitance (Cm) as an index of cell surface. *B*, membrane conductance (Gm). *C*, specific membrane conductance (*G*m/*C*m). One-way ANOVA with repeated measures was used for multiple comparisons. * $P < 0.05$, ** $P < 0.01$ ADPN vs related CTRL. Values are means ± SEM; CTR *n* = 20 cells, ADPN *n*= 20 cells (5 mice).

ADPN affects RMP by inducing hyperpolarization

To evaluate if ADPN affect the RMP we then focused on the membrane electrical activity of SMC by performing experiments in current-clamp conditions. Spontaneous waves of resting membrane potential were detected by intracellular recording in basal condition (-52,2±3mv). When ADPN was added to the bath solution we observed a hyperpolarization, already visible 2-3 min after its application (Fig. 26). RMP reached -59±2 mV in the presence of ADPN after 23 min (longer time not observed).

This prevalent tendency of ADPN to hyperpolarize the RMP and the parallel reduction of the membrane conductance, strongly justify the decrease of the basal tension induced by ADPN observed in the mechanical experiments.

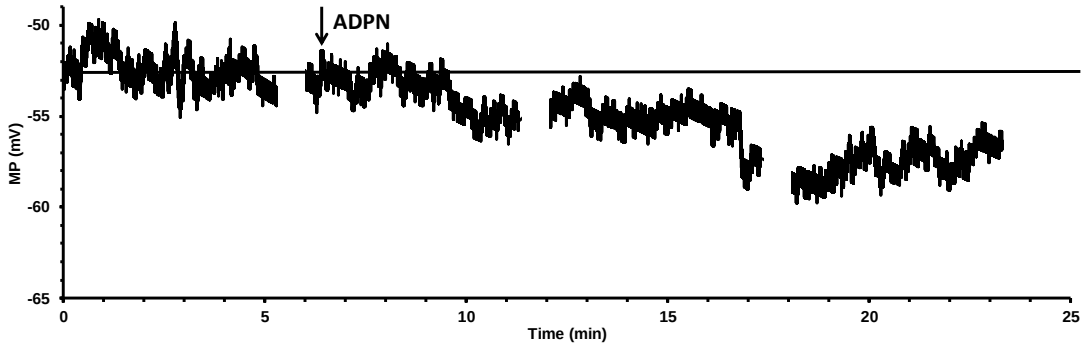

Figure 26. ***Effects of ADPN on resting membrane potential recorded from gastric SMC.***

Typical tracings of membrane potential from a single gastric SMC. Asynchronous and irregular waves of resting membrane potential recorded in basal condition and after 6 min ADPN addition (arrow) induced a persistent hyperpolarization occurring right after about 2-3 min from its application. Continuous line is the mean of resting potential in control.

ADPN influences the voltage-dependent outward K^+ currents

We successively investigated the effect of ADPN (20nM) on the main voltage-dependent delayed rectifier K^+ currents ($I_{K,DR}$) (Fig. 27) . Typical outward K^+ current traces, were evoked by proper voltage pulse stimulation protocol (see method section) and elicited in the modified bath control solution containing nifedipine (10 μM) to avoid the occurrence of inward currents. The different types of voltage-dependent K^+ channels involved in the total K^+ current were separated by pharmacological tools as for the previous study in colonic CMSs. We were consistently able to distinguish the fast activating α-dendrotoxin (α-DTX)-sensitive $I_{Kv,}$ the large conductance Ca^{2+} activated K^+ current that was Iberiotoxin (IbTx) sensitive, namely BK current (I_{BK}) and the slowly activating chromanol (Chr)-sensitive I_{Ks}. The voltage threshold of activation of the different currents was -40±5, -30±5 and -20±4 mV for K_v, I_{BK} and I_{Ks}, respectively (Fig. 28). We could clearly observe that ADPN treatment caused a slight increase of the total outward K^+ current (Fig. 27Ab), and this apparent slight increase was mostly due to the potentiation of the Kv and Ks current amplitude (Fig.27 B,D). In contrast, BK was clearly reduced by ADPN treatment (Fig 27C). To better evaluate the general behaviour of the phenomenon, we calculated the *I-V* relationship related to all the experiments done, reporting the normalized mean I_{Ca} maximal amplitude for any voltage step applied (Fig. 28).

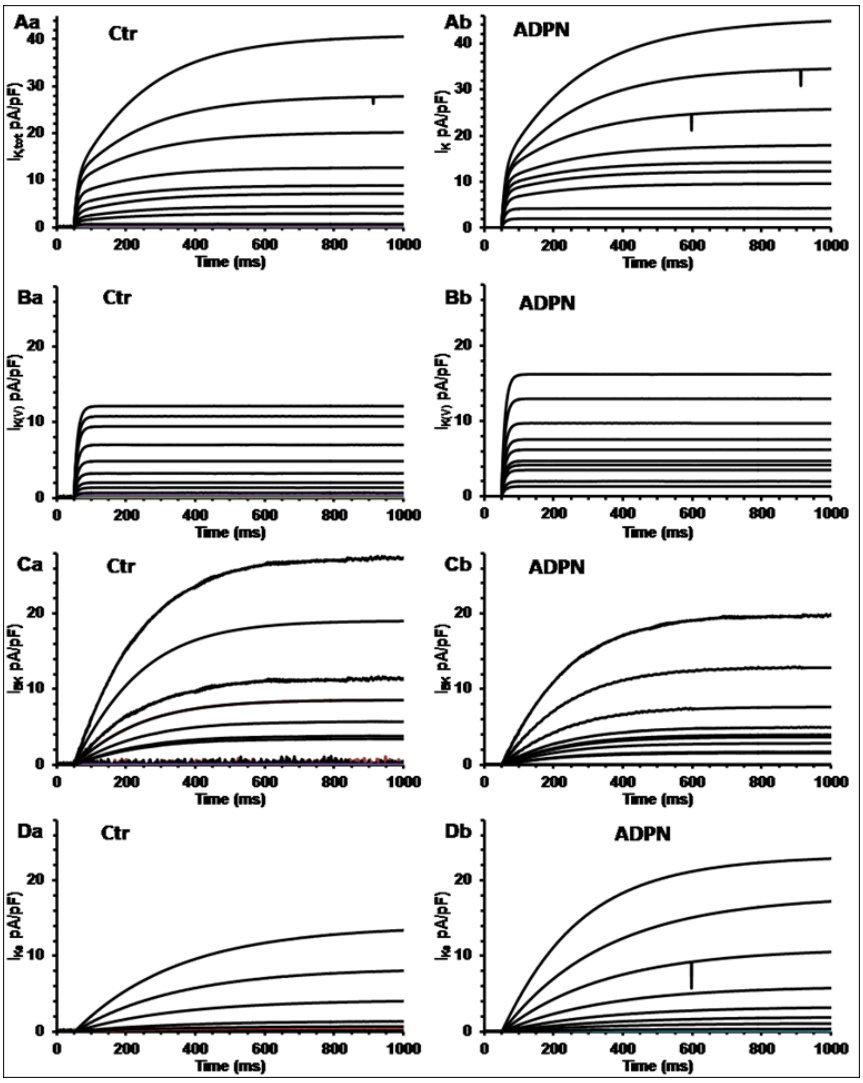

Figure 27. ***Effects of ADPN on K^+ currents of voltage-dependent Kv, BK and Ks currents recorded in a smooth muscle cell from gastric fundus.***
Outward K+ currents, elicited by voltage steps from -80 to 50 mV (HP= -60 mV) in solution containing nifedipine (10 μM). A) Representative total outward K+ currents ($I_{K,tot}$) recorded in Ctr (a) and in the presence of ADPN (b). By pharmacological dissection $I_{K,tot}$ could be systematically distinguished into three kinds of K+ currents: I_{Kv} (B); I_{BK} (C) and I_{Ks} (D), examples of records in control solution are reported in (a), whereas the different components under ADPN treatment are reported in (b). Current values are normalized to cell capacitance.

The analysis of the *I-V* plot confirmed that ADPN treatment mainly reduced the Ca^{2+}-dependent K^+ currents with an intermediate voltage threshold. In contrast, the fast and low threshold I_{Kv} and the slow and high threshold I_{Ks} resulted potentiated by the

hormone (Fig. 28), thus enabling the compensation of the fast and slow changes of the resting membrane potential.

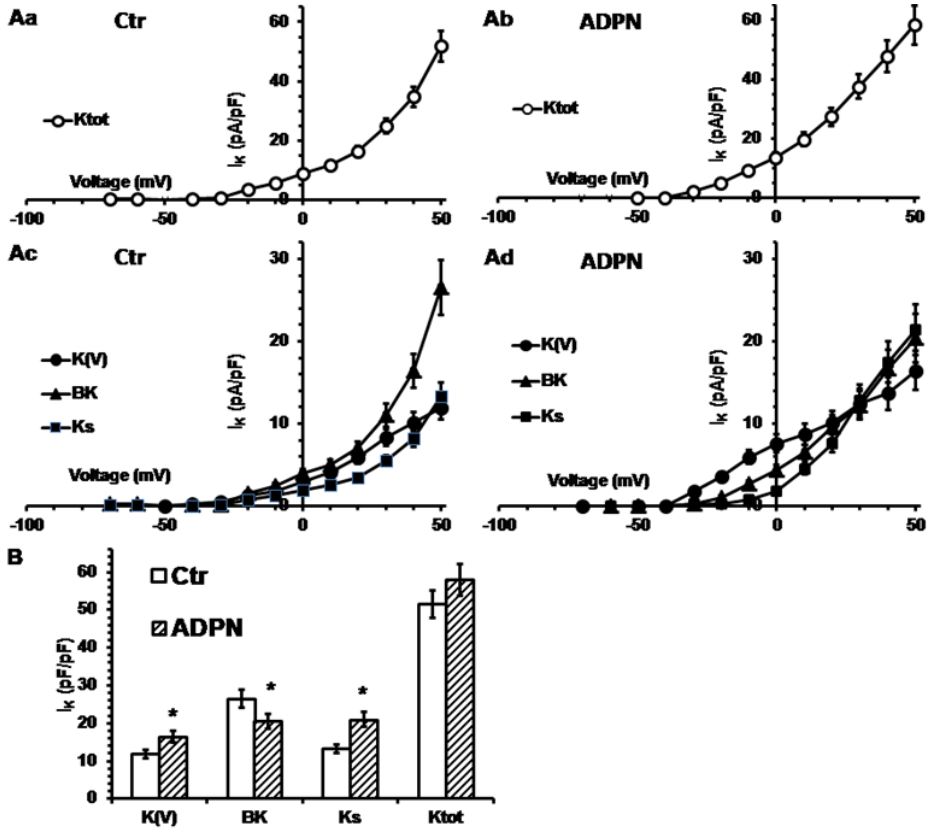

Figure 28. ***ADPN determines different effects on outward delayed rectifier K^+ current types (I_{Kv}, I_{BK} and I_{Ks}) in smooth cells from gastric fundus.***
A) *I-V* plots related to the total delayed rectifier K^+ current ($I_{K,tot}$)) in control (a) and in the presence of ADPN (b); the pharmacologically dissected components I_{Kv}, I_{BK} and I_{Ks} in control (c) and ADPN treated cells (d All data point in b are greater than in a ($P < 0.05$). Current values are normalized to cell capacitance. B) Comparison of the maximal values recorded at 50 mV; * $P < 0.05$ of ADPN versus Ctr. ADPN potentiate I_{Kv} and I_{Ks} but depress I_{BK}. All data are mean values ± SEM. In each experimental condition, data are from 6-8 cells from 3-4 mice. * $P < 0.05$, ** $P < 0.01$ ADPN *vs* related Ctr.

ADPN decreases the voltage-dependent Ca^{2+} current

To explain the origin of the basal tension changes elicited by ADPN in the mechanical experiments, we evaluated (in voltage-clamp condition) the effects of the ADPN on the inward voltage-dependent Ca^{2+} currents (I_{Ca}). This current represents a chief source for intracellular Ca^{2+} elevation useful for SMC contractile activation. Modifications of T- and L-type Ca^{2+} currents ($I_{Ca,T}$ and $I_{Ca,L}$) are a key events that may affect excitation-

contraction coupling in smooth muscle. Since we observed that ADPN affects the mechanical response in gastric longitudinal smooth muscle, it became essential to observe the effect of this peptide on $I_{Ca,T}$ and $I_{Ca,L}$ to evaluate if ADPN acts directly on SMC.

To this end, we made our current records using the high-TEA solution. When a pulse protocol of stimulation for evoking the Ca^{2+} currents (see method section for details) was applied to longitudinal SMCs of the gastric fundus, we constantly recorded inward current traces resembling smooth muscle Ca^{2+} currents. Representative control traces of the total Ca^{2+} current are depicted in Fig. 29Aa: the maximum current amplitude with a peak time (tp) of about 18 ms was observed by applying a 0-mV pulse step. After the addition of ADPN to the bath solution, we observed a decrease in amplitude as well as different voltage dependence, since the maximal peak size was reached by a 10-mV step pulse in the presence of ADPN (Fig. 29Ab). When this type of experiment was performed in the presence of nifedipine (10 µM) to block L-type Ca^{2+} channels, we could observe a residual low voltage activated current with a rapid and transient time course (tp= 5.5±0.5 ms), suggesting the involvement of $I_{Ca,T}$ (Fig. 29Ba). The addition of ADPN decreased the maximal size of $I_{Ca,T}$ slightly affecting its time to peak (5.8 ± 0.5 ms) and negatively shifting the maximal activation from -25 to -30 mV (Fig. 29Bb, Table7). By subtracting the current traces obtained in the presence of nifedipine from the total currents, we obtained the L-type Ca^{2+} channel contribution (Fig. 29Ca): high-voltage-activated current traces with a slow decay were observed with the maximum amplitude reached in 22.7 ± 2 ms by a 0-mV step pulse. Once again, the addition of ADPN decreased the size of $I_{Ca,L}$ (Figs. 29Cb and 30B) apparently without altering its time to peak (Table 7), but shifting the voltage value of the pulse required to evoke the maximal current amplitude from 0 to 10 mV.

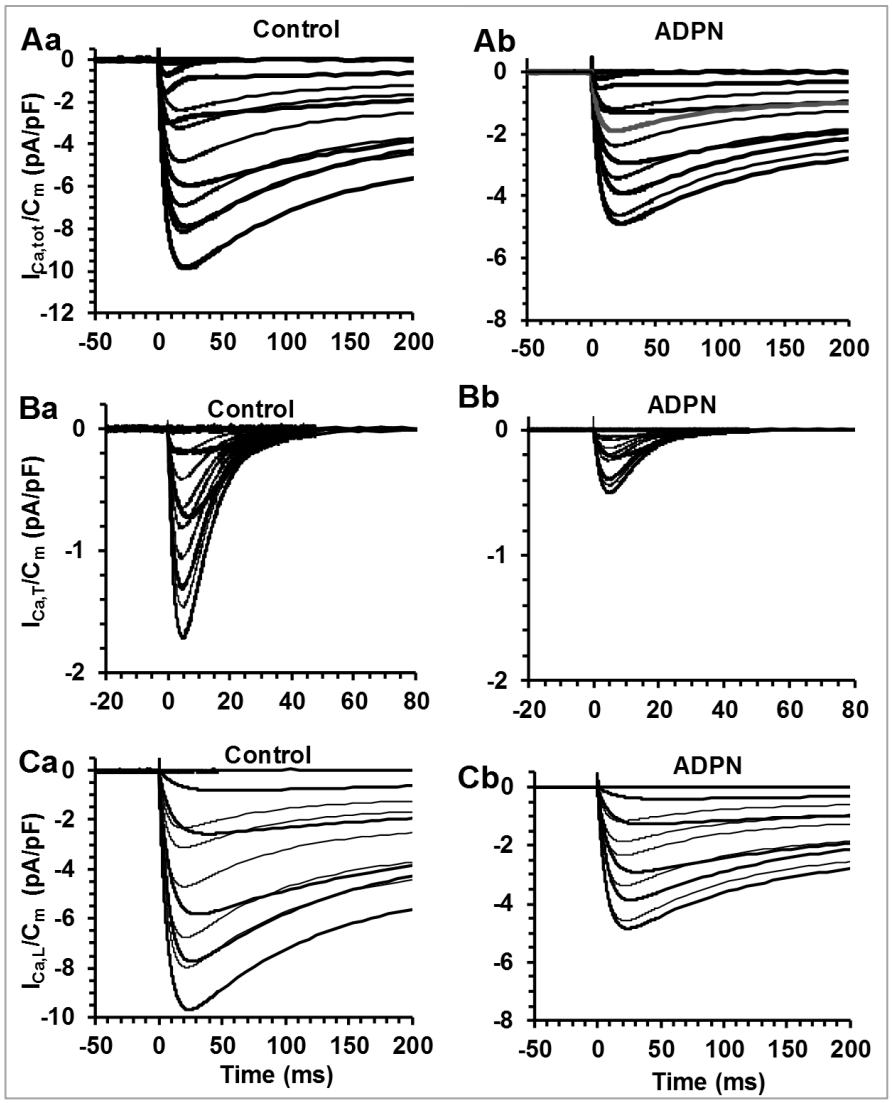

Figure 29. ***Effects of ADPN on Ca^{2+} currents recorded from gastric fundus.***
A: Typical total Ca^{2+} current traces obtained in a control (a) and ADPN treated (b) smooth gastric fundus muscle cell in response to 4-s voltage pulses from -70 to 50 mV applied from a HP of -80 mV, in 10-mV increments, in high–TEA bath solution. B: $I_{Ca,T}$ traces recorded by applying the protocol of stimulation in the presence of nifedipine in control (a) and in the presence of ADPN (b). C: $I_{Ca,L}$ obtained by subtracting $I_{Ca,T}$ from the total I_{Ca} in control (a) and in the presence of ADPN (b). All the current values are normalized for cell capacitance.

The analysis of the current-voltage (*I-V*) curve allowed us to evaluate the voltage dependence of all the Ca^{2+} currents recorded. The study was performed on $I_{Ca,T}$ and $I_{Ca,L}$ separately, in control conditions or under ADPN treatment. Any data point is the mean value ± SEM of the peak amplitude obtained at any voltages in all the experiments done. Figure 30 shows control *I-V* curves related to $I_{Ca,T}$ (C) and $I_{Ca,L}$ (D) recorded from SMCs of gastric fundus. The line through the filled symbols represents the fit of a

Boltzmann function. Adding ADPN caused a strong decrease in size of all the components, but did not affect the voltage dependence of inactivation of both T- and L-type Ca^{2+} current. ADPN positively shifted the half-maximal activation voltage value of $I_{Ca,T}$ activation of 5.1 ± 1 mV and that of $I_{Ca,L}$ of 19.8 ± 4 mV compared to control (Fig. 30D). Boltzmann parameters are showed in the table 7.

Moreover, it is to note that the inactivation curves did not steadily keep on at zero level at positive potentials but progressively increased causing a sort of U-shaped inactivation curve. This behaviour may suggest that inactivation was Ca^{2+} dependent. ADPN depressed this phase, probably due to the minor intracellular $[Ca^{2+}]_i$ as a consequence of the decreased Ca^{2+} influx trough L-type Ca^{2+} channels, as observed in colonic SMC.

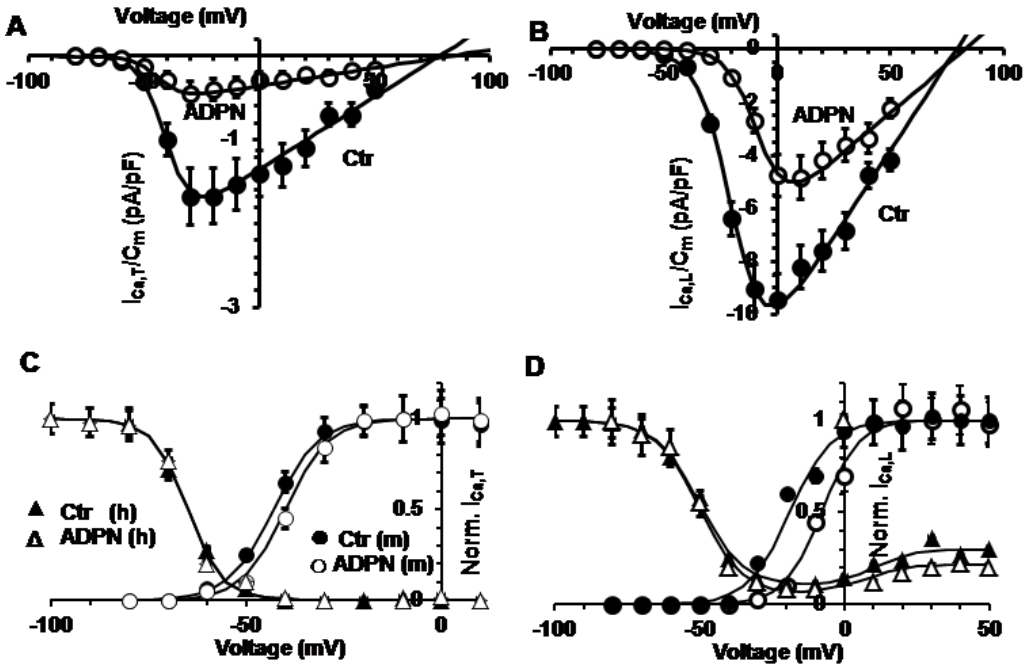

Figure 30. ***Effects of ADPN on the voltage-dependence of T- and L-type activation curves.***
A, B: *I-V* plots related to $I_{Ca,T}$ (A) and $I_{Ca,L}$ (B) in control (Ctr) and ADPN-treated SMCs from gastric fundus. Data are normalized for the mean cell capacitance. The lines through the experimental data are the fit as a Boltzmann function. Steady state activation and inactivation analysis for $I_{Ca,T}$ (C) and $I_{Ca,L}$ (D). Effect of ADPN on I_{CaT} and $I_{Ca,L}$ activation (open circles, m) respect to control (filled circles, m); lack of effects on inactivation (triangles, h). Note the U-shaped inactivation curve at positive potentials for $I_{Ca,L}$ that is depressed in ADPN treated cells. All data are mean values ± SEM. Data in each experimental condition are from 6-8 cells and 3-4 mice.

Table 7. ***Boltzmann parameters of $I_{Ca,T}$ and $I_{Ca,L}$ activation and inactivation in control and in adiponectin (ADPN) treated smooth muscle cells from gastric fundus.***

Parameters	Ctr	ADPN
$I_{Ca,T}$		
$I_{Ca,T}/C_m$ (pA/pF)	1.7 ± 0.2	0.5 ± 0.1***
G_m/C_m (pS/pF)	18 ± 5	5.5 ± 9***
V_{thr} (mV)	-54.8 ± 2	-53.0 ± 2
V_p (mV)	-25.1 ± 2	-30.2 ± 1.6**
V_a (mV)	-42.1 ± 3	-40.0 ± 2
k_a (mV)	7.2 ± 0.4	7.1 ± 0.5
V_r (mV)	76.5 ± 6	80.1 ± 7
V_h (mV)	-64.7 ± 6	-64.8 ± 6
k_h (mV)	4.5 ± 0.5	4.3 ± 0.4
t_p (ms)	5.5 ± 0.5	5.8 ± 0.5
$I_{Ca,L}$		
$I_{Ca,L}/C_m$ (pA/pF)	9.42 ± 0.6	5.2 ± 0.4**
G_m/C_m (pS/pF)	46 ± 5.1	32 ± 3.8**
V_{thr} (mV)	-50.2 ± 3	-48.7 ± 3
V_p (mV)	0.5 ± 0.07	10.2 ± 1***
V_a (mV)	-18.1 ± 2	-10.2 ± 2***
k_a (mV)	7.6 ± 0.3	8.1 ± 0.4
V_r (mV)	79.4 ± 6	81.7 ± 7
V_h (mV)	-51 ± 4	-53 ± 5
k_h (mV)	7.5 ± 0.5	7.4 ± 0.5
t_p (ms)	22.7 ± 2	21.8 ± 3

V_{thr} as voltage threshold and t_p as peak time at the voltage eliciting the maximal current amplitude, other symbols as in previous tables 5 and 6. *, ** and *** P<0.5, P<0.01 and P<0.001 of ADPN versus Ctr data.

Adipo-R1 and Adipo-R2 are expressed in the gastric fundus

Adiponectin receptor expression, of isoform 1 and isoform 2, has been detected in cDNA of murine gastric fundus samples by semiquantitative PCR analysis (Fig.31). Two mice were analysed per group. Positive controls derived from inguinal fat pad cDNA.

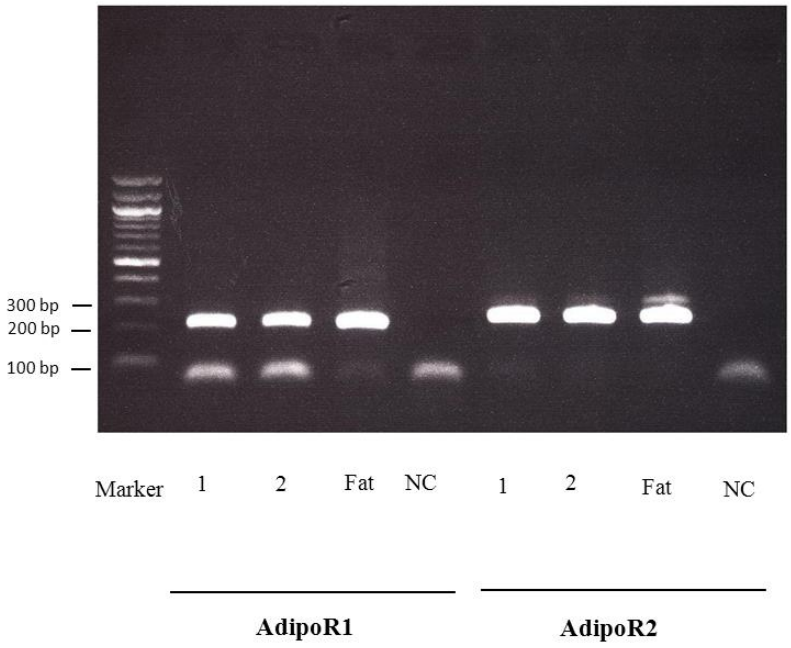

Figure 31. ***Expression of adiponectin receptors, AdipoR1 and AdipoR2, in murine gastric fundus.***
PCR analysis revealed the expression of both AdipoR1 (left hand) and AdipoR2 (right hand) receptors at murine gastric fundus. Two mice were analysed per group: stomach mice 1 and 2 (1 and 2). Positive controls derived from inguinal fat pad cDNA. NC: negative control, H2O. Marker: 100bp marker (NEB)

Chapter 4

Discussion

A number of endogenous substances can modulate the contractile and electric behaviour of the GI smooth muscle. This thesis work is focused on the effects of two hormones, RLX and ADPN, on the GI smooth muscle of female mice. Particularly, the effects of RLX have been studied on both colonic and ileal preparations, whereas those of ADPN in gastric fundus.

The results of the present work actually demonstrate that both RLX and ADPN, acting directly at the muscular level, are able to influence the mechanical activity and the biophysical properties of the SMCs. Particularly, the mechanical experiments have shown that either RLX or ADPN caused a decay of the basal tension in each GI segment investigated. Nevertheless, RLX, other than the common decrease of muscular tone, exerted two different actions in colon and ileum, consisting of an increase of the spontaneous contractions in the first preparation and a decrease in the latter one.

Moreover, despite many similarities such as, the decay of muscular basal tension, the RMP hyperpolarization and the decrease of I_{Ca} and I_{BK}, we obtained some different results (shortly summarized in the table 8) with the two hormones tested in the three different GI regions. For this reason, peculiar aspects of this research will be discussed separately, trying to better clarify the precise aspect of the question arose.

Table 8. ***Principal effects of relaxin on both colon and ileum and of adiponectin on gastric fundus of mice.***

	Effects of RLX on the proximal colon	**Effects of RLX on the distal ileum**	**Effects of ADPN on the gastric fundus**
Basal tension	↓	↓	↓
Spontaneous contractions amplitude	↑	↓	-
RMP	Hyperpolarization/depolarization oscillations, superimposed on a hyperpolarisation trend	Hyperpolarization with irregular waves	Hyperpolarization
L-type Ca^{2+} current	↓	↓	↓
$I_{K,tot}$	↓	↓	↑
I_{BK}	↓	↓	↓
I_{Kv}	↓	↓	↑
I_{Ks}	↑	↓	↑

Effects of RLX on colonic smooth muscle

The increase of the spontaneous contractions due to RLX in the longitudinal muscle layer of proximal colon preparations, observed in this study, had already been reported in the circular ones (*Baccari et al., 2012*) and it was actually unexpected since RLX has been always reported to depress GI motility mainly through the up-regulation of the expression of the different NOS isoforms (*Baccari et al., 2004a; Baccari et al., 2004b*). Indeed, in the colon circular preparations, in addition to the increase of nNOSβ and nNOSγ expression in the myenteric neurons, a significant decrease of nNOSα and eNOS expression induced by RLX has been observed in SMCs (*Baccari et al., 2012*)

(see introduction, section 1.2). Since both these latter enzyme isoforms contribute to regulate cytosolic calcium concentration (*Brenman et al., 1995; Loesch & Burnstock, 1995; Salapatek et al., 1998; Ward et al., 2000; El-Yazbi et al., 2008*), it has been hypothesized that their decreased expression in the colonic SMC induced by RLX and the consequent reduction of NO production, could shift the cytoplasmic free calcium buffering system toward an enhancement of calcium availability to sustain cell contractility. This sustained elevation of intracellular calcium, predisposing cells to myogenic contraction, might account for the increased amplitude of the muscular spontaneous contractions by RLX in colonic preparations.

In order to verify the above hypothesis and to find a possible correlation between the mechanical and electrophysiological effects of the hormone, we decided to investigate its ability to influence the resting membrane potential (RMP) and sarcolemmal ion channels of colonic SMCs. The observed expression of the RLX receptor (RXFP1) in our preparation further supports the effects of the hormone on the proximal colon.

The RMP recorded on the control colonic SMC, was not constant but showed spontaneous rapid rhythmic asynchronous waves without a regular shape or a dominant rhythmicity. This may account for the spontaneous contractile activity, consisting of rhythmic changes in isometric tension, observed in the colonic preparations. We then focused our attention mainly on Ca^{2+} and K^{+} currents. Concerning on Ca^{2+} currents, on colonic SMCs, the high voltage-activated L-type Ca^{2+} channels represent the major path for Ca^{2+} influx useful to activate the contractile machinery in colonic SMCs (*Bolton et al., 1999*); it leads to tension increase and it is responsible of the spontaneous contractions observed in colon (*Lecchini et al., 1991*). We here found that the prevalent calcium-dependent activation of the contractile machinery resulted hampered by the hormone RLX in colon (as well as in ileum), causing a consistent reduction of the Ca^{2+}

current peak size flowing through L-type Ca^{2+} channels and the alteration of the channels kinetics. About the possible mechanism involved, we can suggest the usual channels phosphorylation (by PKA, PKG or PKC) or second messengers cascade. Particularly, cGMP-activated PKG is a well-known negative modulator of L-type Ca^{2+} channels (*Morgado et al., 2012*). Thus RLX may cause the observed effect on L-type Ca^{2+} channels by triggering, at least, the cGMP signalling pathway. In agreement, in these electrophysiological experiments in colon, either ODQ or the specific inhibitor of PKG (KT5823) pre-treatment abolished the effect of RLX, suggesting that the NO/cGMP/PKG pathway is actually downstream to the effect of RLX on RMP. The consequent reduction of Ca^{2+} entry through L-type calcium channels can further justify a scarce availability of Ca^{2+} ions in the internal medium, since also Ca^{2+} released from internal stores mainly depends on extracellular Ca^{2+} influx (*Hennig et al., 2002*), so furnishing an explanation for the decrease of basal tension observed by the mechanical experiments in all our preparations. In this view, muscle relaxation accompanied by a decrease of cytosolic Ca^{2+} concentration, induced by exogenous NO, in the circular muscle of rat distal colon has been also reported (*Colpaert et al., 2005*).

The hyperpolarizing effect of RLX on RMP has been systematically observed in this study in any preparation and may undoubtedly contribute to keep the SMC membrane potential far from the voltage threshold for L-type I_{Ca} (-30 mV) and mechanical activation in any case. However, in colonic smooth muscle we observed an increased mechanical activity that should be somehow justified. Indeed, the membrane hyperpolarization can progressively cause an increase of the driving force value for Ca^{2+} ions entry. Calcium influx can thus take place through a set of ion channels different to the L-type ones, since these channels are not supposed to be activated at a resting potential more negative than -30 mV. Consequently, external Ca^{2+} can only flow

through the NSSC, such as stretch activated channels (*Sbrana et al., 2008*), and this Ca^{2+} influx can slightly depolarize the membrane again. The observation that RLX, in the presence of NSCC blocker ($GdCl_3$), had no longer effects on the membrane potential of colonic SMCs strongly indicates that NSCC are involved in RLX effects, particularly on the cycles of slow hyperpolarization/depolarization oscillations as well as on the increase of the superimposed rapid rhythmic waves. Other than influencing the tension development, the diminished entry of Ca^{2+} ions through L-type Ca^{2+} channels paralleled by a faster kinetics can have a role on regaining a polarized membrane potential after the depolarization: it can be less effective in activating BK channels causing a decrease of K^+ outflow and this was actually what we observed. Since K^+ outflow through BK channels is one of the main responsible of regaining the normally polarized membrane potential, the inhibition of BK channels may tend to keep the colonic SMC depolarized. Moreover, occurring from a more positive membrane potentials eventual spontaneous depolarization may be sometimes smaller in amplitude but higher in frequency. Actually, also this pattern was consistently observed in our records and can partly justify the increase of the spontaneous contractions observed in our mechanical experiments in colon.

It is known that the regulation of RMP is mainly ascribable to K^+ conductance. Indeed, K^+ channel activation is an effective mechanism able to cause hyperpolarization and relaxation of SMCs, where both cGMP and cAMP can modulate K^+ channels activity to elicit this outcome (*Schlossmann et al., 2003*). Based on the important role played by outward ion currents in regulating the RMP and excitability, we also investigated the effect of RLX on K^+ currents known to be expressed on SMCs of GI tract (*Koh et al., 2012*). RLX treatment caused a clear reduction of the voltage- and Ca^{2+}- dependent BK current that can be, at least in part, justified by the reduction of Ca^{2+} entry through

voltage dependent calcium channels. Also in this case, the ODQ pre-treatment in colonic SMC abolished the effect of RLX on SMCs, suggesting that cGMP signalling pathway was necessary for RLX to cause its effect also on K^+ channels. Also I_{Kv} current was reduced by RLX treatment, so it cannot explain a major hyperpolarizing effect. Actually, in this colonic preparation the only current that was slightly increased by RLX was the chromanol-sensitive I_{Ks}, even if the amount of this increase might not be sufficient to justify the resulting membrane hyperpolarization. We can tentatively suggest that other voltage-independent K^+ channels normally involved in the control of colonic cell RMP could be positively influenced by RLX. In this regard, our results indicate that the ATP- and glybenclamide-sensitive K^+ channel could be a good candidate (*Koh et al., 2012*). In fact, under RLX treatment we can reasonably suppose an increase of ATP consumption for different reasons: the activation of NO-cGMP-PKG cascade can lead to an enhanced activity of all the membrane pumps (*Morgado et al., 2012*); the phosphorylation processes triggered by RLX through CG-cGMP-PKG leads to ADP formation. Least, but not last, the increased mechanical activity induced by RLX in colonic preparations could further decrease ATP levels. As a consequence, lowering ATP concentration can activate ATP-sensitive K^+ channels, further accounting for hyperpolarization (*Murphy & Brayden, 1995; Koh et al., 2012*). Actually, in our experiments we found that outward K^+ currents through K_{ATP} channels are required for RLX to exert its effects. In fact, in the presence of the K_{ATP} channel blocker, the hormone was no longer able to induce the cycles of slow hyperpolarization/ depolarization oscillations and the rapid rhythmic waves. These latter may be the cause of maintaining/inducing to the increased spontaneous activity elicited by RLX in the mechanical experiments. Thus, the present mechanical and electrophysiological results confirm that the NO/cGMP pathway is involved in the effects of RLX on colonic SMC.

In keeping, several studies have suggested that RLX acts in different smooth muscles by promoting the biosynthesis of NO (*Baccari & Bani, 2008*). Notably, even if NO is considered as a substance causing GI relaxation (*Grider et al., 1992; Rand, 1992*), NO-mediated contractile effects have also been reported in the cat ileum (*Barthò & Lefebvre 1994*) as well as in the rat small and large intestine (*Barthò & Lefebvre 1995*).

In summary, the results of this study offer the first direct evidence that RLX is able to affect the RMP value and the electrophysiological properties of Ca^{2+} and K^+ channels in colonic SMCs. Particularly, RLX effects may be ascribable to the reduction of Ca^{2+} currents through the voltage-dependent L-type channels and to the increase of K^+ outflow mainly from Ks and K_{ATP} sensitive channels. The resulting membrane hyperpolarization increases the driving force for Ca^{2+} entry through NSCC that, in turn, induces membrane repolarization leading to muscle contraction. This event reduces the intracellular ATP, increasing the K_{ATP} current and inducing again a new hyperpolarization. Taking into account that the hyperpolarization/depolarization cycles are desynchronized among different cells, these observations could explain the mechanical effects exerted by RLX in the whole colonic preparations. In this view, the hyperpolarizing tendency and the greater rate of rapid rhythmic waves induced by RLX in the SMCs could account for the mechanical decrease of the basal tension and the increase in amplitude of the spontaneous contractions, respectively. Thus, RLX may be considered a useful regulator of the GI tract motility since it can directly modulate ion channels activity through the NO/cGMP pathway.

Influence of RLX on ileal smooth muscle

The mechanical and electrophysiological data obtained in ileum indicate that, similarly to what observed in colon, RLX is able to depress the basal muscular tone of the

longitudinal smooth muscle, although in the ileum, it induces also a decrease of the spontaneous contractions.

Moreover, at variance with the results obtained in the colon, in which RLX appears to exert its effects only through cGMP signalling pathway (*Baccari et al., 2012; Squecco et al., 2015b*), in ileal preparations, the cGMP does not appear to be the only signalling pathway involved. RLX in fact, seems to exert its effect acting through a dual pathway, involving both GC/cGMP and AC/cAMP regulation.

It has already been reported that in isolated ileal preparations from female mice (*Bani et al., 2002*), RLX was able to act directly on the smooth muscle causing a decay of muscular tension and a reduction in amplitude of spontaneous contractions. Since these effects were significantly blunted by the NO synthesis inhibitor L-NNA and RLX increased i-NOS and e-NOS expression, it was suggested that the inhibitory effects of the hormone mainly occurred through the activation of intrinsic NO biosynthesis (*Bani et al., 2002*). Nevertheless, the possible involvement of additional signalling pathways could not be completely ruled out. In keeping, in the present mechanical results, the depressant actions of RLX are reduced, not only by the GC inhibitor (ODQ), but also by the AC inhibitor (9-CP-Ade), indicating that both cGMP and cAMP are involved in the effects of the hormone on ileal motility. This conclusion is strongly supported by the observation that the effects of RLX were abolished in the concomitant presence of both inhibitors.

In order to give an explanation to the RLX depressant action, we performed an electrophysiological analysis, demonstrating for the first time in ileal preparations, that RLX is able to hyperpolarize the RMP also in this preparation and to affect the biophysical properties of ion channels that can be involved in cell excitability and mechanical activity.

Some considerations about the RMP, typically considered a main determinant of muscular tone, have been already made for the colonic SMC. In this view, K^+ channel conductance and also the mechano-sensitive channels may have a principal role on regulating RMP and excitability (*Sbrana et al., 2008*). It is to note, however, that the precise role of the different K^+ channels (see *Sanders et al., 2006* for review) in the GI SMC membranes permeability and thus, the negative RMP of these cells, remains controversial. In fact, the blockers of all of these channels only yield partial depolarization of gastrointestinal SMCs. Actually, RMP should be considered as the result of the membrane permeability to several ions, such as K^+, Ca^{2+}, Cl^- and Na^+.

In our ileum preparation we found that RLX determined membrane hyperpolarization but, unexpectedly, in this case we observed a depression of all the delayed rectifier K^+ currents (I_{Ks}, I_{BK}, and I_{Kv}). Therefore, to explain the relatively high resting permeability to K^+ causing the hyperpolarization, a significant background conductance should be also suggested. This background conductance can consist of mechanosensitive- and pH-sensitive K^+ conductance (*Sanders & Koh, 2006*), and/or voltage-independent and Ca^{2+}-dependent small conductance K^+ channel (SK) (*Matsuyama et al., 1999*).

Another novel aspect of this part of the study is the demonstration that both cGMP and cAMP are involved in the hyperpolarization of the SMC induced by RLX in ileum SMCs. In fact, ODQ pre-treatment did not completely abolish the effect of RLX on RMP (at variance with what we previously observed in colon) suggesting that NO/guanylate cyclase pathway, although noticeable, is not the only signalling pathway involved. Notably, the signalling cascade of nitrergic inhibitory action associated to membrane hyperpolarization is complicated and still debated and the type of ion channels involved in cGMP-PKG-mediated smooth muscle hyperpolarization has been controversial (*Omori & Kotera, 2007; He & Goyal, 2012; Morgado et al., 2012*).

Moreover, the reduction of the RLX effect on RMP due to 9-CP-Ade pre-treatment, in ileum, supports the involvement of the cAMP signalling pathway too. In accord with Morgado (*Morgado et al., 2012*), we tentatively suggest a sort of cross-talk between the two pathways since the blockade of the synthesis of each cyclic nucleotide seems to prevent a full RLX action also through the other pathway. Moreover, the intracellular levels of these two second messengers are the result of the balance between the rate of their synthesis and the rate of their degradation due to phosphodiesterase (PDE) cleavage and PDEs themselves are also downstream effectors of cAMP and cGMP (*Omori & Kotera, 2007*).

Remarkably, the hyperpolarization of the SMC membrane, as a proved mechanism causing the smooth cell relaxation (*Morgado et al., 2012*) can be accomplished through various processes like the activation of K^+ and Cl^- channels or/and the inactivation of Na^+ and Ca^{2+} channels. However, in our ileal SMCs, RLX treatment caused RMP hyperpolarization but decreased the K^+ efflux through the voltage-dependent channels. Particularly, the hormone caused a clear reduction of I_{Ks}, I_{Kv} and of the voltage- and Ca^{2+}-dependent I_{BK}. Interestingly, we also observed that RLX induced a faster kinetic of I_{Kv} activation indicating that, under depolarizing stimuli, these channels could be activated faster especially for negative potentials, which is next to the resting potentials, so to regain early the negative potentials leading to muscle relaxation. Moreover, since the delayed rectifier Kv channel has the lowest voltage threshold of activation, it may be the most involved voltage-dependent K^+ channel in the control of the RMP. However, Tanaka *et al.* (*2006*) showed that the contribution of Kv channel is irrelevant for the relaxations induced by NO in thoracic aorta, but is significant in mesenteric artery from the rat, suggesting that cGMP signalling about on K^+ channels could essentially vary in different preparations (*Koh et al, 2012*).

The effects of RLX on RMP and Ca^{2+} currents in ileal SMCs almost resemble the results obtained in colon and, once more, the reduction of BK current observed in our experiments can be, at least in part, justified by the reduction of Ca^{2+} entry through voltage dependent Ca^{2+} channels. This reduction of Ca^{2+} influx fits well with the depressant actions of RLX on the mechanical activity of ileum. The ODQ pre-treatment did not completely abolish the effect of RLX, since the K^+ current amplitude measured was still less than control, suggesting that cGMP was not the only cyclic nucleotide involved in these channels regulation. Again, we suggest the contribution of the other signalling pathway mediated by adenylate cyclase. Indeed, the 9-CP-Ade treatment resulted more efficient in blocking RLX effect on all the voltage-dependent currents investigated in ileum SMCs that was almost completely reversed. The current amplitude was similar to control records suggesting that cAMP could be upstream in the cascade of events induced by RLX action. Accordingly, both the cGMP and the cAMP signalling pathways are involved in the effects of RLX on voltage dependent K^+ channels, but this effect hardly explain the observed hyperpolarization of RMP. Maybe other kinds of K^+ channels can be implied in RLX action on modulating RMP of ileal SMCs, but due to the complexity of K^+ channels expression in the GI tract (*Sanders et al., 2006*) and of their regulation, this aspect deserves a further dedicated study.

Another possible explanation that can, at least in part, justify the detected hyperpolarization can come from the here observed reduction of the resting nonspecific background membrane conductance induced by RLX. Moreover, the detected effect of RLX on $I_{Ca,L}$ decrease may support the above concept: any reduction of Ca^{2+} influx through membrane channels can facilitate the setting of negative charges in the inner side of the membrane. Finally, we should bear in mind that cGMP and cAMP, activating PKG and PKA, can also modulate other transport systems such as electrogenic pumps

increasing their activity (*Morgado et al., 2012*) and thus adding further positive charges on the outer side of the membrane, and contributing to the negative RMP.

In relation to Ca^{2+} influx, we already discussed the role of high voltage-activated L-type Ca^{2+} channels as chief path for Ca^{2+} entry useful to trigger the contractile machinery in intestinal SMCs, and the reason why their modulation represents another effective mechanism playing a role in SMC relaxation. Thus, also in ileum, the reduction of Ca^{2+} entry through L-type calcium channels induced by RLX can further justify its depressant effects observed in the present mechanical experiments. The L-type Ca^{2+} channels activation strictly depends on membrane potential: negative voltages as well as steady-state depolarizations (leading to channel inactivation) lead to channel closure and myorelaxation.

In addition, these voltage-gated Ca^{2+} channels can be also modulated by several signalling systems such as cyclic nucleotides. Even if data about this item are sometimes contradictory (*McDonald et al., 1994*) in general, it is accepted that cAMP and cGMP inhibit L-type Ca^{2+} channels. Our results actually support this clue: L-type Ca^{2+} channels resulted inhibited by RLX treatment and both cGMP and cAMP synthesis are involved in this action. In fact, the ODQ pre-treatment did not completely abolish the effect of RLX, since the current observed was still less than control. This suggests that the L-type Ca^{2+} channel could even be negatively modulated by the other cyclic nucleotide. The 9-CP-Ade treatment resulted more efficient in blocking RLX action: the current amplitude was similar to control records, suggesting that cAMP could be upstream in the RLX action and this signalling pathway is activated earlier than NO-cGMP.

In summary, we found that the peptide hormone RLX is able to modulate the ileal SMCs activity from female mouse still inducing the decrease of basal tone and of the

contraction amplitude and these effects go together with the membrane hyperpolarization, the decrease of resting conductance and the decreased Ca^{2+} influx through L-type channels. However, in ileum SMCs all these actions are exerted by RLX through a dual signalling pathway involving both cGMP and cAMP formation, as strongly suggested by the ability of ODQ plus 9-CP-Ade to antagonize the effects of RLX in either the mechanical or the electrophysiological experiments.

Taken together, all the above results indicate that RLX can be considered an intestinal motility modulator since it is able to induce significant changes in smooth muscle-mechanical and -electrical activity of both colon and ileum preparations.

Effects of ADPN on gastric fundal smooth muscle

The results of the present thesis work indicate that besides RLX, ADPN too is able to influence GI smooth muscle activity.

In this view, it is known, that some adipokines released from the adipose tissue, such as leptin, may influence GI motility (*Yarandi et al., 2011; Okumura & Nozu, 2016*), whose motor changes represent peripheral factors able to invoice signals to the central structures involved in the regulation of food intake (*Duca & Covasa, 2012)*. Among adipokines, ADPN attracted our attention since its physiological effects on the GI smooth muscle motility have been poorly examined. Thus, in order to investigate if ADPN was able to influence gastric smooth muscle activity, we performed mechanical, electrophysiological and immunohistochemical experiments on gastric fundal preparations from female mice.

We revealed the expression of ADPN receptors (AdipoR1 and AdipoR2) in our preparation and we found, for the first time to our knowledge, that ADPN is able to influence either the basal tension or the biophysical properties of the gastric fundus

SMCs. Particularly, the mechanical experiments showed that ADPN caused a long-lasting decay of the basal tension that was unaffected by TTX, indicating that the hormone exerts its effects directly on the smooth muscle. Accordingly, likewise the experiments shown for RLX effect on intestinal SMCs, we performed the electrophysiological analysis to better understand the depressant action of ADPN.

As already discussed for RLX on intestinal SMCs, also ADPN caused a prevalent tendency to hyperpolarize the RMP in gastric preparation. Noteworthy, the present electrophysiological study demonstrates for the first time that the ADPN is able to affect the membrane passive properties of gastric SMCs, inducing the increase of the cell capacitance, index of cell surface, and the decrease of the specific membrane conductance which may justify the decay of the basal tension observed with the mechanical experiments and the hyperpolarization of the RMP in the SMCs.

Once more, since we observed that ADPN was able to affect the mechanical response in gastric longitudinal muscle layer acting directly on smooth muscle, it became essential to study the effect of this peptide on I_{Ca} In agreement with previous studies from our research group on gastric fundus preparations (*Squecco et al., 2013*) we confirmed the occurrence of both T and L-Type calcium currents also in the present preparations and, outstandingly, $I_{Ca,T}$ and $I_{Ca,L}$ represent a key events that may affect excitation-contraction coupling in SMC. Again, as observed with RLX on intestinal SMC, we found that the addition of ADPN to the bath solution induced a decrease of the total current amplitude as well as different voltage dependence. When this type of experiment was performed in the presence of nifedipine to block L-type Ca^{2+} channels, we could observe the residual low voltage activated current, $I_{Ca,T}$, which resulted reduced in amplitude by the addition of the hormone to the bath medium. Moreover, also $I_{Ca,L}$, is decreased in amplitude by the hormone, without altering significantly its time to peak,

but positively shifting of about 10 mV the voltage value of the pulse required to evoke the semi-maximal current amplitude. Over again, the consequent reduction of Ca^{2+} entry through L- and T-type calcium channels due to the hormone, other than leading the SMC to a lower predisposition to myogenic contraction may affect calcium dependent potassium channels (BK) and it was actually what we observed. Adding ADPN to the bath medium induced a slight increase of the total outward k^+ current. Particularly, this apparent slight increase was mostly due to the potentiation of the K_V and K_s current amplitude that may account for the hyperpolarization of the sarcolemma membrane and the decay of the basal tension induced by the hormone. In contrast, as also observed for RLX, the amplitude of I_{BK} was clearly reduced by ADPN treatment, justified, at least in part, by the reduction of Ca^{2+} entry through voltage dependent calcium channels.

Remarkably, since ADPN caused a slow and long-lasting SMC hyperpolarization, resembling the typical features due to NO stimulation (*Matsuyama et al., 1999*), we suggest the involvement of this pathway also in our gastric preparation. In fact this pathway could be involved as one of the possible ways through which the hormone exerts its effects, since it has been already reported as an intracellular pathway in vascular smooth muscle (*Han et al., 2007*). However, further experiments have already been planned to better investigate this and/or other possible signalling pathways through which ADPN may modulate the smooth muscle activity of the gastric fundus.

In summary, this part of my research offers the first direct evidence that ADPN is able to affect the RMP value, the biophysical properties of Ca^{2+} and K^+ channels and to influence the mechanical activity in gastric preparations. Particularly, ADPN effects may be ascribable to the reduction of Ca^{2+} currents through the voltage-dependent L-type and T-type channels and to the increase of K^+ outflow mainly from Ks and Kv sensitive channels.

Conclusions

Our data indicate that both hormones, ADPN and RLX, can be considered valid modulators of the GI smooth muscle activity since they are able to influence the mechanical responses as well as the biophysical properties of GI smooth muscle preparations. At least in part, the hormones induce similar mechanical and electrophysiological effects in the three different preparations used. However, differences were noted among the segments considered suggesting a dissimilar and peculiar sensitivity to the hormonal signals within GI tract. For instance, RLX appears to exert its effects only through cGMP signalling pathway in the colon, while both cGMP and cAMP seem to be involved in ileal preparations.

From a physiological point of view, the results obtained in colonic SMCs can lead to the speculation that the slow hyperpolarization caused by RLX and the consequent decay of the mechanical basal tension, may contribute to retain colonic content in order to favour water absorption. This may account for the constipation symptom frequently observed in pregnancy, during which the hormone attains high levels. On the other hand, the increase of the rapid rhythmic waves rate could contribute to the increased contractile activity, aimed to mix the large intestine content and thus contributing to the absorption. In addition, the dual signalling pathway, activated by RLX in ileal preparation, may represent a reinforcing and cross-talking (redundant) mechanism for the hormone aimed to guarantee its efficacious and to prolong its modulation, since all neural, hormonal, and paracrine regulation of smooth muscle contractions is superimposed upon a basal excitability state of SMC. This underlies the importance of the depressant effects of the hormone directed to slowly emptying in the small intestine, to favour the absorption of nutrients, particularly important during peculiar situation such as pregnancy.

Finally, the results obtained with ADPN in gastric SMCs, such as the hyperpolarization

of SMCs and the consequent decay of the mechanical basal tension together with the reduction of calcium influx, may contribute to muscle relaxation and to increase the organ capacity. Since gastric distension represents, from a physiological point of view, a peripheral satiety signal, it could speculated that the relaxant effects of ADPN might concur to suppress feeding behaviour in rodents. These observations provide a stimulating background to the challenging hypothesis that ADPN could be a potential therapeutic tool in the treatment of obesity and eating disorders and, certainly, this issue deserves to be further investigated.

Chapter 5

My collaboration to other researches during the PhD course

In addition to the above results concerning on the study of the effects of RLX and ADPN on GI smooth muscle, during these three years of PhD course, I had the possibility to collaborate on other different projects, involving also other organs and tissues, in which the mechanical and the electrophysiological techniques have been separately employed. The published results are shortly reported below.

5.1 Glucagon-like peptide 2 counteracts the mucosal damage and the neuropathy induced by chronic treatment with cisplatin in the mouse gastric fundus.

(Pini A, Garella R, **Idrizaj E**, Calosi L, Baccari MC, Vannucchi MG. *Neurogastroenterol Motil.*, 28: 206-216, 2016)

Glucagon-like peptide-2 (GLP-2) is a pleiotropic hormone synthesized and secreted by the enteroendocrine 'L' cells, able to exert intestine-trophic and anti-inflammatory effects. The antineoplastic drug cisplatin causes GI alterations with clinical symptoms (nausea and vomiting) that greatly affect the therapy compliance. Experimentally, it has been reported that chronic cisplatin treatment caused mucosal damage and enteric neuropathy in the rat colon. Thus, through a combined immunohistochemical and functional approach, this study was addressed to investigate if [Gly2]GLP-2 (a GLP-2 analog), was able to counteract the detrimental effects of long-term cisplatin administration in the mucosa and myenteric neurons of mouse gastric fundus. The morphological experiments showed a reduction in the epithelium thickness in cisplatin-treated mice, which was prevented by [Gly2]GLP-2 co-treatment. Immunohistochemistry demonstrated that cisplatin caused a significant decrease in myenteric neurons, mainly those expressing neuronal nitric oxide synthase (nNOS), which was prevented by [Gly2] GLP-2 co-treatment. In the functional experiments, [Gly2]GLP-2 co-treatment counteracted the increase in amplitude of the neurally induced contractions observed in strips from cisplatin-treated animals. The NO synthesis inhibitor, L-NG-nitro arginine, caused an increase in amplitude of the contractile responses that was greater in preparations from cisplatin+[Gly2]GLP-2 treated mice compared to the cisplatin-treated ones. In conclusion, the results of this study demonstrated that in cisplatin long-term treated mice, [Gly2]GLP-2 was able to counteract both the mucosal gastric fundus damage, by preventing the epithelium thickness decrease, and the neuropathy, by protecting the nNOS neurons. Taken together, the present data suggested that [Gly2]GLP-2 could represent an effective strategy to overcome the distressing GI symptoms present during the anti-neoplastic therapy.

5.2 Inhibitory effects of relaxin on cardiac fibroblast-to-myofibroblast transition: an electrophysiological study.

(Squecco R, Sassoli C, Garella R, Chellini F, **Idrizaj E,** Nistri S, Formigli L, Bani D, Francini F. *Exp Physiol*., 100: 652-666, 2015)

This study, performed in collaboration with the section of Anatomy and Histology of our Department, was addressed to investigate the role of RLX as a possible antifibrotic agent. Particularly, the ability of the hormone to influence the electrophysiological events associated with the differentiation of cardiac stromal cells to myofibroblasts was evaluated. Primary cardiac proto-myofibroblasts and NIH/3T3 fibroblasts were induced to myofibroblasts by transforming growth factor-β1, and the electrophysiological features of both cell populations were investigated by whole-cell patch clamp. Myofibroblast differentiation is a key mechanism of wound healing and the reparative response to organ/tissue damage. Physiologically, myofibroblasts progressively disappear upon wound repair, whereas their persistence gives rise to fibrosis and, eventually, organ failure. Previous studies have investigated the electrophysiological changes occurring in myofibroblast differentiation. In particular, the inward-rectifying K^+ (I_{Kir}) current is considered essential for controlling the RMP in both ventricular fibroblasts and myofibroblasts, and its alterations might be involved in the functional derangement of fibroblasts from physiological to fibrogenic function.

On this regard, we demonstrated, for the first time, that RLX was able to reduce both voltage- and Ca^{2+} -dependent delayed-rectifier and inward-rectifying K^+ currents that were typically increased in myofibroblasts compared with proto-myofibroblasts, suggesting that this hormone was able to antagonize the biophysical effects of transforming growth factor-β1 in inducing myofibroblast differentiation. These novel effects of RLX on the electrical properties of cardiac stromal cell membrane correlate well with its well-known ability to suppress myofibroblast differentiation, thus supporting a possible use of RLX on the treatment of cardiac fibrosis.

5.3 Low intensity 635 nm diode laser irradiation inhibits fibroblast-myofibroblast transition reducing TRPC1 channel expression/activity: New perspectives for tissue fibrosis treatment.

(Sassoli C, Chellini F, Squecco R, Tani A, **Idrizaj E,** Nosi D, Giannelli M, Zecchi-Orlandini S. *Lasers Surg Med.*, 48: 318-332, 2016)

Continuing on the study of fibrosis, we investigated the effects of a low intensity 635±5 nm diode laser irradiation on fibroblast-myofibroblast transition, as a key event in the onset of fibrosis, and elucidated some of the underlying molecular mechanisms. Low intensity diode laser is considered a safe technology and is applied in several branches of medicine and dentistry for pain management, to promote coagulation, and reduce inflammation. Moreover, many studies showed the beneficial effects of the photobiomodulation therapy on healing and regeneration processes at different tissues. Along this line, we have demonstrated that therapy with different types of diode lasers was able to improve healing in chronic periodontitis patients. Furthermore, photobiomodulation therapy was reported to have beneficial effects in reducing fibrosis in different damaged organs. However, despite these promising data, the anti-fibrotic potential of this kind of laser therapy needs to be further investigated and confirmed prior to clinical use as new treatment option for fibrosis. On this regard the aim of this study was to further extend the knowledge on the anti-fibrotic action of photobiomodulation by examining the effect of low-energy diode laser irradiation on the in vitro transition of NIH/3T3 fibroblasts into myofibroblasts and to better understand its molecular mechanisms.

We observed that diode laser treatment inhibited TGF-β1-induced fibroblast–myofibroblast transition as judged by reduction of stress fibres formation, a-smooth muscle actin and type-1 collagen expression and by changes in electrophysiological properties such as RMP, cell capacitance and inwardly rectifying K^+ currents. This laser effect was shown to involve also transient receptor potential canonical channel (TRPC1) functionality. Thus, diode laser treatment inhibited TGF-β1/Smad3-mediated fibroblast-myofibroblast transition by involving also the modulation of TRPC1. These data contribute to support the potential anti-fibrotic effect of Low-level laser therapy and may offer further information for considering this therapy as a promising therapeutic tool for the treatment of tissue fibrosis.

5.4 Hyponatremia alters the biophysical properties of neuronal cells independently of osmolarity: a study on Ni^{2+} -sensitive current involvement.

Squecco R, Luciani P, **Idrizaj E,** Deledda C, Benvenuti S, Giuliani C, Fibbi B, Peri A, Francini F. *Exp Physiol*., 101: 1086-100, 2016

Hyponatraemia is an independent predictor of in-hospital mortality and represents a clinical and social burden. This is demonstrated by several studies published in the last few years, which have shown that mild chronic hyponatraemia may lead to negative consequences on health status, such as altered gait and increased risk of falling, attention deficits, fractures and bone loss.

Thus, this study was conducted on SK-N-AS and SH-SY5Y neuronal cell lines in order to verify whether hyponatremic condition can per se cause electrophysiological alterations and if these effects vary over time. Accordingly, we made experiments in low sodium medium either in hypo-, Osm(-), or iso-osmotic condition, Osm(+), for a short (24 h) or long time (7 d). By a patch pipette in voltage clamp condition, we recorded possible modifications of Cm and Gm. Our results indicate that in both Osm(-) and Osm(+) medium, Cm and Gm, show a similar increase but such effects were differently dependent on time in culture. Particularly, regarding to the possibly involved mechanisms for the maintenance of Cm, Gm and Gm /Cm in Osm(+) condition, we observed a greater contribution of Na^+ /Ca^{2+} exchanger respect to Osm(-) and control condition. Thus, the electrophysiological results of this study help us to understand the mechanisms of volume regulation following ionic perturbation. Our results can also have relevance in a translational perspective because the Na^+ /Ca^{2+} exchanger can be considered a target for planning novel therapies.

5.5 An electrophysiological study on the effects of BDNF and FGF2 on voltage dependent Ca^{2+} currents in developing human striatal primordium.

Squecco R, **Idrizaj E,** Morelli A, Gallina P, Vannelli GB, Francini F. *Mol Cell Neurosci*., 75: 50-62, 2016

Selective neuronal loss of the striatum, accounts for most of the clinical features of Huntington's disease (HD). No proven medical treatments are currently available to counteract the devastating course of the disease. Several studies conducted in both HD animal models and pilot clinical trials have demonstrated that the replacement of degenerated striatum and repair of circuitries by grafting fetal striatal primordium was feasible, safe and might counteract disease progression, thus prospecting an effective strategy to treat HD patients. Accordingly, transplantation of human nervous primordia is being explored as a reparative strategy in the treatment of neurodegenerative diseases, such as HD. However, a better comprehension of striatal ontogenesis was required to assess the fetal graft regenerative potential. During neuronal development, neurotrophins exert pleiotropic actions in regulating cell fate and synaptic plasticity. In this regard, brain-derived neurotrophic factor (BDNF) and fibroblast growth factor 2 (FGF2) are crucially implicated in the control of fate choice of striatal progenitor cells. In this study, we intended to refine the functional features of human striatal precursor (HSP) cells isolated from ganglionic eminence of 9-12week old human fetuses, by studying with electrophysiological methods the effect of BDNF and FGF2 on the membrane biophysical properties and the voltage-dependent Ca^{2+} currents. These features are particularly relevant to evaluate neuronal cell functioning and can be considered reliable markers of the developmental phenotype of human striatal primordium. Our results demonstrated that both growth factors induced membrane hyperpolarization, increased the Cm and reduced Gm and Gm/Cm values, suggesting a more efficient control of resting ionic fluxes. Moreover, the treatment with both neurotrophins enhanced N-type Ca^{2+} current amplitude and reduced L- and T-type ones, indicating that BDNF and FGF2 may help HSP cells to attain a more functionally mature phenotype. Moreover, the results of this study can also suggest a possible use of the neurotrophins addition to the culture medium to further improve n-HSP regenerative potential when grafted in patients suffering from neurodegenerative diseases such as HD.

5.6 Tumor Necrosis Factor α Impairs Kisspeptin Signalling in Human Gonadotropin-Releasing Hormone Primary Neurons.

Sarchielli E, Comeglio P, Squecco R, Ballerini L, Mello T, Guarnieri G, **Idrizaj E,** Mazzanti B, Vignozzi L, Gallina P, Maggi M, Vannelli GB, Morelli A. *J Clin Endocrinol Metab*., jc20162115, 2016 [Epub ahead of print]

Previous studies have suggested that inflammatory pathways may impair central regulatory networks involving gonadotropin-releasing hormone (GnRH) neuron activity. Little was known about the effects of circulating proinflammatory molecules on human GnRH neurons. Knowledge about the regulatory network governing GnRH system, in both physiological and pathophysiological conditions, was based on laboratory animals, in particular rodents. Moreover, in vitro studies on GnRH neuron biology used immortalized cell lines either of mouse or rat origin. Hence, the primary objective of this study was to establish a cellular model of GnRH neurons of human origin and analyse the effects of proinflammatory cytokines on their biological properties. We believed that such a model could represent a valuable tool for investigating those factors that might directly influence human GnRH neuron function. For this purpose, the primary human fetal hypothalamic (hfHypo) cell cultures were isolated from brain of three 12 week-old fetuses. Responsiveness to kisspeptin (0.1nM-1μM), the main physiological regulator of GnRH neurons, was evaluated for biological characterization of hfHypo cells. Tumor necrosis factor alpha (TNFα) was used as pro-inflammatory stimulus. The results of the present study indicated that, these primary hfHypo cell cultures were characterized by a high percentage of GnRHpositive cells (80%), abundantly expressing the kisspeptin receptor, KISS1R, and able to release GnRH in response to kisspeptin. Moreover, kisspeptin induced changes in electrophysiological membrane properties. TNFα exposure determined a specific inflammatory intracellular signalling and significantly reduced GnRH secretion, KISS1R expression and kisspeptin-induced depolarizing effect. Thus, in conclusion, the hfHypo cells represent a novel tool for in vitro investigations on human GnRH neuron biology. TNFα may directly affect GnRH neuron function by interfering with KISS1R expression and cyclogenesis, thereby impairing kisspeptin signalling.

5.7 Searching for Classical Brown Fat in Humans: Development of a Novel Human Fetal Brown Stem Cell Model.

Di Franco A, Guasti D, Squecco R, Mazzanti B, Rossi F, **Idrizaj E,** Gallego-Escuredo JM, Villarroya F, Bani D, Forti G, Vannelli GB, Luconi M. *Stem Cells.*, 34: 1679-1691, 2016

Brown adipose tissue (BAT) is a thermogenic organ, densely vascularized that consists of adipocytes filled with small lipid droplets and mitochondria specialized in dissipating energy derived from fatty acid oxidation. This specialized function is due to the unique expression of uncoupling-protein-1 (UCP1), a mitochondrial transmembrane protein that shunts the proton gradient generated by the respiratory chain resulting in heat production. Besides thermoregulation, BAT has also recently been demonstrated to act as an endocrine organ characterized by a specific brown adipokine secretion. Animal studies, showed that BAT transplantation could restore the correct metabolism in diet-induced weight gain and related disorders, as well as evidence from adult humans strongly indicated that stimulating human BAT content and activity might represent a suggestive target for the treatment of obesity and metabolic disorders by increasing energy expenditure.

However, due to the limited extension in adult humans of brown depots, which are dramatically reduced after birth, solid cell models to study human brown adipogenesis and its regulatory factors in pathophysiology were needed. To this end, in this study, we described an innovative human model of brown adipose stem cells, hfB-ASC, derived from fetal interscapular brown fat depots, obtained during medical abortion. Besides the characterization of their stem and classical brown adipose properties, we demonstrated that these cells retain a specific intrinsic differentiation program to functional brown adipocytes, even spontaneously generating organoid structures with brown features. Moreover, this study investigated for the first time the thermogenic and electrophysiological activity of the in vitro-derived fetal brown adipocytes compared to their undifferentiated precursors hfB-ASC, in basal and norepinephrine-induced conditions.

The electrophysiological results showed significant differences between undifferentiated hfB-ASC and adipocytes in vitro differentiated with DIM cocktail. Similar results were obtained when differentiation was conducted with norepinephrine (NE) addition. Undifferentiated stem cells (hfB-ASC) had a rather depolarized resting potential, whereas the corresponding differentiated adipocytes (ADIPO) tended to hyperpolarize:

this hyperpolarization is a typical feature of differentiated and less proliferating cells. Moreover, the Rm and Cm were respectively lower and higher in differentiated brown fat cells vs. undifferentiated hfB-ASC, suggesting a cell enlargement occurring during adipose differentiation, maybe due to cytoskeleton reorganization and lipid droplet accumulation in mature adipocytes. It was also confirmed the mesenchymal nature of these cells characterized by the presence of outwards K^+ currents. The majority of undifferentiated hfB-ASC showed small-amplitude K^+ currents. Similar currents were recorded in differentiated brown ADIPO, however characterized by significantly greater amplitude. Furthermore, a rapid increase in the membrane conductance was recorded in differentiated brown adipocytes after NE acute addition, suggesting the ability of mature adipocytes to depolarize in response to NE.

In conclusion, in this study, from interscapular brown fat of the human fetus we developed and functionally characterized a novel physiological brown adipose stem cell model early programmed to brown differentiation. It may represent a unique opportunity for further studies on brown adipogenesis processes in humans as well as the most suitable target to study novel therapeutic approaches for stimulating brown activity in metabolic pathologies.

Abbreviations

4-AP	4-aminopyridine
9-CP-Ade	9-cyclopentyladenine mesylate
AC	adenylate cyclase
ACRP30	complement-related protein
AdipoR	adiponectin receptor
ADPN	adiponectin
AMPK	AMP-activated protein kinase
ATP	adenosine triphosphate
$BaCl_2$	barium chloride
BH4	tetrahydrobiopterin
BK	Ca^{2+}-dependent K^+ channels
cAMP	cyclic adenosine monophosphate
CCK	cholecystokinin
cGMP	cyclic guanosine monophosphate
Chr	chromanol
C_m	cell linear capacitance
CNS	central nervous system
CPI-17	PKC-potentiated inhibitory protein
Ctr	control
E-C	excitation-contraction
EGTA	ethylene-bis(oxyethylenenitrilo)tetraacetic acid
eNOS	endothelial NOS
ENS	enteric nervous system
FAD	flavin adenine dinucleotide
FMN	flavin mononucleotide
GBP28	gelatin-binding protein-28
GC	guanylate cyclase
$GdCl_3$	gadolinium chloride
GI	gastrointestinal
Glbn	glybenclamide

GLP-1	glucagon-like peptide 1
GLP-2	glucagon-like peptide 2
G_m	membrane conductance
Gm/Cm	specific membrane conductance
H1 relaxin	Human relaxin-1
H2 relaxin	Human relaxin-2/relaxin
H3 relaxin	Human relaxin-3
HEPES	4-(2-hydroxyethyl)-1-piperazineethanesulfonic acid
HMW	high-molecular-mass
HP	holding potential
I_{BK}	BK current/ large conductance Ca^{2+} activated K^+ current
IbTx	iberiotoxin
I_{Ca}	L-type Ca^{2+} current
ICC	interstitial Cajal-cells
IK	intermediate-conductance Ca^{2+}-activated K^+ channels
$I_{K,DR}$	voltage-dependent delayed rectifier K^+ current
I_{Ks}	slowly activating Chr-sensitive K^+ current
I_{Ktot}	total outward K^+ currents
I_{Kv}	fast activating α-DTX-sensitive K^+ current
IL-6	interleukin 6
iNOS	inducible NOS
INSL 3,5,6	insulin like peptides 3,5,6
IRS-2	insulin receptor substrate 2
I_{to}	transient-activated K^+ channels
Ka	steepness factor of activation
K_{ATP}	ATP-sensitive K^+ channels
Kh	steepness factor of inactivation
Ks	slow-activated K^+ channels
Kv	fast-activated K^+ channels
MLC20	20 kDa light chain of myosin
MLCK	myosin light chain kinase
MLCP	myosin light-chain phosphatase
NADPH	Nicotinamide adenine dinucleotide phosphate

NANC	non-adrenergic non-cholinergic
NC	negative control
NFkβ	nuclear factor kappa β
nNOS	neuronal NOS
NO	Nitric oxide
NOS	nitric oxide synthase
NSCC	non-selective cation channels
ODQ	1H-[1,2,4]oxadiazolo[4,3-*a*]-quinoxalin-1-one
OVLT	organum vascuosum of the lamina terminalis
OXM	Oxyntomodulin
PCR	Polymerase chain reaction
PKA	Protein kinase A
PKC	Protein kinase C
PKG	cGMP-dependent protein kinase/ Protein kinase G
PP	pancreatic polypeptide
PPARα	peroxisome proliferator-activated receptor alpha
PYY	peptide YY
RLX	Relaxin
R_m	membrane resistance
RMP	resting membrane potential
ROC	receptor-operated channels
RT-PCR	Reverse Transcription-PCR
RXFP	Relaxin family peptide receptors
S1P	sphingosine-1-phosphate
SAC	stretch-activated channels
SFO	subfornical organ
SK	small conductance Ca^{2+}-activated K^+ channels
SMC	smooth muscle cell
TEA-OH	tetraethylammonium hydroxide
tp	peak time
TTX	Tetrodotoxin
Va	voltages causing the half-maximal activation
VDCC	voltage dependent Ca^{2+} channels

Vh	voltages causing the half-maximal inactivation
VIP	vasoactive intestinal peptide
Vrev	apparent reversal potential
ZIPK	zipper-interacting kinase
α-DTX	α-dendrotoxin
τ_h	current inactivation time constant
τ_m	current activation time constant

Bibliography

- Adham IM, Burkhardt E, Benahmed M, Engel W. Cloning of a cDNA for a novel insulin-like peptide of the testicular Leydig cells. *J Biol Chem.*, **268**: 26668-26672, 1993.

- Akbarali HI, Thatte H, He XD, Giles WR, Goyal RK. Role of HERG-like K(+) currents in opossum esophageal circular smooth muscle. *Am J Physiol*., **277**: C1284-C1290, 1999.

- Andersson U, Filipsson K, Abbott CR, Woods A, Smith K, Bloom SR, Carling D, Small CJ. AMP-activated protein kinase plays a role in the control of food intake. *J Biol Chem*., **279:** 12005-1208, 2004.

- Angel F, Go VLM, Schmalz PF, Szurszewki JH. Vasoactive intestinal polypeptide: a putative transmitter in the canine gastric muscolaris mucosa. *J Physiol*., **341**: 641-645, 1983.

- Arita Y, Kihara S, Ouchi N, Maeda K, Kuriyama H, Okamoto Y, Kumada M, Hotta K, et al. Adipocyte-derived plasma protein adiponectin acts as a platelet-derived growth factor-BB-binding protein and regulates growth factor-induced common postreceptor signal in vascular smooth muscle cell. *Circulation*, **105:** 2893-2898, 2002.

- Arita Y, Kihara S, Ouchi N, Takahashi M, Maeda K, Miyagawa J, Hotta K, Shimomura I, et al. Paradoxical decrease of an adipose-specific protein, adiponectin, in obesity. 1999. *Biochem Biophys Res Commun*., **425:** 560-564, 2012.

- Arita Y, Kihara S, Ouchi N. Paradoxical decrease of an adipose-specific protein, adiponectin, in obesity. *Biochem. Biophys. Res. Commun*., **257:** 79-83, 1999.

- Austin CR & Rowlands JW. Mammalian reproduction. In: Short DJ, Woodnott DP (eds.), The IAT Manual of Laboratory Animal Practice and Technique. 2nd ed. Bungay, UK: Lockwood; 340-349, 1969.

- Azzena GB & Mancinelli R. Nitric oxide regenerates the normal colonic peristaltic activity in mdx dystrophic mouse. *Neurosci Lett.*, **261:** 9-12, 1999.

- Baccari MC & Bani D. Relaxin and nitric oxide signalling. *Curr Protein Pept Sci.*, **9:** 638-645, 2008.

- Baccari MC, Bani D, Bigazzi M, Calamai F. Influence of relaxin on the neurally induced relaxant responses of the mouse gastric fundus. *Biol Reprod*., **71:** 1325-1329, 2004b.

- Baccari MC, Calamai F. Relaxin: new functions for an old peptide. *Curr Protein Pept Sci* **5**: 9-18, 2004.

- Baccari MC, Nistri S, Quattrone S, Bigazzi M, Bani Sacchi T, Calamai F, Bani D. Depression by relaxin of neurally induced contractile responses in the mouse gastric fundus. *Biol Reprod.*, **70:** 222-228, 2004a.

- Baccari MC, Nistri S, Vannucchi MG, Calamai F, Bani D. Reversal by relaxin of altered ileal spontaneous contractions in dystrophic (mdx) mice through a nitric oxide-mediated mechanism. *Am J Physiol Regul Integr Comp Physiol*., **293:** R662-R668, 2007.

- Baccari MC, Romagnani P, Calamai F. Impaired nitrergic relaxations in the gastric fundus of dystrophic (mdx) mice. *Neurosci Lett*, **282:** 105-108, 2000.

- Baccari MC, Traini C, Garella R, Cipriani G, Vannucchi MG. Relaxin exerts two opposite effects on mechanical activity and nitric oxide synthase expression in the mouse colon. *Am J Physiol Endocrinol Metab* **303**: E1142-E1150, 2012.

- Baglioni S, Cantini G, Poli G, Francalanci M, Squecco R, Di Franco A, Borgogni E, Frontera S, et al. Functional differences in visceral and subcutaneous fat pads originate from differences in the adipose stem cell. *PLoS One*, **7:** 365-369, 2012.

- Banerjee A, Shen PJ, Ma S, Bathgate RA, Gundlach AL. Swim stress excitation of nucleus incertus and rapid induction of relaxin-3 expression via CRF1 activation. *Neuropharmacology*., **58**: 145-155, 2010.

- Bani D, Baccari MC, Nistri S, Calamai F, Bigazzi M, Bani Sacchi T. Relaxin up-regulates the nitric oxide biosynthetic pathway in the mouse uterus: involvement in the inhibition of myometrial contractility. *Endocrinology*, **140:** 4434-4441, 1999.

- Bani D, Baccari MC, Quattrone S, Nistri S, Calamai F, Bigazzi M, Bani Sacchi T. Relaxin depresses small bowel motility through a nitric oxide-mediated mechanism. Studies in mice. *Biol Reprod.*, **66:** 778-784, 2002.

- Bani D, Bigazzi M, Masini E, Bani G, Bani Sacchi T. Relaxin depresses platelet aggregation. In vitro studies on isolated human and rabbit platelets. *Lab. Invest.*, **73:** 709-713, 1995.

- Bani D, Failli P, Bello MG, Thiemermann C, Bani ST, Bigazzi M, Masini E. Relaxin activates the L-arginine-nitric oxide pathway in vascular smooth muscle cells in culture. *Hypertension*, **31:** 1240-1247, 1998.

- Bani D. Relaxin: a pleiotropic hormone. *Gen Pharmacol*., **28:** 13-22, 1997.

- Barnes PJ. The third nervous system in the lung: physiology and clinical perspectives. *Thorax* **39**: 561-567. 1984.

- Barthó L & Lefebvre RA. Nitric oxide causes contraction in the rat isolated small intestine. *Eur J Pharmacol*., **259:** 101-4, 1994.

- Barthó L & Lefebvre RA. Nitric oxide-mediated contraction in enteric smooth muscle. *Arch Int Pharmacodyn Ther.,* **329:** 53-66, 1995.

- Bathgate RA, Halls ML, van der Westhuizen ET, Callander GE, Kocan M, Summers RJ. Relaxin Family Peptides and Their Receptors. Physiological Reviews **93**: 405-480, 2013.

- Bathgate RA, Hsueh AJ, Sherwood OD. Physiology and molecular biology of the relaxin peptide family. J.D. Neill (Ed.), The Physiology of Reproduction (3rd edn), Raven Press, New York, 701-790, 2006a.

- Bathgate RA, Ivell R, Sanborn BM, Sherwood OD, Summers RJ. International Union of Pharmacology LVII: recommendations for the nomenclature of receptors for relaxin family peptides. *Pharmacol Rev* **58**: 7-31, 2006b.

- Bathgate RA, Ivell R, Sanborn BM, Sherwood OD, Summers RJ. Receptors for relaxin family peptides. *Ann N Y Acad Sci*., **1041**: 61-76, 2005.

- Bathgate RA, Lin F, Hanson NF, Otvos L Jr, Guidolin A, Giannakis C, Bastiras S, Layfield SL, Ferraro T, Ma S, Zhao C, Gundlach AL, Samuel CS, Tregear GW, Wade JD. Relaxin-3: improved synthesis strategy and demonstration of its high-affinity interaction with the relaxin receptor LGR7 both in vitro and in vivo. *Biochemistry* **45**: 1043-1053, 2006c.

- Bathgate RA, Samuel CS, Burazin TC, Layfield S, Claasz AA, Reytomas IG, Dawson NF, Zhao C, Bond C, Summers RJ, Parry LJ, Wade JD, Tregear GW. Human relaxin gene 3 (H3) and the equivalent mouse relaxin (M3) gene. Novel members of the relaxin peptide family. *J Biol Chem.,* **277**: 1148-1157, 2002.

- Batterham RL, Le Roux CW, Cohen MA, Park AJ, Ellis SM, Patterson M, Frost GS, Ghatei MA, Bloom SR. Pancreatic polypeptide reduces appetite and food intake in humans. *J Clin Endocrinol Metab*., **88:** 3989-3992, 2003.

- Belai A, Lefebvre RA, Burnstock G. Motor activity and neurotransmitter release in the gastric fundus of streptozonic-diabetic rats. *Eur J Pharmacol*., 194: 225-234, 1991.

- Bell RJ, Eddie LW, Lester AR, Wood EC, Johnston PD, Niall HD. Relaxin in human pregnancy serum measured with an homologous radioimmunoassay. *Obstet Gynecol*., **69**: 585-589, 1987.

- Benham CD, Bolton TB, Lang RJ, Takewaki T. The mechanism of action of Ba^{2+} and TEA on single Ca^{2+}-activated K+-channels in arterial and intestinal smooth muscle cell membranes. *Pflugers Arch* **403**: 120-127, 1985.

- Biancani P, Walsh JH, Behar J. Vasoactive intestinal peptide: a neurotransmitter for relaxation of the rabbit internal anal shinter. *Gastroenterology*, **89**: 867-874, 1985.

- Blüher M, Bullen JW Jr, Lee JH, Kralisch S, Fasshauer M, Klöting N, Niebauer J, Schön MR et al. Circulating adiponectin and expression of adiponectin receptors in

human skeletal muscle: associations with metabolic parameters and insulin resistance and regulation by physical training, *J. Clin. Endocrinol. Metab*., **91:** 2310-2316, 2006.

❖ Boels K & Schaller HC. Identification and characterisation of GPR100 as a novel human G-protein-coupled bradykinin receptor. *Br J Pharmacol.,* **140:** 932-938, 2003.

❖ Bolton TB, Prestwich SA, Zholos AV, Gordienko DV. Excitation-contraction coupling in gastrointestinal and other smooth muscles. *Ann Rev Physiol*., **61:** 85-115, 1999.

❖ Boyraz M, Cekmez F, Karaoglu A, Cinaz P, Durak M, Bideci A. Serum adiponectin, leptin, resistin and RBP4 levels in obese and metabolic syndrome children with nonalcoholic fatty liver disease. *Biomark Med*., **7:** 737-745, 2013.

❖ Brenman JE, Chao DS, Xia H, Aldape K, Bredt DS. Nitric oxide synthase complexed with dystrophin and absent from skeletal muscle sarcolemma in Duchenne muscular dystrophy. *Cell,* **82:** 743-752, 1995.

❖ Burns AJ, Lomax AE, Torihashi S, Sanders KM, Ward SM. Interstitial cells of Cajal mediate inhibitory neurotransmission in the stomach. *Proc Natl Acad Sci U S A*., **93**: 12008-12013, 1996.

❖ Burnstock G. Comparative studies of purinergic nerves. *J Exp Zool*., **194**: 103-134, 1975.

❖ Burnstock G, Campbell G, Bennet M, Holman ME. Inhibition of the smooth muscle of the taenia coli. *Nature,* **200:** 581-582, 1963.

❖ Burnstock G. Neurotrasmitters and trophic factors in the autonomic nervous system. *J Physiol*., **313**: 1-35, 1981.

❖ Burnstock G. Purinergic nerves. *Pharmac Rev.*, **24:** 509-581, 1972.

❖ Burnstock G. The changing face of autonomic neurotransmission. *Acta Physiol Scand*., **126**: 67-91, 1986.

❖ Calabrese V, Mancuso C, Calvani M, Rizzarelli E, Butterfield DA, Stella AM. Nitric oxide in the central nervous system: neuroprotection versus neurotoxicity. Nat Rev Neurosci., **8:** 766-775, 2007.

❖ Carl A & Sanders KM. Ca^{2+}-activated K channels of canine colonic myocytes. *Am J Physiol*., **257**: C470-C480, 1989.

❖ Chassin D, Laurent A, Janneau JL, Berger R, Bellet D. Cloning of a new member of the insulin gene superfamily (INSL4) expressed in human placenta. *Genomics* **29**: 465-470, 1995.

- Chen H, Montagnani M, Funahashi T, Shimomura I, Quon MJ. Adiponectin stimulates production of nitric oxide in vascular endothelial cells. *J Biol Chem*., **278**: 45021-45026, 2003.

- Chinetti G, Zawadski C, Fruchart J, Staels B. Expression of adiponectin receptors in human macrophages and regulation by agonists of the nuclear receptors PPAR alpha, PPAR gamma and LXR. *Biochem Biophys Res Com*., **314:** 151-158, 2004.

- Cho SY, Beckett EA, Baker SA, Han I, Park KJ, Monaghan K, Ward SM, Sanders KM, Koh SD. A pH-sensitive potassium conductance (TASK) and its function in the murine gastrointestinal tract. *J Physiol*., **565**: 243-259, 2005.

- Cnop M, Havel PJ, Utzschneider KM. Relationship of adiponectin to body fat distribution, insulin sensitivity and plasma lipoproteins: evidence for independent roles of age and sex. *Diabetologia* **46:** 459-469, 2003.

- Coburn RF, Tomita T. Evidence for nonadrenergic inhibitory nerves in guinea pig trachealis muscle. *Am J Physiol.,* **224**: 1072-80. 1973.

- Coeskum T, Sevinec A, Tevetoaglu I, Alican I, Kurtel H, Yeagen BC. Delayed gastric emptyng in conscious male rats following chronic estrogen and progesterone treatment. *Res Exp Med (Berl).*, **195:** 49-54, 1995.

- Colpaert EE1, Levent A, Lefebvre RA. Nitric oxide relaxes circular smooth muscle of rat distal colon through RhoA/Rho-kinase independent Ca^{2+} desensitisation. *Br J Pharmacol*., **144:** 588-94, 2005.

- Conklin D, Lofton-Day CE, Haldeman BA, Ching A, Whitmore TE, Lok S, Jaspers S. Identification of INSL5, a new member of the insulin superfamily. *Genomics*., **60:** 50-56. 1999.

- Coope A, Milanski M, Araújo EP, Tambascia M, Saad MJ, Geloneze B, Velloso LA. AdipoR1 mediates the anorexigenic and insulin/leptin-like actions of adiponectin in the hypothalamus. *FEBS Lett*., **582:** 1471-1476, 2008.

- Currò, D. K^+ channels as potential targets for the treatment of gastrointestinal motor disorders. *Eur J Pharmacol.,* **733:** 97-101, 2014.

- Datta S, Hey VM, Pleuvry BJ. Effects of pregnancy and associated hormones in mouse intestine, in vivo and in vitro. *Plueg Arch*., **346**: 87-95, 1974.

- Dehghan F, Haerian BS, Muniandy S, Yusof A, Dragoo JL, Salleh N. The effect of relaxin on the musculoskeletal system. *Scand J Med Sci Sports*., **24:** e220-e229, 2014.

- Dekeratry DR, Ducker TE, Clench MH, Mathias JR. Progesterone and relaxin disrupt the migrating myoelectric complex (MMC) of the small intestine in rats. *Gastroenterology,* **104:** A1036, 1993.

- Del Angel Meza AR, Beas-Zárate C, Alfaro FL, Morales-Villagran A. A simple biological assay for relaxin measurement. *Comp Biochem Physiol C.*, **99:** 35-39, 1991.

- Delort L, Jardé T, Dubois V, Vasson MP, Caldefie-Chézet F. New insights into anticarcinogenic properties of adiponectin: a potential therapeutic approach in breast cancer, *Vitam. Horm.*, **90**: 397-417, 2012.

- Denzel MS, Scimia MC, Zumstein PM, Walsh K, Ruiz-Lozano P, Ranscht B. T-cadherin is critical for adiponectin-mediated cardioprotection in mice. *J Clin Invest*., **120:** 4342-52, 2010.

- Desai KM, Sessa WC, Vane JR. Involvement of nitric oxide in the reflex relaxation of the stomach to accommodate food or fluid. *Nature*, **351:** 477-479, 1991.

- Dirk H & Richard W. Physiology and Pathophysiology of Potassium Channels in Gastrointestinal Epithelia. *Physiological Reviews,* **88:** 1119-1182, 2008.

- Dowing SJ & Hollingsworth M. Action of relaxin on uterine contractions- a review. *J Reprod Fertil.*, **99:** 275-282, 1993.

- Dschietzig T, Richter C, Bartsch C, Laule M, Armbruster FP, Baumann G, Stangl K. The pregnancy hormone relaxin is a player in human heart failure. *FASEBJ* **15:** 2187-2195, 2001.

- Du XJ, Samuel CS, Gao XM, Zhao L, Parry LJ, Tregear GW. Increased myocardial collagen and ventricular diastolic dysfunction in relaxin deficient mice: a gender-specific phenotype. *Cardiovascular research*. **57:** 395-404, 2003.

- Duca FA & Covasa M. Current and emerging concepts on the role of peripheral signals in the control of food intake and development of obesity. *Br J Nutr.,* **108:** 778-793, 2012.

- Dwyer L, Rhee PL, Lowe V, Zheng H, Peri L, Ro S, Sanders KM, Koh SD. Basally activated nonselective cation currents regulate the resting membrane potential in human and monkey colonic smooth muscle. *Am J Physiol Gastrointest Liver Physiol.*, **301:** G287-G296, 2011.

- El-Yazbi AF, Cho WJ, Cena J, Schulz R, Daniel EE. Smooth muscle NOS, colocalized with caveolin-1, modulates contraction in mouse small intestine. J. Cell. Mol. Med., **12:** 1404-1415, 2008.

- Everson GT. Gastrointestinal motility in pregnancy. *Gastroenterol Clin North Am*., **21**: 751-756, 1992.

- Ewart MA1, Kohlhaas CF, Salt IP. Inhibition of tumor necrosis factor alpha-stimulated monocyte adhesion to human aortic endothelial cells by AMP-activated protein kinase. *Arterioscler Thromb Vasc Biol*., **28:** 2255-2257, 2008.

- Farrelly AM, Ro S, Callaghan BP, Khoyi MA, Fleming N, Horowitz B, Sanders KM, Keef KD. Expression and function of KCNH2 (HERG) in the human jejunum. *Am J Physiol Gastrointest Liver Physiol*., **284**: G883-G895, 2003.

- Fevold HL, Hisaw FL, Meyer RK. The relaxative hormone of the corpus luteum. Its purification ad concentration. *J Am Chem Soc*., 52: 3340-3348, 1930.

- Fink RHA & Veigel C. Calcium uptake and release modulated by counter-ion conductances in the sarcoplasmic reticulum of skeletal muscle. Review. *Acta Physiol Scand*., **156:** 387-96, 1996.

- Francisco C, Neves JS, Falcão-Pires I, Leite-Moreira A. Can Adiponectin Help us to Target Diastolic Dysfunction? *Cardiovasc Drugs Ther*., 2016 [Epub ahead of print]

- Frati A, Ricci B, Pierucci F, Nistri S, Bani D, Meacci E. Role of sphingosine kinase/S1P axis in ECM remodeling of cardiac cells elicited by relaxin. *Mol Endocrinol.*, **29**: 53-67, 2015.

- Friedrich O, Ehmer T, Fink RHA. Calcium currents during contraction and shortening in enzymatically isolated murine skeletal muscle fibres. *J Physiol*., **517**: 757-770, 1999.

- Fu Y, Luo N, Klein RL, Garvey WT. Adiponectin promotes adipocyte differentiation, insulin sensitivity, and lipid accumulation. *J Lipid Res*., **46:** 1369-1379. 2005.

- Fu Z, Gong Y, Löfqvist C, Hellström A, Smith LE. Review: adiponectin in retinopathy. *Biochimica et Biophysica Acta.*, **1862:** 1392-1400, 2016.

- Fujimoto N, Matsuo N, Sumiyoshi H, Yamaguchi K, Saikawa T, Yoshimatsu H, Yoshioka H. Adiponectin is expressed in the brown adipose tissue and surrounding immature tissues in mouse embryos. *Biochim Biophys Acta.*, **1731:** 1-12, 2005.

- Ganella DE, Callander GE, Ma S, Bye CR, Gundlach AL, Bathgate RA. Modulation of feeding by chronic rAAV expression of a relaxin-3 peptide agonist in rat hypothalamus. *Gene Ther.*, **20**:703-716, 2013.

- Garber SL, Mirochnik Y, Brecklin CS, Unemori EN, Singh AK, Slobodskoy L, Grove BH, Arruda JA, Dunea G. Relaxin decreases renal interstitial fibrosis and slows progression of renal disease. *Kidney Int.*, **59:** 876-882, 2001.

- Garella R, Baccari MC. Contribution of endogenous nitrergic and peptidergic influences to the altered neurally-induced gastric contractile responses in strips from dystrophic (mdx) mice. *Regul Pept* **160:** 57-63, 2010.

- Ghantous CM, Azrak Z, Hanache S, Abou-Kheir W, Zeidan A. Differential Role of Leptin and Adiponectin in Cardiovascular System. *Int J Endocrinol*., **2015:** 534320, 2015 Review.

- Glister C, Satchell L, Bathgate RA, Wade JD, Dai Y, Ivell R, Anand-Ivell R, Rodgers RJ, Knight PG. Functional link between bone morphogenetic proteins and insulin-like peptide 3 signaling in modulating ovarian androgen production. *Proc Natl Acad Sci U S A.*, **110**: E1426-E1435, 2013.

- González CR, Caminos JE, Gallego R, Tovar S, Vázquez MJ, Garcés MF, Lopez M, García-Caballero T, et al. Adiponectin receptor 2 is regulated by nutritional status, leptin and pregnancy in a tissue-specific manner. *Physiol Behav*, **99:** 91-99, 2010.

- Grider JR, Murthy KS, Jin JG, Makhlouf GM Stimulation of nitric oxide from muscle cells by VIP: prejunctional enhancement of VIP release. *Am J Physiol*., **262:** G774-G778, 1992.

- Grosse J, Heffron H, Burling K, Akhter Hossain M, Habib AM, Rogers GJ, Richards P, Larder R, et al. Insulin-like peptide 5 is an orexigenic gastrointestinal hormone. *Proc Natl Acad Sci U S A.*, **111:** 11133-11138, 2014.

- Grossman J, Frishman WH. Relaxin: a new approach for the treatment of acute congestive heart failure. *Cardiol Rev*., **18**: 305-312, 2010.

- Halls ML, Bathgate RA, Sutton SW, Dschietzig TB, Summers RJ. International Union of Basic and Clinical Pharmacology. XCV. Recent advances in the understanding of the pharmacology and biological roles of relaxin family peptide receptors 1-4, the receptors for relaxin family peptides. *Pharmacol Rev* **67**: 389-440, 2015.

- Halls ML, van der Westhuizen ET, Bathgate RA, Summers RJ. Relaxin family peptide receptors--former orphans reunite with their parent ligands to activate multiple signalling pathways. *Br J Pharmacol*., **150:** 677-691, 2007.

- Han SH, Quon MJ, Kim JA, Koh KK. Adiponectin and cardiovascular disease: response to therapeutic interventions. *J Am Coll Cardiol*., **49**: 531-538, 2007.

- Hansell DJ, Bryant-Greenwood GD, Greenwood FC. Expression of the human relaxin H1 gene in the decidua, trophoblast, and prostate. *J Clin Endocrinol Metab*., **72**: 899-904, 1991.

- Harwood HJ Jr. The adipocyte as an endocrine organ in the regulation of metabolic homeostasis. *Neuropharmacology*, **63**: 57-75, 2012.

- He XD & Goyal RK. CaMKII inhibition hyperpolarizes membrane and blocks nitrergic IJP by closing a Cl(-) conductance in intestinal smooth muscle. *Am J Physiol Gastrointest Liver Physiol*., **303:** G240-G246, 2012.

- Hennig GW, Smith CB, O'Shea DM, Smith TK. Patterns of intracellular and intercellular Ca^{2+} waves in the longitudinal muscle layer of the murine large intestine in vitro. *J Physiol*., **543:** 233-253, 2002.

- Hisaw FL. Experimental relaxation of the pubic ligament of guinea-pig. *Proc Soc Exp Biol Med*., **23**: 661-663, 1926.

- Holland WL, Miller RA, Wang ZV, Sun K, Barth BM, Bui HH, Davis KE, Bikman BT. Receptor-mediated activation of ceramidase activity initiates the pleiotropic actions of adiponectin. *Nat Med*., **17:** 55-63, 2011.

- Holzer P. Peptidergic sensory neurons in the control of vascular functions: mechanisms and significance in the cutaneous and splanchic vascular beds. *Rev Physiol Biochem Pharmacol*., **121:** 49-146, 1992.

- Hotta K, Funahashi T, Arita Y, Takahashi M, Matsuda M, Okamoto Y, Iwahashi H, Kuriyama H, et al. Plasma concentrations of a novel, adipose-specific protein, adiponectin,in type 2 diabetic patients. *Arterioscler. Thromb. Vasc. Biol*., **20:** 1595-1599, 2000.

- Hotta K, Funahashi T, Bodkin NL. Circulating concentrations of the adipocyte protein adiponectin are decreased in parallel with reduced insulin sensitivity during the progression to type 2 diabetes in rhesus monkeys. *Diabetes* **50:** 1126-1133, 2001.

- Hsu SY, Nakabayashi K, Nishi S, Kumagai J, Kudo M, Sherwood OD, Hsueh AJ. Activation of orphan receptors by the hormone relaxin. *Science*, **295:** 671-674, 2002.

- Hu E, Liang P, Spiegelman BM. AdipoQ is a novel adipose-specific gene dysregulated in obesity. *J. Biol. Chem*., **271:**10697-10703, 1996.

- Hu Z, Cha SH, Chohnan S, Lane MD. Hypothalamic malonyl-CoA as a mediator of feeding behavior. *Proc Natl Acad Sci U S A.*, **100:** 12624-12629, 2003.

- Huber A, Saur D, Kurjak M, Schusdziarra V, Allescher HD. Characterization and splice variants of neuronal nitric oxide synthase in rat small intestine. Am. J. Physiol. Gastrointest. Liver. Physiol., 275: G1146-G1156, 1998.

- Hudson P, Haley J, John M, Cronk M, Crawford R, Haralambidis J, Tregear G, Shine J, and Niall H. Structure of a genomic clone encoding biologically active human relaxin. *Nature,* **301**: 628-631, 1983.

- Hudson P, John M, Crawford R, Haralambidis J, Scanlon D, Gorman J, Tregear G, Shine J, Niall H. Relaxin gene expression in human ovaries and the predicted structure of a human preprorelaxin by analysis of cDNA clones. *EMBO J* **3**: 2333-2339, 1984.

- Hug C, Wang J, Ahmad NS, Bogan JS, Tsao TS, Lodish HF, T-cadherin is a receptor for hexameric and high-molecular-weight forms of Acrp30/adiponectin. *Proc. Natl. Acad. Sci. U. S. A.*, **101:** 10308-10313, 2004.

- Hui X, Lam KS, Vanhoutte PM, Xu A. Adiponectin and cardiovascular health: an update. *British Journal of Pharmacology*, **165:** 574-590, 2012.

- Ivell R, Hunt N, Khan-Dawood F, Dawood MY. Expression of the human relaxin gene in the corpus luleum of the menstrual cycle and in the prostate. *Mol Cell Endocrinol*., **66**: 251-255, 1989.

- James R, Niall H, Kwok S, Bryand-Greenwood G. Primary structure of porcine relaxin: homology with insulin and related growth factors. *Nature* **267**: 544-546. 1977.

- Kadowaki T, Yamauchi T, Kubota N, et al. Adiponectin and adiponectin receptors in insulin resistance, diabetes, and the metabolic syndrome. *J Clin Invest*., **116:** 1784-1792, 2006.

- Kadowaki T, Yamauchi T, Kubota N. The physiological and pathophysiological role of adiponectin and adiponectin receptors in the peripheral tissues and CNS. *FEBS Lett.*, **582:** 74-80, 2008.

- Kadowaki, T & Yamauchi T. Adiponectin and adiponectin receptors. *Endocr. Rev*., **26:** 439–451, 2005.

- Kaser S, Moschen A, Cayon A, Kaser A, Crespo J, Pons-Romero F, Ebenbichler CF, Patsch JR, Tilg H. Adiponectin and its receptors in non-alcoholic steatohepatitis. *Gut*, **54:** 117-121, 2005.

- Kawamura K, Kumagai J, Sudo S, Chun SY, Pisarska M, Morita H, Toppari J, Fu P, Wade JD, Bathgate RA, Hsueh AJ. Paracrine regulation of mammalian oocyte maturation and male germ cell survival. *Proc Natl Acad Sci U S A*., **101**: 7323-7328, 2004.

- Kemp BE & Niall HD. Relaxin. *Vitamins and Hormones **41**:* 79-115, 1984.

- Kentish SJ, Ratcliff K, Li H, Wittert GA, Page AJ. High fat diet induced changes in gastric vagal afferent response to adiponectin. *Physiol Behav.*, **152(Pt B):**354-362, 2015.

- Kershaw EE, Flier JS. Adipose tissue as an endocrine organ. *J Clin Endocrinol Metab.*, **89:** 2548-2556, 2004.

- Kharroubi I, Rasschaert J, Eizirik D, Cnop M. Expression of adiponectin receptors in pancreatic beta cell. *Biochem Biophys Res Commun.*, **312**: 1118-1122, 2004.

- Koh SD, Bradley KK, Rae MG, Keef KD, Horowitz B, Sanders KM. Basal activation of ATP-sensitive potassium channels in murine colonic smooth muscle cell. *Biophys J*., **75**: 1793-800, 1998.

- Koh SD, Dick GM, Sanders KM. Small-conductance Ca^{2+} dependentK^{+} channels activated byATPin murine colonic smooth muscle. *Am J Physiol*., **273**: C2010-C2021, 1997.

- Koh SD, Sanders KM. Stretch-dependent potassium channels in murine colonic smooth muscle cells. *J Physiol*., **533**: 155-163, 2001.

- Koh SD, Ward SM, Sanders KM. Ionic conductances regulating the excitability of colonic smooth muscles. *Neurogastroenterol Motil*., **24:**705-718, 2012.

- Konturek SJ, Konturek JW, Pawlik T, Brzozowski T. Brain-gut axis and its role in the control of food intake. *J Physiol Pharmacol.* **55:** 137-154, 2004.

- Kos K, Harte AL, da Silva NF, Tonchev A, Chaldakov G, James S, Snead DR, Hoggart B, O'Hare JP, McTernan PG, Kumar S. Adiponectin and resistin in human cerebrospinal fluid and expression of adiponectin receptors in the human hypothalamus. *J Clin Endocrinol Metab*., **92:** 1129-1136, 2007.

- Kubota N, Yano W, Kubota T, Yamauchi T, Itoh S, Kumagai H, Kozono H, Takamoto I, et al. Adiponectin stimulates AMP-activated protein kinase in the hypothalamus and increases food intake. *Cell Metab*., **6:** 55-68, 2007.

- Kumar D. In vitro inhibitory effect of progesterone on extrauterine human smooth muscle. Am J Obstet Gynecol., **84:** 1300-1304, 1962.

- Langley K. The neuroendocrine concept today. *Ann NY Acad Sci*., **733:** 1-17, 1994.

- Lawson M, Kern F Jr, Everson GT. Gastrointestinal transit time in human pregnancy: prolongation in the second and third trimesters followed by postpartum normalization. *Gastroenterology,* **89:** 996-999, 1985.

- Lecchini S, Marcoli M, De Ponti F, Castelletti CA, Frigo GM. Selectivity of Ca^{2+} channel blockers in inhibiting muscolar and nerve activities in isolated colon. *Br J Pharmacol*., **102:** 735-741,1991.

- Lefebvre RA. Non-adrenergic, non-cholinergic neurotransmission in the proximal stomach. *Gen Pharmacol*., **24**: 257-266, 1993.

- Lefebvre RA. Study on the possible neurotransmitter of the non-adrenergic, non-cholinergic innervations of the rat gastric fundus. *Arch Int Pharmacodyn*., **280**: 110-136, 1986.

- Loesch A & Burnstock G. Ultrastructural localization of nitric oxide synthase and endothelin in coronary and pulmonary arteries of newborn rats. *Cell Tissue Res.*, **279:** 475-483, 1995.

- Lok S, Johnston DS, Conklin D, Lofton-Day CE, Adams RL, Jelmberg AC, Whitmore TE, Schrader S, Griswold MD, Jaspers SR. Identification of INSL6, a new member of the insulin family that is expressed in the testis of the human and rat. *Biol Reprod.*, **62**: 1593-1599, 2000.

- Lorenz M, Hewing B, Hui J, Zepp A, Baumann G, Bindereif A, Stangl V, Stangl K. Alternative splicing in intron 13 of the human eNOS gene: a potential mechanism for regulating eNOS activity. FASEB J., 21: 1556-1564, 2007.

- Ma S, Bonaventure P, Ferraro T, Shen PJ, Burazin TC, Bathgate RA, Liu C, Tregear GW, Sutton SW, Gundlach AL. Relaxin-3 in GABA projection neurons of nucleus incertus suggests widespread influence on forebrain circuits via G-protein-coupled receptor-135 in the rat. *Neuroscience.*, **144**: 165-190, 2007.

- Maeda K, Okubo K, Shimomura I, Funahashi T, Matsuzawa Y, Matsubara K. cDNA cloning and expression of a novel adipose specific collagen-like factor, apM1 (AdiPose Most abundant Gene transcript 1). *Biochem. Biophys. Res. Commun*., **221:** 286-289, 1996.

- Maeda K, Okubo K, Shimomura I, Mizuno K, Matsuzawa Y, Matsubara K. Analysis of an expression profile of genes in the human adipose tissue. *Gene*, **190:** 227-235, 1997.

- Martinson J & Muren A. Excitatory and inhibitory effects of vagus stimulation on gastric motility in the cat. *Acta Physiol Scand*., **57**: 309-316, 1963.

- Masini E, Bani D, Bigazzi M, Mannaioni PF, Bani-Sacchi T. Effects of relaxin on mast cells. In vitro and in vivo studies in rats and guinea pigs. *J Clin Invest*., **94:** 1974-1980, 1994.

- Mathias JR, Clench MH, Roberts PH, Reeves-Darby VG. Serum relaxin levels detected in women with functional bowel disease and reduced by leuprolide acetate (LA) therapy. *Gastroenterology*, **104:** 549, 1993.

- Matsuyama H, Thapaliya S, and Takewaki T. Cyclic GMP-associated apamin-sensitive nitrergic slow inhibitory junction potential in the hamster ileum. *Br J Pharmacol.,* **128:** 830-836, 1999.

- Matsuzaki U, Hamasaki Y, Said S. Vasoactive intestinal peptide: a possible transmitter of non-adrenergic relaxation of guinea-pig airways. *Science*, **210**: 1252-1253, 1980.

- Mayer B & Hemmens B. Biosynthesis and action of nitric oxide in mammalian cells. *Trends Biochem Sci.,* **12**: 477-481, 1997.

- McDonald TF, Pelzer S, Trautwein W, Pelzer DJ. Regulation and modulation of calcium channels in cardiac, skeletal, and smooth muscle cells. *Physiol Rev.,* **74:** 365-507, 1994.

- McGowan BM, Stanley SA, Smith KL, White NE, Connolly MM, Thompson EL, Gardiner JV, Murphy KG, Ghatei MA, Bloom SR. Epub 2005 Apr 21. Central relaxin-3 administration causes hyperphagia in male Wistar rats. *Endocrinology* **146**: 3295-3300, 2005.

- Mercado-Simmen RC, Bryant-Greenwood GD, Greenwood FC. Relaxin receptor in the rat myometrium: regulation by estrogen and relaxin. *Endocrinology,* **110:** 220-226, 1980.

- Minokoshi Y, Alquier T, Furukawa N, Kim YB, Lee A, Xue B, Mu J, Foufelle F, Ferré P, Birnbaum MJ, Stuck BJ, Kahn BB. AMP-kinase regulates food intake by responding to hormonal and nutrient signals in the hypothalamus. *Nature*, **428:** 569-574, 2004.

- Moncada S & Higgs EA. Endogenous nitric oxide: physiology, pathology and clinical relevance. *Eur J Clin Invest* **4**: 361-374, 1991.

- Moncada S & Palmer RMJ. Nitric oxide release accounts for the biological activity of endothelium derived relaxion factor. *Nature Lond*., **327**: 524-526, 1987.

- Morgado M, Cairrão E, Santos-Silva AJ, Verde I. Cyclic nucleotide-dependent relaxation pathways in vascular smooth muscle. *Cell Mol Life Sci*., **69:** 247-66, 2012.

- Morgan KG, Muir TC, Szurszewski JH. The electrical basis for contraction and relaxation in canine fundal smooth muscle. *J Physiol*., **311**: 475-488, 1981.

- Mulè F, Vannucchi MG, Corsani L, Serio R, Faussone-Pellegrini MS. Myogenic NOS and endougenous NO production are defective in colon from dystrophic (mdx) mice. *Am J Physiol.,* **281:** G1264-G1270, 2001.

- Murphy KG & Bloom SR. Gut hormones in the control of appetite. *Exp Physiol.,* **89:** 507516, 2004.

- Murphy ME & Brayden JE. Nitric oxide hyperpolarizes mesenteric arteries via ATP-sensitive potassium channels. *J Physiol* **486:** 47-58, 1995.

- Nakano Y, Tobe T, Choi-Miura NH, Mazda T, Tomita M. Isolation and characterization of GBP28, a novel gelatin-binding protein purified from human plasma. *J Biochem*., **120:** 803-812, 1996.

- Nedergaard J, Bengtsson T, Cannon B. Unexpected evidence for active brown adipose tissue in adult humans. *Am J Physiol Endocrinol Metab*., **293:** E444-E452, Review 2007.

- Oh DK, Ciaraldi T, Henry RR. Adiponectin in health and disease. *Diabetes Obes Metab*., **9:** 282-289, 2007.

- Ohya S, Asakura K, Muraki K, Watanabe M, Imaizumi Y. Molecular and functional characterization of ERG, KCNQ, and KCNE subtypes in rat stomach smooth muscle. *Am J Physiol Gastrointest Liver Physiol*., **282**: G277-G287, 2002.

- Okamoto Y, Kihara S, Funahashi T, Matsuzawa Y, Libby P. Adiponectin: a key adipocytokine in metabolic syndrome. *Clinical Science* **110:** 267-278, 2006.

- Okumura T & Nozu T. Role of brain orexin in the pathophysiology of functional gastrointestinal disorders. *J Gastroenterol Hepatol.,* **26:** 61-6, Review. 2011.

- Omori K & Kotera J. Overview of PDEs and Their Regulation. *Circ Res.,* **100:** 309-327, 2007.

- Ouchi N, Kihara S, Arita Y, Okamoto Y, Maeda K, Kuriyama H, Hotta K, Nishida M, et al. Adiponectin, an adipocyte-derived plasma protein, inhibits endothelial NF-kappaB signaling through a cAMP-dependent pathway. *Circulation*, **102:** 1296-1301, 2000.

- Palin MF, Bordignon VV, Murphy BD. Adiponectin and the control of female reproductive functions. *Vitam Horm*., **90**: 239-287, 2012.

- Pini A, Boccalini G, Baccari MC, Becatti M, Garella R, Fiorillo C, Calosi L, Bani D, Nistri S. Protection from cigarette smoke-induced vascular injury by recombinant human relaxin-2 (serelaxin). *J Cell Mol Med.*, **20:** 891-902, 2016.

- Psilopanagioti A, Papadaki H, Kranioti EF, Alexandrides TK, Varakis JN, Expression of adiponectin and adiponectin receptors in human pituitary gland and brain. *Neuroendocrinology* **89**: 38-47, 2009.

- Qi Y, Takahashi N, Hileman SM, Patel HR, Berg AH, Pajvani UB, Scherer PE, and Ahima RS. Adiponectin acts in the brain to decrease body weight. *Nat Med.*, **10:** 524-529, 2004.

- Rand MJ. Nitrergic transmission: nitric oxide as mediator of non-adrenergic, non-cholinergic neuro-effector transmission. *Clin Exp Pharmacol Physiol.*, **19:** 147-169, 1992.

- Rubino A. Non-adrenergic non-cholinergic (NANC) neural control of the atrial myocardium. *Gen Pharmacol*., **24**: 539-545, 1993.

- Ryan JP & Bhoiwani A. Colonic transit in rats: effect of ovariectomy sex steroid hormones, and pregnancy. *Am J Physiol*., **251:** G46-G50, 1986.

- Ryan PJ, Büchler E, Shabanpoor F, Hossain MA, Wade JD, Lawrence AJ, Gundlach AL. Central relaxin-3 receptor (RXFP3) activation decreases anxiety- and depressive-like behaviours in the rat. *Behav Brain Res*., **244**: 142-151, 2013

- Rybalkin SD, Yan C, Bornfeldt KE, Beavo JA. Cyclic GMP phosphodiesterases and regulation of smooth muscle function. *Circ Res*., **93:** 280-291, 2003

- Ryo M, Nakamura T, Kihara S. Adiponectin as a biomarker of the metabolic syndrome. *Circ. J*. **68:** 975-981, 2004.

- Ryoo SB, Oh HK, Yu SA, Moon SH, Choe EK, Oh TY, Park KJ. The effects of eupatilin (stillen®) on motility of human lower gastrointestinal tracts. *Korean J Physiol Pharmacol.*, **18:** 383-390, 2014.

- Salapatek AM, Wang YF, Mao YK, Mori M, Daniel EE. Myogenic NOS in canine lower esophageal sphincter: enzyme activation, substrate recycling, and product actions. *Am. J. Physiol. Cell. Physiol.*, **274:** C1145-C1157, 1998.

- Samuel CS, Du XJ, Bathgate RA, Summers RJ. 'Relaxin' the stiffened heart and arteries: the therapeutic potential for relaxin in the treatment of cardiovascular disease. *Pharmacol Ther.*, **112**: 529-52, 2006.

- Samuel CS & Hewitson TD. Relaxin in cardiovascular and renal disease. *Kidney Int*., **69**: 1498-502, 2006.

- Samuel CS, Unemori EN, Mookerjee I, Bathgate RA, Layfield SL, Mak J. et al. Relaxin modulates cardiac fibroblast proliferation, differentiation, and collagen production and reverses cardiac fibrosis in vivo. *Endocrinology* 145: 4125-4133, 2004.

- Sanders KM & Koh SD. Two-pore-domain potassium channels in smooth muscles: new components of myogenic regulation. *J Physiol*., **570**: 37-43. 2006.

- Sanders KM, Koh SD, Ward SM. Interstitial cells of cajal as pacemakers in the gastrointestinal tract. *Annual review of physiology,* **68**: 307-43, 2006.

- Sanders KM. Regulation of smooth muscle excitation and contraction. *Neurogastroenterol Motil.,* **20**: 39-53, 2008.

- Sarwar M, Du XJ, Dschietzig TB, Summers RJ. The actions of relaxin on the human cardiovascular system. *Br. J. Pharmacol.,* 13523, 2016 [Epub ahead of print]

- Sarwar M, Samuel CS, Bathgate RA, Stewart DR, Summers RJ. Serelaxin-mediated signal transduction in human vascular cells: bell-shaped concentration-response curves reflect differential coupling to G proteins. *Br J Pharmacol*., **172:** 1005-1019, 2015.

- Saur D, Paehge H, Schusdziarra V, Allescher HD. Distinct expression of splice variants of neuronal nitric oxide synthase in the human gastrointestinal tract. *Gastroenterology,* **118:** 849-858, 2000.

- Sbrana F, Sassoli C, Meacci E, Nosi D, Squecco R, Paternostro F, Tiribilli B, Zecchi-Orlandini S, Francini F, Formigli L. Role for stress fiber contraction in surface tension development and stretch-activated channel regulation in C2C12 myoblasts. *Am J Physiol Cell Physiol.,* **295:** C160-C172, 2008.

- Scherer PE, Williams S, Fogliano M, Baldini G, Lodish HF. A novel serum protein similar to C1q, produced exclusively in adipocytes. *J Biol Chem*., 270: 26746-26749, 1995.

- Scherer PE. Adipose tissue: from lipid storage compartment to endocrine organ. *Diabetes*, **55**: 1537-1545, Review 2006.

- Schlossmann J, Fiel R, Hofmann F. Signalling through NO and cGMP-dependent protein kinases. *Ann Med*., **35:** 21-27, 2003.

- Schmalz F, Kinsella J, Koh SD, Vogalis F, Schneider A, Flynn ER, Kenyon JL, Horowitz B. Molecular identification of a component of delayed rectifier current in gastrointestinal smooth muscles. *Am J Physiol*., **274**: G901-G911, 1998.

- Schwabe C, McDonald JK, Steinetz BG. Primary structure of the A chain of porcine relaxin. *Biochem Biophys Res Commun.,* **70**: 397-405, 1976.

❖ Schwabe C, Steinetz B, Weiss G, Segaloff A, McDonald JK, O'Byrne E, Hochman J, Carriere B, Goldsmith L. Relaxin. *Recent Prog Horm Res.*, **34**: 123-211, 1978.

❖ Sherwood CD & O'Byrne EM. Purification and characterization of porcine relaxin. *Arch Biochem Biophys* **160**: 185-96, 1974.

❖ Sherwood O.D. Relaxin's physiological roles and other diverse actions. *Endocr Rev.*, **25:** 205-234, 2004.

❖ Sherwood OD. Purification and characterization of rat relaxin. *Endocrinology* **104**: 886-892. 1979.

❖ Shklyaev S, Aslanidi G, Tennant M, Prima V, Kohlbrenner E, Kroutov V, Campbell-Thompson M, Crawford J, et al., Sustained peripheral expression of transgene adiponectin offsets the development of diet-induced obesity in rats. *Proc Natl Acad Sci USA.*, **100:** 14217-14222, 2003.

❖ Sims SM, Singer JJ, Walsh JV Jr. Cholinergic agonists suppress a potassium current in freshly dissociated smooth muscle cells of the toad. *J Physiol*., **367**: 503-529, 1985.

❖ Smith CM, Chua BE, Zhang C, Walker AW, Haidar M, Hawkes D, Shabanpoor F, Hossain MA, Wade JD, Rosengren KJ, Gundlach AL. Central injection of relaxin-3 receptor (RXFP3) antagonist peptides reduces motivated food seeking and consumption in C57BL/6J mice. *Behav Brain Res*., **268**:117-126, 2014.

❖ Smith SR, Lovejoy JC, Greenway F, Ryan D, de Jonge L, de la Bretonne J, Volafova J, Bray GA. Contributions of total body fat, abdominal subcutaneous adipose tissue compartments, and visceral adipose tissue to the metabolic complications of obesity. *Metabolism.*, **50:** 425-435, 2001.

❖ Sokol RZ, Wang XS, Lechago J, Johnston PD, Swerdloff RS. Immunohistochemical localization of relaxin in human prostate. *J Histochem Cytochem*., **37:** 1253-1255, 1989.

❖ Spanel-Borowski K, Schäfer I, Zimmermann S, Engel W, Adham IM. Increase in final stages of follicular atresia and premature decay of corpora lutea in Insl3-deficient mice. *Mol Reprod Dev*., **58**: 281-286, 2001.

❖ Squecco R, Garella R, Francini F, Baccari MC. Influence of obestatin on the gastric longitudinal smooth muscle from mice: mechanical and electrophysiological studies. *Am J Physiol Gastrointest Liver Physiol.*, **305:** G628-G637, 2013.

❖ Squecco R, Garella R, Luciani G, Francini F, Baccari MC. Muscular effects of orexin A on the mouse duodenum: mechanical and electrophysiological studies. *J Physiol* **589**: 5231-5246, 2011.

❖ Squecco R, Sassoli C, Garella R, Chellini F, Idrizaj E, Nistri S, Formigli L, Bani D, Francini F. Inhibitory effects of relaxin on cardiac fibroblast-to-myofibroblast transition: an electrophysiological study. *Exp Physiol*., **100:** 652-666, 2015a.

- Squecco, R.; Garella, R.; Idrizaj, E.; Nistri, S.; Francini, F.; Baccari, M.C. Relaxin affects smooth muscle biophysical properties and mechanical activity of the female mouse colon. *Endocrinology,* **156:** 4398-4410, 2015b.

- Stanley S, Wynne K, McGowan B, Bloom S. Hormonal Regulation of Food Intake. *Physiol Rev.*, **85:** 1131-1158, 2005.

- Sudo S, Kumagai J, Nishi S, Layfield S, Ferraro T, Bathgate RA, and Hsueh AJ. H3 relaxin is a specific ligand for LGR7 and activates the receptor by interacting with both the ectodomain and the exoloop 2. *J Biol Chem.*, **278:**7855-7862, 2003.

- Szurszewski JH. Electrical basis of gastrointestinal motility. In: Johnson LR, editor. *Physiology of the Gastrointestinal Tract*, 2nd edn. New York: Raven press, 383-422, 1987.

- Tanaka M, Iijima N, Miyamoto Y, Fukusumi S, Itoh Y, Ozawa H, Ibata Y. Neurons expressing relaxin 3/INSL 7 in the nucleus incertus respond to stress. *Eur J Neurosci*., **21**: 1659-1670, 2005.

- Tanaka Y, Tang G, Takizawa K, Otsuka K, Eghbali M, Song M, Nishimaru K, Shigenobu K, Koike K, Stefani E, Toro L. Kv channels contribute to nitric oxide- and atrial natriuretic peptide-induced relaxation of a rat conduit artery. *J Pharmacol Exp Ther*., **317:** 341-354, 2006.

- Teichman SL, Unemori E, Dschietzig T, Conrad K, Voors AA, Teerlink JR, Felker GM, Metra M, Cotter G. Relaxin, a pleiotropic vasodilator for the treatment of heart failure. Heart *Fail Rev.,* **4**: 321-329, 2009.

- Tschöp M, Weyer C, Tataranni PA, Devanarayan V, Ravussin E, Heiman ML. Circulating ghrelin levels are decreased in human obesity. *Diabetes,* **50:** 707-709, 2001.

- Unemori EN & Amento EP. Relaxin modulates synthesis and secretion of procollagenase and collagen by human dermal fibroblasts. *J Biol Chem*., **265:** 10681-10685, 1990.

- Unemori EN1, Pickford LB, Salles AL, Piercy CE, Grove BH, Erikson ME, Amento EP. Relaxin induces an extracellular matrix-degrading phenotype in human lung fibroblasts in vitro and inhibits lung fibrosis in a murine model in vivo. *J Clin Invest*., **98:** 2739-2745, 1996.

- Vallance P. Nitric oxide: therapeutic oppurtunies. Fundam Clin Pharmacol., **17:** 1-10, 2003.

- van der Westhuizen ET, Halls ML, Samuel CS, Bathgate RA, Unemori EN, Sutton SW, Summers RJ. Relaxin family peptide receptors--from orphans to therapeutic targets. *Drug Discov Today*., **13:** 640-51, 2008.

❖ Vannucchi MG, Corsani L, Bani D, Faussone-Pellegrini MS. Myenteric neurons and interstitial cells of Cajal of mouse colon express several nitric oxide synthase isoforms. *Neurosci Lett.,* **326:** 191-195, 2002.

❖ Vannucchi MG, Garella R, Cipriani G, Baccari MC. Relaxin counteracts the altered gastric motility of dystrophic (mdx) mice: functional and immunohistochemical evidence for the involvement of nitric oxide. *Am J Physiol Endocrinol Metab*., **300**: E380- E391, 2011.

❖ Vogalis F & Goyal RK. Activation of small conductance Ca^{2+}-dependent K^{+} channels by purinergic agonists in smooth muscle cells of the mouse ileum. *J Physiol*., **502**: 497-508, 1997.

❖ Wajchenberg BL. Subcutaneous and visceral adipose tissue: their relation to the metabolic syndrome. *Endocr Rev.,* **21:** 697-738, 2000.

❖ Wald A, Van Thiel DH, Hochstetter L, Gavaler JS, Egler KM, Verm R, Scott L, Lester R. Effects of pregnancy on gastrointestinal transit. *Dig Dis Sci*., **27:** 1015-1018, 1982.

❖ Wang GR, Zhu Y, Halushka PV, Lincoln TM, Mendelsohn ME. Mechanism of platelet inhibition by nitric oxide: in vivo phosphorylation of thromboxane receptor by cyclic GMP-dependent protein kinase. *Proc Natl Acad Sci U S A.,* **95**: 4888-93, 1998.

❖ Wang H, Kohr MJ, Traynham CJ, Ziolo MT. Phosphodiesterase 5 restricts NOS3/soluble guanylate cyclase signaling to L-type Ca^{2+} current in cardiac myocytes. *J Mol Cell Cardiol*. **47:** 304-314, 2009.

❖ Ward SM, Ordog T, Koh SD, Baker SA, Jun JY, Amberg G, Monaghan K, Sanders KM. Pacemaking in interstitial cells of Cajal depends upon calcium handling by endoplasmic reticulum and mitochondria. *J. Physiol.,* **525:** 355-361, 2000.

❖ Weiss G, O'Byrne EM, Steinetz BG. Relaxin: a product of the human corpus luteum of pregnancy. *Science* **194**: 948-949, 1976.

❖ Weyer C, Funahashi T, Tanaka S, Hotta K, Matsuzawa Y, Pratley RE, Tataranni PA. Hypoadiponectinemia in obesity and type 2 diabetes: close association with insulin resistance and hyperinsulinemia. *J. Clin.Endocrinol. Metab.* **86:** 1930-1935, 2001.

❖ Wilding JP. Neuropeptides and appetite control. *Diabet Med*., **19:** 619-627, 2002.

❖ Wilkinson TN, Speed TP, Tregear GW, Bathgate RA. Evolution of the relaxin-like peptide family. *BMC Evol Biol.,* **12**: 5-14, 2005.

❖ Williams G, Bing C, Cai XJ, Harrold JA, King PJ, Liu XH. The hypothalamus and the control of energy homeostasis: different circuits, different purposes. *Physiol Behav.,* **74:** 683-701, 2001.

- Winslow JW, Shih A, Bourell JH, Weiss G, Reed B, Stults JT, Goldsmith LT. Human seminal relaxin is a product of the same gene as human luteal relaxin. *Endocrinology*, **130**: 2660-2668, 1992.

- Wolf G1. The regulation of food intake by hypothalamic malonyl-coenzyme A: the MaloA hypothesis. *Nutr Rev*., **64:** 379-383, 2006.

- Wong GW, Wang J, Hug C, Tsao TS, Lodish HF. A family of Acrp30/adiponectin structural and functional paralogs. *Proc Natl Acad Sci U S A.*, **101:** 10302-10307, 2004.

- Xiong Z, Sperelakis N, Noffsinger A, Fenoglio-Preiser C. Ca^{2+} currents in human colonic smooth muscle cells. *Am J Physiol*., **269**: G378-G385, 1995.

- Yamauchi T & Kadowaki T, Adiponectin receptor as a key player in healthy longevity and obesity-related diseases. *Cell Metab.,* **17:** 185-196, 2013.

- Yamauchi T, Kamon J, Ito Y, et al. Cloning of adiponectin receptors that mediate antidiabetic metabolic effects. *Nature,* **423:** 762-769, 2003.

- Yamauchi T, Nio Y, Maki T, Kobayashi M, Takazawa T, Iwabu M, Okada Iwabu M, Kawamoto S, et al. Targeted disruption of AdipoR1 and AdipoR2 causes abrogation of adiponectin binding and metabolic actions. *Nat. Med.*, **13:** 332-339, 2007.

- Yarandi SS, Hebbar G, Sauer CG, Cole CR, Ziegler TR. Diverse roles of leptin in the gastrointestinal tract: modulation of motility, absorption, growth, and inflammation. *Nutrition*, **27:** 269-275, Review. 2011.

- Yatagai T, Nishida Y, Nagasaka S. Relationship between exercise training-induced increase in insulin sensitivity and adiponectinemia in healthy men. *Endocr. J*., **50:** 233-238, 2003.